Peer Effects in Social Networks: Search, Matching Markets, and Epidemics

Thesis by

Elizabeth Bodine-Baron

In Partial Fulfillment of the Requirements

for the Degree of

Doctor of Philosophy

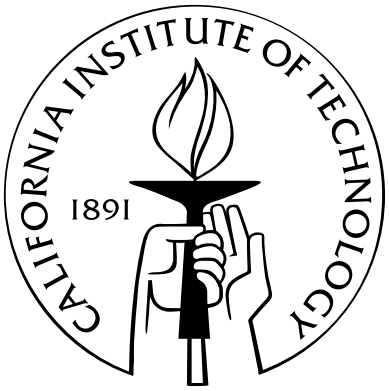

California Institute of Technology

Pasadena, California

2012

(Defended May 11, 2012)

Acknowledgements

I would like to thank my advisor, Dr. Babak Hassibi, for his tireless dedication to my research and willingness to let me explore a rather non-traditional research topic. From the beginning of my career at Caltech to now, his belief in my ability to succeed as an independent researcher has given me the confidence to reach for something a little different, to make my own path and study the topics that excite me. I would also like to thank Dr. Adam Wierman for taking me on as a student four years ago. His commitment to improving and guiding my research as well as his dedication to the art of presentation, have been and will continue to be invaluable, in my work here at Caltech and in my future career. Whether in research meetings or casual conversation, both Babak and Adam have been essential source of advice and critique for everything from my job search to my writing skills to my actual research. I have been truly spoiled by their dedication to me – not every advisor is willing to sit down with students on a regular basis and work with them directly. Being able to observe the way they think and solve problems has not only improved my own work but also the way that I mentor and interact with other students.

I also must thank my thesis committee, each of whom has had an impact on my research. Dr. Shuki Bruck was my co-advisor for my first year at Caltech; in addition to introducing me to graduate-level research, he has always given me honest and very useful advice for both my research and life in general. Dr. Steven Low has always given me useful feedback on my research, even when I was a first year graduate student and unsure of which direction to take. Without Dr. Leeat Yariv's class on matching markets and her very useful input, this thesis would look very different. Watching all of my committee members and other faculty interact in various research

meetings around campus, I am struck by the level of cooperation across disciplines and interest in other areas; without this collaborative environment, it is unlikely that I would have been able to do such interdisciplinary research.

I would definitely be remiss if I did not thank the students, both undergraduate and graduate, that I have been lucky enough to collaborate with at Caltech. Daniel Thai was the first undergraduate student I mentored – special thanks go to him for being patient as I figured out my mentor role. Anthony Chong and Christina Lee were both very talented CS undergraduate students I had the chance to collaborate with and mentor; it was amazing to watch them both develop as researchers and I wish them the best in their future careers. I would also like to thank Subhonmesh Bose; it was a pleasure to work with such a brilliant student and I cannot wait to see where his career takes him. Much thanks goes to the students in Babak's research group, both for making the lab enjoyable and for always showing interest in my work, especially to those who started with me: Teja Sukhavasi, Wei Mao, and Amin Khajehnejad.

In my last year at Caltech, I had the chance to work with Dr. Sarah Nowak, Dr. Raffaele Vardavas, and Dr. Neeraj Sood. I would like to thank all of them for taking the time work with me, both during and after my internship at RAND. Our work on peer effects in vaccination decisions was not only fascinating in itself, but has also spawned a number of other ideas which I cannot wait to pursue.

Finally, I have to thank my family. My mother, Mel, my father, Harvey, and brother, John, have always been my staunchest (and most vocal) supporters. My parents inspired me from an early age to tackle challenging problems, always pushing myself and following my own path. Without my dad and his Lincoln Labs journals, I would not have have pursued an internship there, sparking my interest in research (and meeting my husband). Without my mom, I would not have gotten a double major in liberal arts, introducing me to social networks. As for my husband, Josh, his unwavering support of me through both the good times and the bad deserves more thanks than I can give. Without him and his insistence that I never give up, I would not be where I am, or at least not here and mostly sane. They all deserve my love, and much thanks.

Abstract

Social network analysis emerged as an important area in sociology in the early 1930s, marking a shift from looking at individual attribute data to examining the relationships between people and groups. Surveying many different types of real-world networks, researchers quickly found that different types of social networks tend to share a common set of structural characteristics, including small diameter, high clustering, and heavy-tailed degree distributions. Moving beyond real networks, in the 1990s researchers began to propose random network models to explain these commonly observed social network structures. These models laid the foundation for investigation into problems where the underlying network plays a key role, from the spread of information and disease, to the design of distributed communication and search algorithms, to mechanism design and public policy. Here we focus on the role of peer effects in social networks. Through this lens, we develop a mathematically tractable random network model incorporating searchability, propose a novel way to model and analyze two-sided matching markets with externalities, model and calculate the cost of an epidemic spreading on a complex network, and examine the impact of conforming and non-conforming peer effects in vaccination decisions on public health policy.

Throughout this work, the goal is to bring together knowledge and techniques from diverse fields like sociology, engineering, and economics, exploiting our understanding of social network structure and generative models to understand deeper problems that — without this knowledge — could be intractable. Instead of crippling our analysis, social network characteristics allow us to reach deeper insights about the interaction between a particular problem and the network underlying it.

Contents

List of Figures

Chapter 1

Introduction

Social network research, and more generally, network science, is more than just a current hot topic. With the global spread of technology over the last century, we find ourselves in an increasingly networked world. What started as a relatively minor student protest in Tunisia quickly spread to Egypt and the entire Middle East, fueled by social media technology like Twitter. Companies seeking to improve their visibility and attract new customers attend social media marketing seminars where they learn the right way to advertise on Facebook. In 2009, swine flu in Mexico spread to the United States and from there to Europe, Africa, and Asia, quickly jumping countries and ethnicities. Clearly, peer effects in both on-line and physical social networks have the potential to affect our day-to-day lives and the technology we develop. Understanding and analysis of social networks and their impact on different applications can often be complex and difficult, but the potential reward of such research cannot be overstated.

Social network analysis emerged as an important field in sociology in the 1930s, marking a shift from studying attribute data (this person has this characteristic) to relational data (these people share these relationships) [51, 122]. With these "sociograms", sociologists began to define metrics for determining the importance and influence of individuals and groups in a given society [131, 122], paving the way for modern analyses of everything from terrorist networks to the interactions of Fortune-500 companies in financial markets. In the most basic of these networks, relationships between individuals are characterized by a set of nodes (representing individual peo-

ple) and edges (representing the relationships between individuals) and summarized in a symmetric, binary adjacency matrix. Each entry in such a matrix is either one or zero, representing either the presence or absence of a particular type of relationship. Note that this type of network is undirected – all relationships are symmetric. More sophisticated social networks can capture directed relationships, different levels of relationships (using signed edge weights), and even different types of relationships (multi-graphs).

Surveying many different types of real-world networks, researchers quickly found that different types of social networks tended to share a common set of characteristics. For example, many social networks exhibit a small diameter, meaning that the average (or maximum) distance between nodes scales logarithmically rather than linearly with the number of nodes in the network [89, 132]. Further, researchers also observed the tendency of nodes to cluster together — many tightly knit groups of nodes characterized by a relatively high density of ties [63, 133]. This could partly be explained by the presence of homophily, the tendency of individuals to associate with similar people, a characteristic that has been observed in many real-world studies and documented in [88], but has also been observed in other types of complex networks, including the Internet and biological networks. Finally, many social networks (particularly those representing on-line relationships) were observed to be scale-free, meaning that the networks' degree distribution follows some sort of power law [11, 1]. This branch of social network research can broadly be classified as *measurement* — using surveys and studies of real-world and on-line social networks to determine a set of universal characteristics present in all social networks.

Moving beyond measurement, however, we move into the world of *modeling*, emerging as an important area of social network research in the 1990s. Researchers in this area propose random and deterministic network models to explain some of the commonly observed social network structures described above. For example, the Erdös-Rényi random network model, while not initially designed to model a social network, exhibits small diameter and the emergence of a giant component for various input parameters [97]. An explosion of papers looking at random network models

followed the seminal paper by Watts and Strogatz in 1998, which proposed a random network model that exhibits the small-world effect — combining small diameter with high clustering [133]. Around the same time, Barabási and Albert proposed the preferential attachment model explaining scale-free networks, in which new nodes entering a network preferentially attach to higher-degree nodes, creating a "rich get richer" effect. Countless models have since been proposed that exhibit more and more of the commonly observed social network structures and growth, though as of yet there does not exist the "holy grail" of social network modeling, a mathematically tractable random network model exhibiting all characteristics.

Incorporating both measurement and modeling, current social network research focuses on *applications* — developing and studying algorithms and processes operating on networks, as well as studying the role of network structure in various types of problems. We use the broad term *peer effects* to refer to the role of the social network in a given problem; for example, when "peers" or neighbors on a network dictate the preferences or strategies of individual nodes, or when a system's transition states are governed by the links available between peers, we say this is an example of "peer effects." This type of research brings together knowledge and techniques from diverse fields like sociology, engineering, and economics, exploiting our understanding of social network structure and generative models to understand deeper problems that without this knowledge, could be intractable. Social network structure affects a wide range of problems from the spread of information and disease to the design of distributed communication and search algorithms to mechanism design and public policy. Using fully realistic networks often renders mathematical analysis intractable, therefore this work seeks to leverage existing knowledge of social networks and random models to simplify hard problems and provide solutions and insights not otherwise possible. Instead of crippling analysis, social network characteristics allow us to reach deeper insights about the interaction between a particular problem and the network underlying it. In this thesis our particular focus is on the role of peer effects in the context of distributed search, matching markets, and epidemics. We discuss each of these domains in more detail in the following.

1.1 Distributed search in social networks

One of the ways in which people use their social networks in day-to-day life is to find individuals or information not immediately available through their direct social contacts. In 1967, Stanley Milgram tested this ability by sending chain letters to individuals in Nebraska and Kansas, attempting to see if people could use their local social contacts to reach a destination individual in Boston, Massachusetts. Not only were people able to succeed at this task, they were able complete it using remarkably few steps, leading to the popular "six degrees of separation" expression [89]. Milgram's experiment was a real-life version of the distributed search problem, in which a routing algorithm uses only local information to find a (hopefully short) path through a network. Though this problem is known to be hard for complex networks, humans were able to solve it using their social networks, leading to the question:

What makes a (social) network searchable?

Kleinberg first addressed this problem in [75], linking the searchability of a network to the distance-dependent probability of long-range connection (related to Granovetter's weak ties in social networks [56]). Unfortunately, the networks generated by Kleinberg's proposed model lack an important feature in social networks — a power-law degree distribution. We extend Kleinberg's result by focusing on constructing a mathematically tractable network generation model that maintains the unique properties of social networks (as listed above) while also being searchable. Our results show that searchable networks must be embedded in some sort of underlying space, where the probability of long-range connections between nodes is dependent on the underlying distance between them. We define a generalization of Kronecker graphs, first proposed in [81], using a new "Kronecker-like" operation to build a random graph model, which we denote distance-dependent Kronecker graphs [16, 18]. We prove that a decentralized search algorithm will be able to find short paths through networks generated by our model, just as in Milgram's real-world experiment. In this case, peer effects, if the links are generated in a particular way, lead to a searchable social network.

1.2 Peer effects and stability in matching markets

Many-to-one matching markets exist in numerous forms, such as college admissions, the national medical residency program and college housing assignment. These markets are widely studied in academia and have been applied to other areas, such as FCC spectrum allocation and supply chain networks. Early results demonstrated the existence of stable matchings and created matching mechanisms [54], leading to the National Resident Matching Program (NRMP), heralded as the greatest practical success of matching market theory. In the real world, however, problems quickly arose: couples preferred to make their own matches rather than participate in the NRMP. When matching students to housing at Caltech, administrators often find that students collude with their friends and attempt to "game the system" in order to be in the same house as their friends. These real-world problems point at a deeper underlying theoretical problem in matching markets — that in the presence of externalities such as peer effects and complementarities[1], a stable matching may not exist, and further, that even if it does exist, it may be computationally difficult to find. Our research has focused on answering the following questions:

Can stable matchings exist when peer effects are present?

In our work, the key idea is that peer effects are often the result of an underlying social network; agents care about other agents' matches when they are friends. Focusing on utility functions that depend on a social network and using a specific type of stability, we prove that *a stable matching will always exist*, and further, that in certain cases the social welfare-maximizing matching is stable [19]. We propose two algorithms to find stable (and optimal) matchings for the college housing assignment problem: (1) a simple distributed greedy algorithm, and (2) a centralized mechanism employing MCMC methods. To evaluate these algorithms, we employ a real social network (Caltech undergraduate friendship network [47]); our results show that even

[1]Peer effects in this case are instances where students, for example, care about where other students are matched; complementarities are instances where houses, for example, care about the diversity of the group of students matched to them.

relatively simple mechanisms using social information can achieve better matchings than mechanisms that ignore peer effects. However, we can also show that stable matchings may exist outside of the local maxima of social welfare — indicating that stability alone is not the appropriate measure of a "good" matching.

How far from optimal can a stable matching be?

To answer this question, we obtain bounds and tightness results on the "price of anarchy." Further, we prove that impact of social network structure on the price of anarchy happens only through the clustering of the network, which is well understood for social networks. Finally, it turns out that the price of anarchy has a dual interpretation in our context; in addition to providing a bound on the inefficiency caused by enforcing stability, it turns out to also provide a bound on the loss of efficiency due to peer effects.

1.3 Epidemic spread in human contact networks

Though the study of epidemics in networks was initially motivated by the spread of disease, the results have far reaching applications. For example, applications such as (i) network security, where the goal is to limit the spread of computer viruses, (ii) viral advertising, where the goal is to maximize product interest through social media, and (iii) information propagation, where the goal is to understand how new ideas propagate through a network, all have their roots in mathematical infection models. Early models assumed infection could be spread from any individual to another. However, real infection can only spread through some sort of contact between individuals, and so looking at the spread of a disease on a social network is extremely relevant. While the original epidemiological models are easily described by a set of differential equations and steady-state solutions are relatively easy to obtain, the spread of a disease on a network, when peer effects play an important role, is much more difficult to analyze. Our work in this area focuses on the following question:

What is the "social cost" of an epidemic?

The "social cost" of an epidemic includes the cost of immunization (e.g. vaccine cost) as well the cost of infection in a given period of time (e.g. doctor's visits, medication); to calculate this cost requires knowledge of the total number of nodes infected over the entire time period of interest, not just the steady-state fraction of infected nodes. In our work, we use tools from random matrix theory to make the analysis tractable — to our knowledge, we are the first to adapt this approach and proof techniques for this sort of problem. Using a new random graph model, we derive solutions for (i) the exact cost of an epidemic in the large-graph limit and (ii) bounds on the cost of an epidemic for finite graphs [17, 26]. To illustrate the usefulness of these cost calculations, we study random and degree-based centralized immunization strategies for balancing the cost of disease with the cost of immunization. Our approach demonstrates the practicality of analyzing epidemic spread on networks — despite the complexity of the network, we are able to obtain simple solutions highlighting the importance of the structure of the underlying social network in the final cost of an epidemic.

1.4 Peer effects in vaccination decisions

Recent vaccine scares and subsequent outbreaks of diseases that have long been under control highlight the need to understand how people decide whether or not to vaccinate themselves against an infectious disease, in order to better design public health policy to meet changing demands. When making a vaccination decision, individuals weigh the risk of the disease (i.e., the likelihood of contracting the disease, its morbidity and mortality) against the risk and cost of the vaccine. However, the risk of contracting the disease depends on how many individuals in the population are already vaccinated. Recent research focuses on game-theoretical models that assume that individuals perceived risk of infection strictly decreases with vaccination intake; this inverse relationship is an example of a *nonconforming peer effect* [13]. Under these assumptions, the equilibrium vaccination coverage will be lower than what is required to eradicate the disease, as individuals try to "free-ride" on others' decisions

to vaccinate. In our work, we try to answer the question:

What is a realistic vaccination decision model?

The current approach to modeling vaccination decisions makes two limiting assumptions: (1) that individuals have full information and know exactly their probability of being infected and (2) that individuals are perfectly rational and only nonconforming peer effects affect their decision. We develop a new model for vaccination decisions, adding a very specific form of irrationality through *conforming peer effects*. Basically, in addition to the nonconforming peer effects described above, individuals may also be influenced by their social contacts and may decide whether or not to vaccinate based on following majority wisdom. Our research models these apparently conflicting desires to provide a more accurate picture of the vaccination decision process, suggesting that conforming peer effects lead to higher vaccination rates, and further, that through the use of public health policies like government subsidies, populations can be "pushed" to make vaccination decisions that achieve disease eradication [20]. This work highlights the need for models of human decisions and peer effects that account for actual human behavior and limitations; accounting for even a very simple form of irrationality can lead to different recommendations in terms of public health policy.

Chapter 2

Search

2.1 Introduction

Beginning with the simple Erdös-Rényi model of random networks [97], network science has attempted to capture the key characteristics of complex networks such as power networks, the Internet, protein interaction networks, and social networks with a simple, mathematically tractable model. Social networks in particular have generated much interest due to the consistency of their characteristics. These networks tend to exhibit small diameter, high clustering, scale-free degree distributions, and perhaps most importantly, they are searchable by a local greedy algorithm; see [93], [1], and [76] for thorough surveys of this area.

The Erdös-Rényi random graph maintains a small diameter but fails to capture many of the other key properties [25], [97]. The combination of small diameter and high clustering is often called the "small-world effect", and Watts and Strogatz (see Section 2.3) generated much interest when they proposed a model that maintains these two characteristics simultaneously [133]. Several models were then proposed to explain the heavy-tailed degree distributions and densification of complex networks; these include the preferential attachment model [11], the forest-fire model [82], [10], Kronecker graphs [81], [80], and many others [93]. As demonstrated by Milgram's 1967 experiment using real people, individuals can discover and use short paths using only local information [89]. Kleinberg focuses on this searchability characteristic in his lattice model and proves searchability for a precise set of input parameters, but

his model lacks any heavy-tailed distributions [75], [76], [86]. The Kronecker graphs described in [81], [80], and [85] are simple to generate, mathematically tractable, and have been shown to exhibit several important social network characteristics such as heavy-tailed degree and eigen-distributions, high clustering, small diameter, and network densification. However, Kronecker graphs are not searchable by a distributed greedy algorithm [85].

In this chapter, we extend the model proposed in [16], a generalization of stochastic Kronecker graphs that can generate searchable networks. Instead of using the traditional Kronecker operation, we introduce a new "Kronecker-like" operation and a family of generator matrices, $\mathcal{H}$, both dependent upon the distance between two nodes. This new generation method yields networks that have both a local (lattice-based) and global (distance-dependent) structure. This dual structure is what allows a greedy algorithm to search the network using only local information. Additionally, the networks generated have a high clustering (due to the lattice structure) and a small diameter (due to the addition of long-range links).

As part of the analysis of this new model, we provide a general framework for analyzing degree distributions and the performance of greedy search algorithms on a general lattice-based network. We use this framework to study one example in detail: an expanding hypercube with distance-dependent long-range connections. We give an explicit description of its degree distribution, the circumstances under which it will be searchable by a local greedy algorithm, and a lower bound on its diameter. We support our findings with simulations. This example is chosen because it mimics the defining feature of tree metrics and hyperbolic space — exponentially expanding neighborhoods — which are thought to be representative of both the Internet and social networks [5], [78], [38], [108]. Exponentially expanding neighborhoods lead to very small diameters ($O(\log\log n)$ as opposed to $O(\log n)$) and we can show that, as in [22], a local greedy algorithm on the hypercube will find ultrashort paths, $O((\log\log n)^2)$.

This chapter is organized as follows. Section 2.2 briefly defines some key concepts frequently used in social network literature. Section 2.3 describes in detail our model

and its relation to the original Kronecker graph model and other traditional models. Section 2.4 explores the connection between a Kleinberg-like expanding hypercube example and the hidden metric space models proposed in [5]. Section 2.5 describes a general analysis of degree distributions for lattice-based networks and gives a theorem showing that all such networks will have a Poisson degree distribution provided that $P(d)$ is sufficiently small, and gives the relevant degree distribution for the expanding hypercube example. Section 2.6 gives a general framework for proving searchability of a lattice-based distance-dependent network model and recovers the searchability result of [75] and finally proves that the expanding hypercube is in fact searchable. Section 2.7 explores the diameter of the expanding hypercube example and Section 2.8 concludes with proposed future work. Sections 2.9 and 2.9.3 support the proof of searchability for the expanding hypercube example in Section 2.6.

2.2 Preliminaries

Before continuing further, it will be useful to define several terms commonly used in social network literature. A social network is represented by a graph $G = (V, E)$, where V and E are the sets of vertices and edges, respectively. There is one vertex for each agent, or person, in the network, and the edges represent the relationships between individuals. These relationships can be summarized in an adjacency matrix A where

$$A_{ij} = \begin{cases} 1 & \text{if nodes } i \text{ and } j \text{ are connected} \\ 0 & \text{otherwise.} \end{cases}$$

We note that while we will be working with undirected and unweighted graphs, in general, the edges in an adjacency matrix representing a social network can be both directed and weighted, showing the direction and the values of different relationships. The *neighborhood* $\mathcal{N}_i$ of a node i is defined as the set of its immediately connected neighbors. The *degree* k_i of a node is defined as the size of its neighborhood. We define the *geodesic* between two nodes u and v as the shortest path connecting them. The *diameter* of a network, for our purposes, is the length of the maximum geodesic

for that network. Note that in some cases, what is meant by diameter is the average of all geodesics; however, for this chapter we focus on the maximum. In social and most complex networks, the diameter of the network grows logarithmically with the number of nodes int the network [133], [67]. Another useful and commonly used term is clustering, which measures the amount of community structure present in a network. For an individual node, we define a *clustering coefficient* C_i where

$$C_i = \frac{2 \mid \{e_{jk}\} \mid}{k_i(k_i - 1)} : v_j, v_k \in \mathcal{N}_i, e_{jk} \in E$$

The clustering coefficient for the entire graph is then the average of the clustering coefficients over all n nodes [133].

$$\bar{C} = \frac{1}{n} \sum_{i=1}^{n} C_i$$

Finally, we call a network *searchable* if a distributed search algorithm can find paths through the network of length on the order of the diameter. For example, in Kleinberg's lattice model, a network has diameter $O(\log n)$, and is called searchable if a distributed algorithm can find paths of length $O((\log n)^2)$ [75]. For more details on the distributed search algorithm, see Section 2.6.

2.3 Distance-dependent Kronecker graphs

In this section we describe the original formulation of stochastic Kronecker graphs as well as our new "distance"-dependent extension of the model. We then present a few examples illustrating how to generate existing network models using the "distance"-dependent Kronecker graph.

2.3.1 Stochastic Kronecker graphs

Stochastic Kronecker graphs[1] are generated by recursively using a standard matrix operation, the Kronecker product [81]. Beginning with an initiator probability matrix P_1, with N_1 nodes, where the entries p_{ij} denote the probability that edge (i, j) is present, successively larger graphs $P_2, \ldots, P_n$ are generated such that the k^{th} graph P_k has $N_k = N_1^k$ nodes. The Kronecker product is used to generate each successive graph.

Definition 1. *The k^{th} power of P_1 is defined as the matrix $P_1^{\otimes k}$, such that:*

$$P_1^{\otimes k} = P_k = \underbrace{P_1 \otimes P_1 \otimes \ldots P_1}_{k\ times} = P_{k-1} \otimes P_1$$

For each entry p_{uv} in P_k, include an edge in the graph G between nodes u and v with probability p_{uv}. The resulting binary random matrix is the adjacency matrix of the generated graph.

Kronecker graphs have many of the static properties of social networks, such as small diameter and a heavy-tailed degree distribution, a heavy-tailed eigenvalue distribution, and a heavy-tailed eigenvector distribution [81]. In addition, they exhibit several temporal properties such as densification and shrinking diameter. Using a simple 2x2 P_1, Leskovec demonstrated that he could generate graphs matching the patterns of the various properties mentioned above for several real-world data-sets [81]. However, as shown by Mahdian and Xu, stochastic Kronecker graphs are not searchable by a distributed greedy algorithm [85] — they lack the necessary spatial structure that allows a local greedy agent to find a short path through the network. This is the motivation for the current chapter.

2.3.2 Distance-dependent Kronecker graphs

In this section, we propose an extension to Kronecker graphs incorporating the spatial structure necessary to have searchability. We add to the framework of Kronecker

[1] For a description of deterministic Kronecker graphs, see Leskovec et al., [81].

graphs a notion of "distance", which comes from the embedding of the graph, and extend the generator from a single matrix to a family of matrices, one for each distance, defining the likelihood of a connection occurring between nodes at a particular "distance". We accomplish this with a new "Kronecker-like" operation. Specifically, whereas in the original formulation of Kronecker graphs one initiator matrix is iteratively Kronecker-multiplied with itself to produce a new adjacency or probability matrix, we define a "distance"-dependent Kronecker operator. Depending on the distance between two nodes u and v, $d(u,v) \in \mathbb{Z}$, a different matrix from a defined family will be selected to be multiplied by that entry, as shown below.

$$\mathbf{C} = \mathbf{A} \otimes_d \mathcal{H} = \begin{pmatrix} a_{11}H_{d(1,1)} & a_{12}H_{d(1,2)} & \dots & a_{1n}H_{d(1,n)} \\ a_{21}H_{d(2,1)} & a_{22}H_{d(2,2)} & \dots & a_{2n}H_{d(2,n)} \\ \vdots & \vdots & \ddots & \vdots \\ a_{n1}H_{d(n,1)} & a_{n2}H_{d(n,2)} & \dots & a_{nn}H_{d(n,n)} \end{pmatrix}$$

where

$$\mathcal{H} = \{H_i\}_{i \in \mathbb{Z}}$$

So, the k^{th} Kronecker power is now

$$G_k = \underbrace{G_1 \otimes_d \mathcal{H} \cdots \otimes_d \mathcal{H}}_{k\ times}$$

In the Kronecker-like multiplication, the choice of H_i from the family $\mathcal{H}$, multiplying entry (u,v), is dependent upon the distance $d(u,v)$. Note that our $d(u,v)$ is not a true distance measure—we can have negative distances. Further, $d(u,v)$ is not symmetric ($d(u,v) \neq d(v,u)$) since we need to maintain symmetry in the resulting matrix. Instead, $d(u,v) = -d(v,u)$ and $H_{d(u,v)} = H'_{d(v,u)}$.

This change to the Kronecker operation makes the model more complicated, and we do give up some of the beneficial properties of Kronecker multiplication. Potentially, we could have to define a large number of matrices for $\mathcal{H}$. However, for the models we want to generate, there are actually only a few parameters to define, as

$d(i,j)$ and a simple function defines H_i for $i > 1$. The underlying reason for this simplicity is that the local lattice structure is usually specified by H_0 and H_1, while the global, distance-dependent probability of connection can usually be specified by an H_i with a simple form. So, while we lose the benefits of true Kronecker multiplication, we gain generality and the ability to create many different lattices and probability of long-range contacts. We note in passing that the generation of these lattice structures is not possible with the original formulation of the Kronecker graph model. For example, it is impossible to generate the Watts-Strogatz model with conventional Kronecker graphs. However, it can be done with the current generalization. This is illustrated in our examples below.

Example 1 (Original Kronecker Graph)**.** *The simplest example is that of the original Kronecker graph formulation. For this case, the "distance" can be arbitrary, and the family of matrices, $\mathcal{H}$, is simply G_1, the same G_1 used in the original definition. Thus, we define*

$$G_k = \underbrace{G_1 \otimes_d \mathcal{H} \cdots \otimes_d \mathcal{H}}_{k\ times} = \underbrace{G_1 \otimes G_1 \otimes \ldots G_1}_{k\ times}$$

Example 2 (Watts-Strogatz Small-World Model)**.** *The next example we consider, the Watts-Strogatz model, consists of a ring of n nodes, each connected to their neighbors within distance k on the ring. The probability of a connection to any other node on the ring is then $P(u,v) = p$ [133]. To generate the underlying ring structure with $k = 1$, start with an initiator matrix K_1, representing the graph in Figure 2.1(a).*

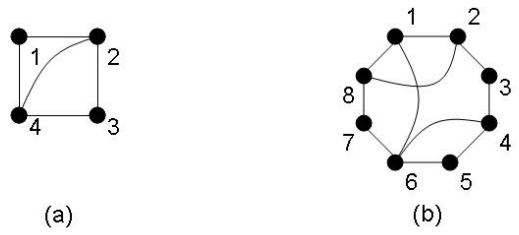

Figure 2.1: Generating the Watts-Strogatz model

In order to obtain the sequence of matrices representing the graphs in Figure 2.1, we define a "distance" measure as the number of hops from one node to another along

the ring, where clockwise hops are positive, and counter-clockwise hops are negative. Recall that the definition of "negative distance" is required only to keep the matrix symmetric. The "negative" matrix is just the transpose of the matrix defined for the "positive" direction. After each operation, the distance between nodes is still the number of hops along the ring, though the number of nodes doubles each time. We then define the following family of matrices, $\mathcal{H}$:

$$H_0 = \begin{pmatrix} 1 & 1 \\ 1 & 1 \end{pmatrix}, H_1 = \begin{pmatrix} p & p \\ 1 & p \end{pmatrix}, H_i = \begin{pmatrix} 1 & 1 \\ 1 & 1 \end{pmatrix} \ \forall i > 1$$

Note that $H_{-i} = H_i'$. So, starting from the initiator matrix in Figure 2.1(a), we have the following progression of matrices:

$$G_1 = \begin{pmatrix} 1 & 1 & p & 1 \\ 1 & 1 & 1 & p \\ p & 1 & 1 & 1 \\ 1 & p & 1 & 1 \end{pmatrix},$$

$$G_2 = G_1 \otimes_d \mathcal{H} = \begin{pmatrix} 1\times H_0 & 1\times H_1 & p\times H_2 & 1\times H_{-1} \\ 1\times H_{-1} & 1\times H_0 & 1\times H_1 & p\times H_2 \\ p\times H_2 & 1\times H_{-1} & 1\times H_0 & 1\times H_1 \\ 1\times H_1 & p\times H_2 & 1\times H_{-1} & 1\times H_0 \end{pmatrix} = \begin{pmatrix} 1 & 1 & p & p & p & p & p & 1 \\ 1 & 1 & 1 & p & p & p & p & p \\ p & 1 & 1 & 1 & p & p & p & p \\ p & p & 1 & 1 & 1 & p & p & p \\ p & p & p & 1 & 1 & 1 & p & p \\ p & p & p & p & 1 & 1 & 1 & p \\ p & p & p & p & p & 1 & 1 & 1 \\ 1 & p & p & p & p & p & 1 & 1 \end{pmatrix}$$

Note that the W-S model is not searchable by a greedy agent; however, if $P(u,v) = \frac{1}{d(u,v)}$, it becomes searchable [75], [76]. It is possible to model this $P(u,v)$ by simply adjusting $H_i, i \geq 1$ as follows:

$$H_0 = \begin{pmatrix} 1 & 1 \\ 1 & 1 \end{pmatrix}, H_i = i \begin{pmatrix} \frac{1}{2i} & \frac{1}{2i+1} \\ \frac{1}{2i-1} & \frac{1}{2i} \end{pmatrix}, \forall i \geq 1, i \neq \frac{n}{2},$$

$$H_i = i \begin{pmatrix} \frac{1}{2i} & \frac{1}{2i-1} \\ \frac{1}{2i-1} & \frac{1}{2i} \end{pmatrix}, \forall i \geq 1, i = \frac{n}{2}$$

As in the previous examples, $H_{-i} = H'_i$. The different definition for the middle node in the ring is due to the fact that we need the probability of a connection to reach a minimum at this point, and then start to rise again. With this new definition of $H_i, i \geq 1$, we have the following progression of matrices:

$$G_1 = \begin{pmatrix} 1 & 1 & 1/2 & 1 \\ 1 & 1 & 1 & 1/2 \\ 1/2 & 1 & 1 & 1 \\ 1 & 1/2 & 1 & 1 \end{pmatrix},$$

$$G_2 = G_1 \otimes_d \mathcal{H} = \begin{pmatrix} 1{\times}H_0 & 1{\times}H_1 & 1/2{\times}H_2 & 1{\times}H_{-1} \\ 1{\times}H_{-1} & 1{\times}H_0 & 1{\times}H_1 & 1/2{\times}H_2 \\ 1/2{\times}H_2 & 1{\times}H_{-1} & 1{\times}H_0 & 1{\times}H_1 \\ 1{\times}H_1 & 1/2{\times}H_2 & 1{\times}H_{-1} & 1{\times}H_0 \end{pmatrix} = \begin{pmatrix} 1 & 1 & 1/2 & 1/3 & 1/4 & 1/3 & 1/2 & 1 \\ 1 & 1 & 1 & 1/2 & 1/3 & 1/4 & 1/3 & 1/2 \\ 1/2 & 1 & 1 & 1 & 1/2 & 1/3 & 1/4 & 1/3 \\ 1/3 & 1/2 & 1 & 1 & 1 & 1/2 & 1/3 & 1/4 \\ 1/4 & 1/3 & 1/2 & 1 & 1 & 1 & 1/2 & 1/3 \\ 1/3 & 1/4 & 1/3 & 1/2 & 1 & 1 & 1 & 1/2 \\ 1/2 & 1/3 & 1/4 & 1/3 & 1/2 & 1 & 1 & 1 \\ 1 & 1/2 & 1/3 & 1/4 & 1/3 & 1/2 & 1 & 1 \end{pmatrix}$$

This example already illustrates that the generalized operator we have defined allows the generation of searchable networks, but we will provide another more realistic example in the next example.

Example 3 (Kleinberg-like Model)**.** *The final example we consider, Kleinberg's lattice model, is particularly pertinent as it was shown to be searchable [75]. In the original formulation, local connections of nodes are defined on a k-dimensional lattice, and long-range links occur between two nodes at distance d with probability proportional to $d^{-\alpha}$. We focus on a "Kleinberg-like" model here, where instead of a k-dimensional lattice, we have an "expanding hypercube" as our underlying lattice. In this example,*

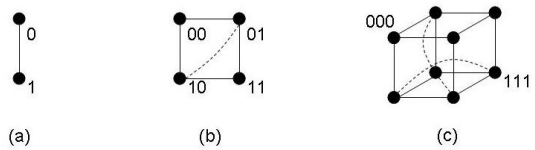

Figure 2.2: Example: the growth of an expanding hypercube

at any point, the graph is a hypercube with some extra long-range connections, and when it grows, it grows by doubling the number of nodes and adding a dimension to

the hypercube. Note that we will have n nodes arranged on a $k = \log n$*-dimensional hypercube. This example is of particular interest due to recent work suggesting that many networks have an underlying hyperbolic or tree-metric structure [38],[78]. The expanding hypercube captures the key feature of these topologies, as the number of nodes at distance d grows exponentially in d. This example is also very naturally represented using our "distance"-dependent Kronecker operation and a Hamming distance as our "distance" measure.*

To define the expanding hypercube, we define a graph G with n nodes, numbered $1...n$*, where each node is labeled with its corresponding* $\log n$*-length bit vector. We define the "distance" between two nodes as the Hamming distance between their labels. The family of matrices* $\mathcal{H}$ *is as follows:*

$$H_0 = \begin{pmatrix} 1 & 1 \\ 1 & 1 \end{pmatrix}, H_i = \begin{pmatrix} 1 & \beta_i \\ \beta_i & 1 \end{pmatrix}, \textit{for all } i \geq 1$$

where $\beta_1 =$ *a normalizing constant,* $\beta_i = \frac{P(i+1)}{P(i)}$*. The graph may or may not be searchable depending on* $P(i)$*. To mimic Kleinberg's model, we let* $P(i) = i^{-\alpha}$*, so that* $\beta_i = \left(\frac{i+1}{i}\right)^{-\alpha}$*. Thus, for the sequence of graphs shown in the figure above, we have the following sequence of matrices:*

$$G_1 = \begin{pmatrix} 1 & 1 \\ 1 & 1 \end{pmatrix}, G_2 = \begin{pmatrix} 1 & 1 & 1 & \beta_1 \\ 1 & 1 & \beta_1 & 1 \\ 1 & \beta_1 & 1 & 1 \\ \beta_1 & 1 & 1 & 1 \end{pmatrix}, G_3 = \begin{pmatrix} 1 & 1 & 1 & \beta_1 & 1 & \beta_1 & \beta_1 & \beta_1\beta_2 \\ 1 & 1 & \beta_1 & 1 & \beta_1 & 1 & \beta_1\beta_2 & \beta_1 \\ 1 & \beta_1 & 1 & 1 & \beta_1 & \beta_1\beta_2 & 1 & \beta_1 \\ \beta_1 & 1 & 1 & 1 & \beta_1\beta_2 & \beta_1 & \beta_1 & 1 \\ 1 & \beta_1 & \beta_1 & \beta_1\beta_2 & 1 & 1 & 1 & \beta_1 \\ \beta_1 & 1 & \beta_1\beta_2 & \beta_1 & 1 & 1 & \beta_1 & 1 \\ \beta_1 & \beta_1\beta_2 & 1 & \beta_1 & 1 & \beta_1 & 1 & 1 \\ \beta_1\beta_2 & \beta_1 & \beta_1 & 1 & \beta_1 & 1 & 1 & 1 \end{pmatrix}$$

From the matrix, we can tell that in each step,

$$P(u,v) = \begin{cases} 1 & \textit{if } d(u,v) = 0, 1 \\ d(u,v)^{-\alpha} & \textit{otherwise} \end{cases}$$

In the original k-dimensional lattice, a distributed algorithm (as defined in Section V), can find paths of length $O(\log n)$ *only if* $\alpha = k$ *[75]; in the modified case presented*

above, we will see in section V that we need a different probability of connection to find short paths.

2.4 Connection to hidden hyperbolic space model

As mentioned previously, the expanding hypercube model in Example 3 resembles models proposed in [5] and extended in [78], [22], and [23]. In [5], every node in the network has a hidden variable — their location in a hidden metric space. The probability of a connection between two nodes is based upon the distance between them in this hidden space. The resulting degree distribution depends on the curvature of this hidden space; if the space has negative curvature, the degree distribution will be scale-free with $P(k) = k^{-\gamma}$ [79].

In the distance-dependent Kronecker graph described in this chapter and [16], the probability of a connection is based on the distance between two nodes in the given lattice, defined usually by H_0 and H_1 in the family of matrices $\mathcal{H}$. As a result, the lattice, or metric space, is not really hidden since neighbors are explicitly connected in the lattice. It is important to note that both models incorporate a distance-dependent probability of connection. As will be defined formally in Section 2.6, a local greedy search algorithm can take advantage of this embedding into a hidden or physical space to forward a message to a destination. If a given node u has a message to forward to a destination t, it can use its knowledge of the embedding to forward the message to its neighbor closest to the destination in the embedding. It is not necessary that the embedding be physical, as shown in [78] and [22]; rather, what is necessary is that the the probability of a connection between two nodes is dependent on the distance between them. In most social networks the abstract distance is a measure of "social distance" — the likelihood of two individuals being connected depends on their memberships in various groups, among other factors.

In addition, in the models of [5], a hyperbolic space results in exponentially expanding neighborhoods around each node. In the distance-dependent hypercube example, there are $\binom{k}{d}$ nodes at each distance d, also resulting in exponentially expand-

ing neighborhoods. However, the hidden metric space model necessarily includes the notion of a core and periphery of the network, where high-degree nodes form the core connecting many low-degree nodes at the periphery [22]. In the hypercube example, all nodes are homogeneous in expected degree — there is no notion of a core.

In [78], as nodes are located further from the origin in the hidden hyperbolic space their expected degree decreases exponentially ($\propto e^{-\beta r}$). When this is combined with the exponentially expanding neighborhoods ($\propto e^{\alpha r}$), the result is a scale-free distribution with $\gamma = 1 + \frac{\alpha}{\beta}$. It is important to note that an exponential decrease in expected degree is not strictly necessary; to see this, let the number of nodes at distance r from a reference origin in the hyperbolic space be $n(r) = e^{\alpha r}$ and let the average degree of nodes at distance r be $k(r) = r^{-\delta}$, so that $r(k) = k^{-\frac{1}{\delta}}$. Using $n(k) \propto n[r(k)]\,|r'(k)|$, we have

$$n(k) \propto e^{\alpha k^{-1/\delta}} k^{-1/\delta - 1}$$

which asymptotically behaves like a power law with $\gamma = 1 + 1/\delta$. In the hypercube example, despite the exponential expansion of neighborhoods, the resulting degree distribution will always be Poisson as long as the probability of connection is sufficiently small, as shown in the next section.

Nevertheless, the connection between this model and those based on tree metrics and hidden metric spaces is important to note, as one key factor emerges: a distance-dependent relation is necessary for a greedy algorithm to succeed in finding shortest paths.

2.5 Degree distribution

In this section we describe a general characteristic function-based analysis of degree distributions for lattice-based networks, and apply it to the expanding hypercube example in Section 2.3. In general, any lattice-based network with a distance-dependent probability of connection will have a Poisson degree distribution, as long as the prob-

ability of a connection at a distance d is sufficiently small. Formally,

Theorem 2.1. *The degree distribution of a general lattice-based network with a distance-dependent probability of connection $P(d)$ and maximum distance d_{max} will have the following degree distribution:*

$$P(\nu = i) = \frac{e^{-\alpha}\alpha^i}{i!}\left(1 + d_{max}O(P^2(d))\right)$$

where

$$\alpha = \sum_{d=1}^{d_{max}} P(d)\sigma(d) \tag{2.1}$$

and $\sigma(d)$ = number of nodes at distance d from a reference node in the lattice. We note that if $\lim_{n\to\infty} d_{max}P^2(d) = 0$, then the degree distribution is Poisson.

Proof. Let ν denote the degree of an arbitrary node u in a general lattice-based network with n nodes. Thus, $\nu = v_1 + v_2 + \cdots + v_n$ where

$$v_i = \begin{cases} 1 & \text{if link to node } i, \\ 0 & \text{otherwise.} \end{cases}$$

We define the characteristic function of the degree distribution as

$$E[e^{it\nu}] = E[e^{it(v_1+v_2+\cdots+v_n)}] = E[e^{itv_1}]E[e^{itv_2}]\ldots E[e^{itv_n}]$$

We can then group the expectations

$$\begin{aligned} E[e^{it\nu}] &= \prod_{d=1}^{d_{max}} (1 - P(d) + P(d)e^{it})^{\sigma(d)} \\ &= \prod_{d=1}^{d_{max}} (1 - P(d)(1 - e^{it}))^{\sigma(d)} \\ &= \prod_{d=1}^{d_{max}} \left(e^{-P(d)(1-e^{it})} + O(P^2(d))(1 - e^{it})^2\right)^{\sigma(d)} \end{aligned} \tag{2.2}$$

as $e^{-x} = 1 - x + O(x^2)$. Thus, we can pull out the first term and using binomial

approximation of $(1+x)^c = 1 + cx + O(x^2)$, we have

$$\begin{aligned} E[e^{it\nu}] &= \prod_{d=1}^{d_{max}} e^{-P(d)(1-e^{it})\sigma(d)} \left(1 + \frac{O(P^2(d))(1-e^{it})^2\sigma(d)}{e^{-P(d)(1-e^{it})}}\right) \\ &= e^{-(1-e^{it})\sum_{d=1}^{d_{max}} P(d)\sigma(d)} \prod_{d=1}^{d_{max}} \left(1 + O(P^2(d))(1-e^{it})^2\sigma(d)e^{P(d)(1-e^{it})}\right) \\ &\approx e^{\alpha(e^{it}-1)}(1 + d_{max}O(P^2(d))) \end{aligned}$$

Expanding, we see that the characteristic function is

$$E[e^{it\nu}] = \left(1 + d_{max}O(P^2(d))\right) e^{-\alpha} \left(1 + \alpha e^{it} + \frac{(\alpha e^{it})^2}{2!} + \dots\right)$$

From such a representation of the characteristic function, we can clearly see the degree distribution as

$$P(\nu = i) = \frac{e^{-\alpha}\alpha^i}{i!}\left(1 + d_{max}O(P^2(d))\right)$$

□

We now turn to a specific lattice-based network, the hypercube distance-dependent Kronecker graph described in Example 3 in Section 2.3. In this example, $\sigma(d) = \binom{k}{d}$, and the maximum distance in the network is $k = \log n$. We use a particular $P(d) = \left[\binom{k-\frac{2d}{3}}{\frac{d}{3}} d \log k \ln 3\right]^{-1}$ optimized for searchability, as determined in Section 2.6.

Theorem 2.2. *The degree distribution of the expanding hypercube is given by the following Poisson distribution,*

$$P(\nu = i) = \frac{e^{-\alpha}\alpha^i}{i!} \text{ where } \alpha \approx \frac{3.6919\, n^{.4703}}{\log\log n\sqrt{\log n}} \tag{2.3}$$

Proof. We use the same framework as in the proof of Theorem 2.1, and let $e^{it} = x$ for simplicity. In this case, the characteristic function becomes

$$E[x^\nu] = e^{-(1-x)\sum_{d=1}^{k} P(d)\sigma(d)}$$

so that

$$\alpha = \sum_{d=1}^{k} P(d)\sigma(d) = \sum_{d=1}^{k} \left[\binom{k - \frac{2d}{3}}{\frac{d}{3}} d \log k \ln 3 \right]^{-1} \binom{k}{d}$$

To calculate α, we use the entropy approximation $\binom{k}{d} \approx 2^{kH(\frac{d}{k})}$, which holds as $\binom{n}{k} = 2^{n(H(p)+o(1))}$ when $k \propto pn$, so that

$$\alpha \approx \frac{1}{\log k \ln 3} \sum_{d=1}^{k} d^{-1} 2^{kH\left(\frac{d}{k}\right) - \left(k - \frac{2d}{3}\right) H\left(\frac{\frac{d}{3}}{k - \frac{2d}{3}}\right)}$$

We can approximate the sum by using saddle point integration.

$$\int g(y) e^{kf(y)}\, dy = \sqrt{\frac{2\pi}{k\,|f''(y_0)|}} g(y_0) e^{kf(y_0)} \left(1 + O\left(\frac{1}{\sqrt{k}}\right)\right) \tag{2.4}$$

where y_0 is the saddle point of the function $f(y)$, i.e., the point at which $f'(y) = 0$.

We rewrite the sum $S(k)$ in nats, leaving out the constants in front,

$$S(k) = \frac{1}{k} \sum_{d=1}^{k} \frac{k}{d} e^{k\left[H\left(\frac{d}{k}\right) - \left(1 - \frac{2d}{3k}\right) H\left(\frac{\frac{d}{3k}}{1 - \frac{2d}{3k}}\right)\right]}$$

and then we let $y = \frac{d}{k}$,

$$S(y) = \int_{\frac{1}{k}}^{1} \frac{1}{y} e^{k\left[H(y) - \left(1 - \frac{2}{3y}\right) H\left(\frac{\frac{y}{3}}{1 - \frac{2}{3y}}\right)\right]} dy$$

so that, with the saddle point approximation of line (4), $g(y) = \frac{1}{y}$ and $f(y) = H(y) - (1 - \frac{2}{3y}) H(\frac{\frac{y}{3}}{1 - \frac{2}{3}y})$. Using Mathematica, we find

$$\begin{aligned} y_0 &= 0.417 \\ f(y_0) &= 0.326 \\ g(y_0) &= 2.4 \\ |f''(y_0)| &= 2.2 \end{aligned}$$

yielding,

$$S(k) \approx \sqrt{\frac{2\pi}{2.2k}}(2.4)e^{0.326k} \tag{2.5}$$

So, our α is now

$$\alpha \approx \frac{1}{\log k \ln 3}\sqrt{\frac{2\pi}{2.2k}}(2.4)e^{0.326k} \approx \frac{3.6919\, n^{0.4703}}{\log\log n\sqrt{\log n}}$$

With the results of Theorem 2.1, we have a Poisson degree distribution with parameter α. □

2.5.1 Expected degree

From the characteristic function, we can also determine the expected degree.

$$E[\nu] = \frac{\partial}{\partial x}E[x^{\nu}]\bigg|_{x=1} = \frac{\partial}{\partial x}[e^{-(1-x)\alpha}]\bigg|_{x=1} = \alpha$$

Thus, the expected degree of the expanding hypercube example is a growing function of n.

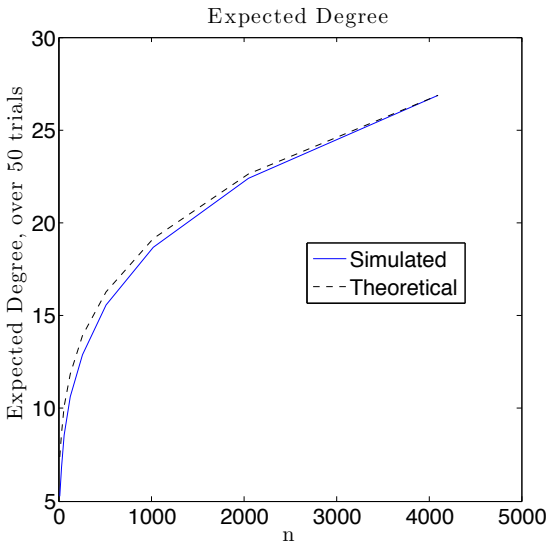

Figure 2.3: Expected degree of expanding hypercube

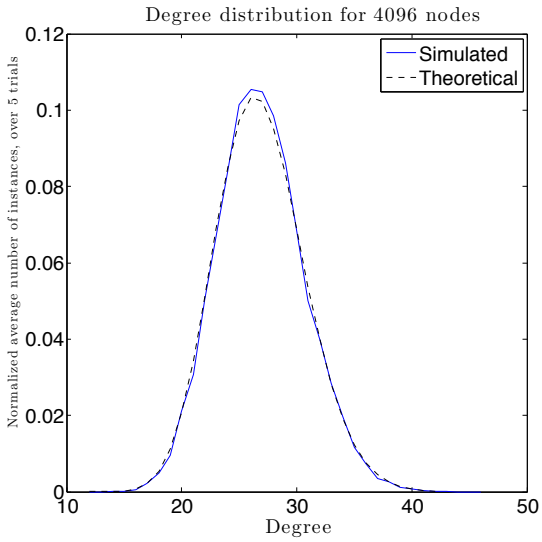

Figure 2.4: Example histogram with $n = 4096$

2.5.2 Simulation of expanding hypercube example

Simulating the expanding hypercube with the $P(d)$ determined in Section 2.6 yields results that match well, within a constant, the analysis above. Figure 2.3 shows the comparison of the theoretical and simulated expected degrees, while Figure 2.4 shows an example histogram of the degree distribution, both theoretical and simulated, with $n = 4096$. The Poisson nature of the distribution is clearly visible, as is the growth of the expected degree as a function of n.

2.6 Proving searchability

While the distance-dependent Kronecker graph model is more complicated than the original Kronecker graph model, it can capture several existing network models, and it incorporates "distance" into the probability of connection, allowing for several cases in which searchability can be proven. In this section, we first give a general framework within which a lattice-based network can be proven searchable and then proceed to the specific cases of the Kleinberg model [75] and the expanding hypercube model of Example 3 in Section 2.4.

2.6.1 General searchability theorem

We define a decentralized algorithm $\mathcal{A}$ similar to [75]. In each step, the current message-holder u passes the message to a neighbor that is closest to the destination, t. Each node only has knowledge of its address on the lattice (given by its bit vector label in the case of the expanding hypercube), the address of the destination, and the nodes that have previously come into contact with the message. For the graph to be searchable, we need to have that the distributed algorithm $\mathcal{A}$ is able to find short paths through the network, which are usually $O(D)$ where D is the diameter of the network.

Let the current message-holder be node u and the destination node t. We will say that the execution of a decentralized search algorithm $\mathcal{A}$ is in phase j when $2^j < d(u,t) \leq 2^{j+1}$, where $d(u,t)$ is the distance between node u and node t. Thus, the largest value of j in a general lattice-based network is $j_{max} = \log d_{max}$ where d_{max} denotes the maximum geodesic in the network. For example, in a hypercube, the maximum geodesic is $d_{max} = \log n = k$, so $j_{max} = \log\log n = \log k$. We define $N_{u,t}(d) = \{v : d(v,t) \leq 2^j, d(u,v) = d\}$ and $\min|N(d)| = \min_{u,t,d(u,t)=d}|N_{u,t}(d)|$.

Theorem 2.3. *A decentralized algorithm $\mathcal{A}$ will find short paths of length $O(\log^2(d_{max}))$, when the probability of a connection is*

$$P(u,v) = [c\, d \min|N(d)|]^{-1} \tag{2.6}$$

where $c \propto \log d_{max}$.

Proof. Suppose we are in phase j with current message-holder node u; we want to determine the probability that the phase ends at this step. This is equivalent to the

probability that the message enters a set of nodes B_j where $B_j = \{v : d(v,t) \leq 2^j\}$.

$$\begin{aligned}\Pr(\{\text{message enters } B_j\}) =& 1 - \prod_{v \in B_j} (1 - P(u, v : v \in B_j)) \\ =& 1 - \prod_{d=d(u,t)-2^j}^{d(u,t)+2^j} (1 - P(d))^{|N_{u,t}(d)|} \\ \geq& 1 - \prod_{d=d(u,t)-2^j}^{d(u,t)+2^j} (1 - P(d))^{\min|N(d)|}\end{aligned}$$

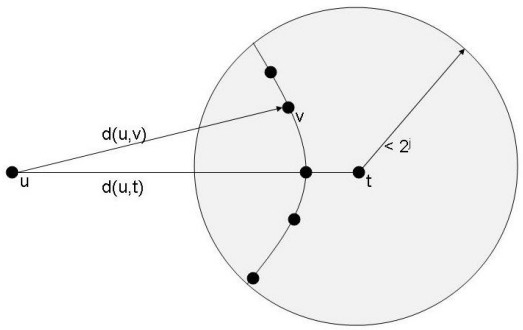

Figure 2.5: Relative positions of nodes u,v, and t in phase j

In any network model, enforcing searchability boils down to determining this $\min |N(d)|$, the minimum number of nodes at a distance d from a given node u within a ball of nodes centered around the destination, t, as illustrated in Figure 2.5. Once this $\min |N(d)|$ is found, if we set the probability of a connection between two nodes distance d apart as in Theorem 2.3, with an appropriate constant, we will find that each phase described above will end in approximately j_{max} steps, and, as there are only j_{max} such phases, our greedy forwarding algorithm will be able to find very short paths of length $O(j_{max}^2)$.

Thus, we have

$$\begin{aligned}
\Pr(\{\text{message enters } B_j\}) &\geq 1 - \prod_{d=d(u,t)-2^j}^{d(u,t)+2^j} (1-P(d))^{\min|N(d)|} \\
&\approx 1 - e^{-\sum_{d=d(u,t)-2^j}^{d(u,t)+2^j} \min|N(d)|P(d)} \qquad (2.7) \\
&= 1 - e^{-\frac{1}{c}\sum_{d=d(u,t)-2^j}^{d(u,t)+2^j} d^{-1}} \\
&\geq 1 - e^{-\frac{1}{c}\ln\frac{d(u,t)+2^j}{d(u,t)-2^j}} \\
&\geq 1 - e^{-\frac{1}{c}\ln\frac{3\,2^j}{2^j}} \\
&= 1 - e^{-\frac{1}{c'}} \\
&\geq \frac{1}{c'} \qquad (2.8)
\end{aligned}$$

where the approximation in (2.7) requires that $\lim_{n\to\infty} d_{max}P^2(d) = 0$, which holds with the $P(d)$ as specified in (2.6) (see proof of Theorem 2.1 for extra order terms), and (2.8) comes from the power series expansion of e^{-x}. Let X_j denote the total number of steps spent in phase j. Then,

$$EX_j = \sum_{i=1}^{\infty} \Pr[X_j \geq i] \leq \sum_{i=1}^{\infty} \left(1 - \frac{1}{c'}\right)^{i-1} = c'$$

Let X denote the total number of steps taken by the algorithm $\mathcal{A}$.

$$X = \sum_{j=0}^{j_{max}} X_j$$

and

$$EX = \sum_{j=0}^{j_{max}} EX_j \leq (1 + j_{max})(c') = (1 + \log d_{max}) \log d_{max} \leq \delta(\log d_{max})^2$$

where the last bound holds $\forall\, \delta \geq 2$, $\log d_{max} \geq 2$. □

With this framework, we can explore the searchability of any lattice-based network model with distance-dependent connection probability.

2.6.2 Searchability in original Kleinberg model

In the original Kleinberg two-dimensional lattice [75], the number of nodes at a distance d from a reference node is approximately $4d$, ignoring edge effects. The maximum distance between any two nodes is $O(n)$, so $j_{max} \approx \log n$. Additionally, the diameter of the graph is on the order of $\log n$. In general, $\min |N(d)| \propto d$ for a fixed j, resulting in the probability of connection optimized for searchability, $P(d) = [\alpha \log(n) d^2]^{-1}$. Using this $P(d)$,

$$\begin{aligned}
\Pr(\{\text{message enters } B_j\}) &\geq 1 - \prod_{d=d(u,t)-2^j}^{d(u,t)+2^j} (1 - P(d))^{\min|N(d)|} \\
&\approx 1 - e^{-\frac{1}{\alpha \log n} \sum_{d=d(u,t)-2^j}^{d(u,t)+2^j} d^{-1}} \qquad (2.9) \\
&\geq 1 - e^{-\frac{1}{\alpha' \log n}} \\
&\geq \frac{1}{\alpha' \log n} \qquad (2.10)
\end{aligned}$$

where (2.9) holds for the $P(d)$ specified, and (2.10) comes from the power series expansion of e^{-x}. Therefore,

$$EX_j \leq \alpha' \log n$$

and

$$EX = \sum_{j=0}^{\log n} EX_j \leq \delta (\log n)^2.$$

where the bound above holds $\forall\, \delta \geq 2$, $\log n \geq 2$.

2.6.3 Searchability in expanding hypercube example

In the expanding hypercube example of Section 2.3, each node has $\log n$ neighbors from the lattice itself. With the addition of long-range links, we expect the diameter to be $O(\log \log n)$, similar to [78]. Note that with this example, $j_{max} = \log \log n = \log k$ and the number of nodes at distance d equals $\binom{n}{d}$. Using Theorem 2.3, we can prove the following result:

Theorem 2.4. *A decentralized algorithm $\mathcal{A}$ will find paths of length $O((\log\log n)^2)$ in the expanding hypercube example when*

$$\begin{aligned}\beta_0 =&1,\ \beta_1 = [2\log k \ln 3]^{-1},\\ \beta_i =&\left[\binom{k-\frac{2i}{3}}{\frac{i}{3}} i\right]\left[\binom{k-\frac{2(i+1)}{3}}{\frac{i+1}{3}}(i+1)\right]^{-1} \quad \forall i \geq 2\end{aligned} \tag{2.11}$$

such that the probability of a connection is

$$P(u,v) = \begin{cases} 1 & \text{if } d(u,v) = 0,1 \\ \left[\binom{k-\frac{2d}{3}}{\frac{d}{3}} d\log k \ln 3\right]^{-1} & \text{if } d(u,v) = d \end{cases} \tag{2.12}$$

Proof. Using Theorem 2.3, all that remains is to find $\min|N(d)|$ and to determine the appropriate constants to use. Without loss of generality, we assume that the destination node t is the all-zero node (i.e., its label is the zero vector) so that we can write $d(u,t) = \|u\|$. To determine $\min|N(d)|$ in our case, since the distance measure is a Hamming distance, we must count the number of possible bit vectors that are at a specific distance d from a node u while still being within a certain distance of the destination. We prove that $\min|N(d)| = \binom{k-\frac{2d}{3}}{\frac{d}{3}}$ in 2.9. We then let $c = \log k \ln 3$ for reasons that will be clear below. Using the same framework as in Theorem 2.3 we have that

$$\begin{aligned}\Pr(\{\text{msg enters } B_j\}) &\geq 1 - \prod_{d=\|u\|-2^j}^{\|u\|+2^j} (1-P(d))^{\min|N(d)|} \\ &\approx 1 - e^{-\frac{1}{\log k \ln 3}\sum_{d=\|u\|-2^j}^{\|u\|+2^j} d^{-1}} \qquad (2.13)\\ &\geq 1 - e^{-\frac{1}{\log k}} \\ &\geq \frac{1}{\log k} \qquad (2.14)\end{aligned}$$

where (2.13) holds for the $P(d)$ specified, and (2.14) comes from the power series

expansion of e^{-x}. Therefore, we have

$$EX_j \leq \log k$$

and

$$EX = \sum_{j=0}^{\log k} EX_j \leq \delta(\log k)^2, \; \forall\, \delta \geq 2, \; \log k \geq 2$$

Since the expected number of steps in phase j is $\log k$, and there are at most $\log k$ phases, the expected amount of steps taken by the algorithm $\mathcal{A}$ is at most $\delta \log^2 k$. So, with this definition of $P(d)$, the distributed algorithm provides searchability. $\square$

2.6.4 Simulation of distributed search algorithm

We simulated the local greedy algorithm described above in MATLAB for $16 \leq n \leq 4096$ with the probability distribution as in Theorem 2.4 and appropriate floor functions. We found that the greedy algorithm finds a path between two nodes with an average length of a constant factor away from the diameter of the simulated network, where diameter is defined as the maximum geodesic in the network. Note that the two nodes selected for the simulation are actually the "worst-case" nodes - the distance between them in the network is exactly the diameter. Figure 2.6 illustrates the results of the greedy algorithm simulations.

2.6.5 Path length with suboptimal P(d)

In this section we analyze the performance of the local greedy search algorithm on the expanding hypercube when $P(d)$ is not optimal, as in Theorem 2.4. For this example, let $P(d) = [\log k \binom{k}{d}]^{-1}$, which is clearly not $\min |N(d)|$ from Lemma 2.5. We will show that this suboptimal $P(d)$ also allows for searchability.

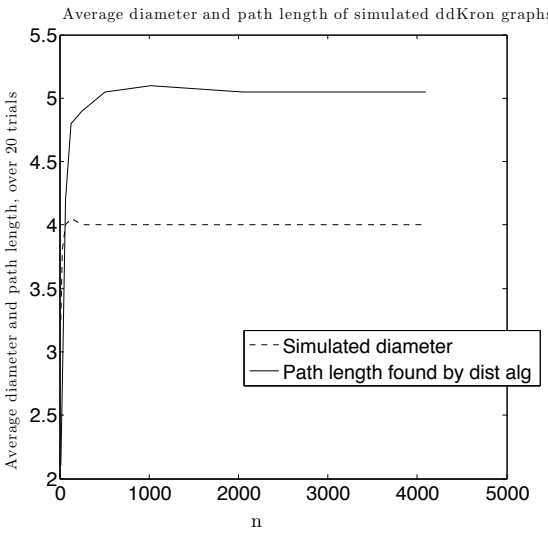

Figure 2.6: Average path length found by greedy algorithm using local information

Using the same framework as in Theorem 2.3,

$$\begin{aligned}
\Pr(\{\text{msg enters } B_j\}) &\geq 1 - \prod_{d=d(u,t)-2^j}^{d(u,t)+2^j} (1-P(d))^{\min|N(d)|} \\
&\approx 1 - e^{\sum_{d=d(u,t)-2^j}^{d(u,t)+2^j} P(d)\min|N(d)|} \qquad (2.15) \\
&= 1 - e^{-\sum_{d=d(u,t)-2^j}^{d(u,t)+2^j} P(d)\binom{k-\frac{2d}{3}}{\frac{d}{3}}} \\
&= 1 - e^{-\frac{1}{\log k}S(k,d)} \\
&\geq 1 - e^{-\frac{1}{\log k}\min S(k,d)}
\end{aligned}$$

where line (2.15) holds for the specified $P(d)$ and where

$$\begin{aligned}
S(k,d) &= \sum_{d=2^j}^{3*2^j} \binom{k}{d}^{-1} \binom{k-\frac{2d}{3}}{\frac{d}{3}} \\
&\approx \sum_{d=2^j}^{3*2^j} 2^{(k-\frac{2d}{3})H(\frac{\frac{d}{3}}{k-\frac{2d}{3}})-kH(\frac{d}{k})} \qquad (2.16) \\
&\geq \min_d \sum_{d=2^j}^{3*2^j} 2^{(k-\frac{2d}{3})H(\frac{\frac{d}{3}}{k-\frac{2d}{3}})-kH(\frac{d}{k})} \\
&\geq 2^{\max_d (k-\frac{2d}{3})H(\frac{\frac{d}{3}}{k-\frac{2d}{3}})-kH(\frac{d}{k})}
\end{aligned}$$

where we have used the approximation $\binom{k}{d} \approx 2^{kH(\frac{d}{k})}$, which holds as $\binom{n}{k} = 2^{n(H(p)+o(1))}$ when $k \propto pn$, in line (2.16). Since the exponent is convex in d, the maximum will be at either the upper or lower bound of the sum. For $0 \leq j \leq \log k$ the lower bound ($d = 2^j$) yields the maximal exponent. So, we have

$$\Pr(\{\text{msg enters } B_j\}) \geq 1 - e^{-\frac{1}{\log k} 2^{f(k,j)}} \geq \frac{2^{f(k,j)}}{\log k}$$

where we have used the power series expansion of e^{-x} and where

$$f(k,j) = (k - \frac{2^{j+1}}{3}) H(\frac{\frac{2^j}{3}}{k - \frac{2^{j+1}}{3}}) - kH(\frac{2^j}{k}). \tag{2.17}$$

Continuing with the proof of searchability, we have

$$EX_j = \sum_{i=1}^{\infty} \Pr[X_j \geq i] \leq \log k \, 2^{-f(k,j)}$$

and

$$EX = \sum_{j=0}^{\log k} EX_j \leq (1 + \log k) \log k \, 2^{-\min_j f(k,j)} \leq \delta (\log k)^2, \; \forall \, \delta \geq 2, \; \log k \geq 2$$

since $f(k,j)$ is convex but its minimum occurs close to $\log k$. As a result, even for suboptimal $P(d)$, a local greedy algorithm can find short paths. However, the bounds used in the analysis above are looser than those in previous sections, so the final expected number of steps taken by $\mathcal{A}$ is not as tight. This analysis is supported by simulation results as shown in the figure below. Finally, if $P(d) = [d \log k \binom{k}{d}]^{-1}$, using the same sort of techniques as above we can show that $EX \leq \delta k (\log k)^2$ for a large enough δ. Note that in this case, the paths found will be $O(\log n \log \log n)$, which are longer than before. Simulation results with this $P(d)$ are shown in Figure 2.8.

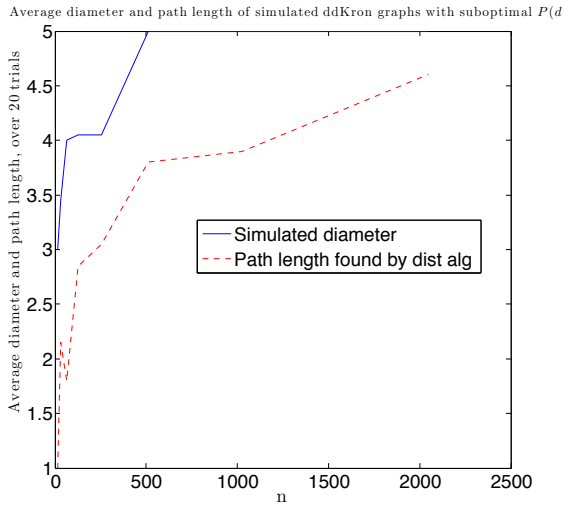

Figure 2.7: Performance of greedy algorithm when $P(d) = [\log k\binom{k}{d}]^{-1}$

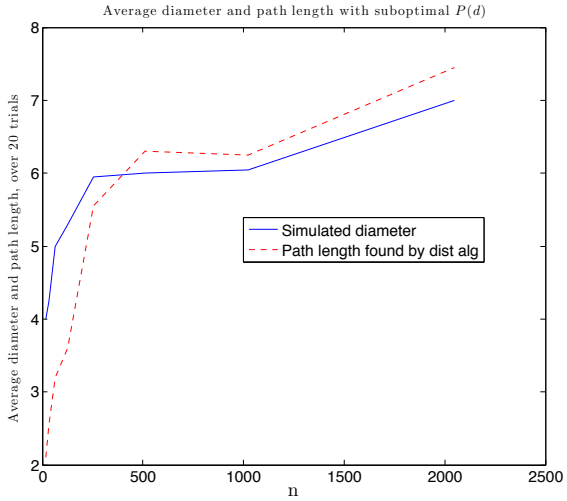

Figure 2.8: Performance of greedy algorithm when $P(d) = [d \log k\binom{k}{d}]^{-1}$

2.7 Brief diameter analysis of hypercube

In this section, we briefly discuss the diameter of a general random graph. Finding the actual diameter, defined as either the maximum or the average geodesic in the network, can be very complicated. We discuss a simple lower bound of the hypercube example here, which can be applied to any random graph.

If we assume that the expected degree of the hypercube example in Section 2.3 is

polynomial in n, say n^β, similar to what was found in Section 2.4 for the expanding hypercube, we can lower bound the diameter as follows. We assume that at each step, every node has d neighbors and that it takes α steps to reach all n nodes. Therefore, to reach all n nodes in the network, we have

$$d^\alpha = n \Rightarrow (n^\beta)^\alpha = n \Rightarrow \alpha = \frac{1}{\beta} \Rightarrow \text{Constant diameter}$$

Thus, a simple lower bound for the diameter of a graph with polynomial expected degree is some constant, $\frac{1}{\beta}$. We can also work backwards, assuming a $\log\log n$ diameter. In this case, we have

$$d^\alpha = n \Rightarrow d^{\log\log n} = n \Rightarrow d = n^{\frac{1}{\log\log n}} = e^{\frac{\log n}{\log\log n}}$$

which is less than a polynomial in n, but still grows with n. Figure 2.9 compares the simulated diameter of the expanding hypercube example with the two lower bounds discussed above. For $16 \leq n \leq 4096$, both lower bounds appear to be a good match.

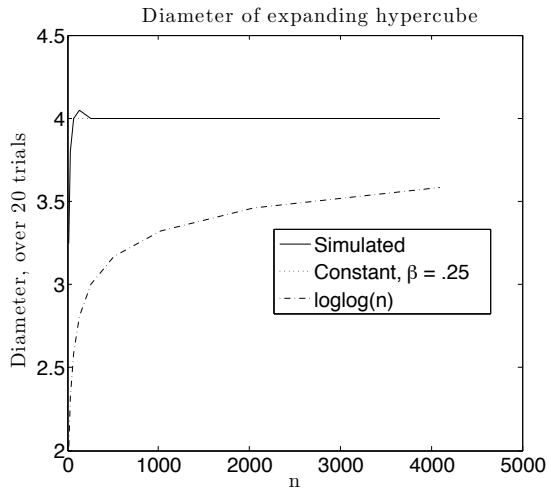

Figure 2.9: Simulated and theoretical diameter of expanding hypercube

2.8 Conclusion

We have presented a generalization of Kronecker graphs by defining a family of "distance"-dependent matrices and a new Kronecker-like operation. As a result, the network model defines both local regular structures and global distance-dependent connections. Though the model is more complicated than the original Kronecker graph model, it is more general, as it can generate existing social network models, and more importantly, networks that are searchable. These properties emerge naturally from the definition of the embedding of the nodes and the probability of connection within the family of matrices $\mathcal{H}$. Any lattice-based network model with distance-dependent connection probabilities can be analyzed using the framework described in Sections 2.5, 2.6, and 2.7 for exploring degree distribution, diameter, and searchability. Most importantly, the searchability analysis shows how to make any network model searchable by defining the appropriate probability of connection based upon $|N(d)|$. The particular expanding hypercube example explicitly described here shares characteristics with those based upon hidden hyperbolic spaces [5], [78], though it has one major difference — degree homogeneity across nodes. Nevertheless, its exponentially expanding neighborhoods and distance-dependent probability of connection make it a good model for social networks as people tend to exhibit strong homophily, i.e., associating with other people most like themselves. In addition, in contrast to Kleinberg's lattice-based model [75], the searchability of the expanding hypercube is not too sensitive to the choice of $P(d)$.

Though this chapter gives a near complete description of the characteristics of "distance"-dependent Kronecker graphs, there are many interesting questions that remain. These include how to parameterize the model from real-world data sets, and how to incorporate network dynamics. Ideally, given any data set, we would like to be able to find an appropriate family of distance-dependent matrices to match any desired characteristic of the data set. Additionally, while the current model incorporates some measure of growth, growing from a small initiator matrix to a final nxn adjacency matrix, we would like to better incorporate mobility into the model

so that it is not just a static description of the network at one point in time.

2.9 Appendix: Calculating the size of $N_{u,t}(d)$

In this section, we show a lower bound for $|N_{u,t}(d)|$, the number of nodes at distance d from a given node u, still within distance 2^j of the destination, t.

Lemma 2.5. $\min |N_{u,t}(d)| = \binom{k-\frac{2d}{3}}{\frac{d}{3}}$

Proof. We first count exactly the number of nodes in $N_{u,t}(d)$, the number of nodes at a distance d from a given node u within a ball of nodes centered around the destination, t, as illustrated in Figure 2.5. Without loss of generality, define t as the all-zero node, $t = (00...0)$. Arrange the label of u such that $u = (1 \ldots 1\, 0 \ldots 0)$. Define $v = (v_{11}\ v_{10}\ v_{01}\ v_{00})$ according to this partition of u, so that v_{11} and v_{01} have "1" entries and v_{10} and v_{00} have "0" entries. Let $\|x\|$ denote the weight, or number of ones, of the label of node x. We know the following:

$$\begin{aligned} v_{11} + v_{10} + v_{01} + v_{00} &= k \\ v_{11} + v_{10} &= \|u\| \\ v_{01} + v_{10} &= d \\ v_{11} + v_{01} &= \|v\| \end{aligned}$$

We can solve in terms of v_{11}, yielding

$$\begin{aligned} v_{00} &= k - d - v_{11} \\ v_{10} &= \|u\| - v_{11} \\ v_{01} &= d - \|u\| + v_{11} \end{aligned}$$

We also know that we must satisfy the following:

$$\begin{aligned} v_{11}, v_{10}, v_{01}, v_{00} &\geq 0 \\ 2^j < \|u\| &\leq 2^{j+1} \\ \|u\| - 2^j \leq d &\leq \|u\| + 2^j \\ \|v\| &\leq 2^j \end{aligned}$$

From these bounds we have

$$\max(0, \|u\| - d) \leq v_{11} \leq \min(\|u\|, k - d, \frac{1}{2}(2^j + \|u\| - d))$$

Note that the second and third bounds do not affect v_{11}. Counting the number of nodes in the ball, we have

$$|N_{u,t}(d)| = \sum_{v_{11}=v_l}^{v_u} \binom{\|u\|}{v_{11}} \binom{k - \|u\|}{d - \|u\| + v_{11}}$$

where we have substituted v_u and v_l, for the upper and lower bounds above, respectively. We can now approximate the number of nodes in $N_{u,t}(d)$, using the entropy approximation for combinations. Let $\|u\| = ak, d = bk, 2^j = ck, x = v_{11}$. Using this notation, we have

$$\begin{aligned} |N_{u,t}(d)| =& \sum_{x=v_l}^{v_u} \binom{ak}{x} \binom{k(1-a)}{k(1-b)+x} \\ \approx& \sum_{x=v_l}^{v_u} 2^{k(aH\left(\frac{x}{ak}\right)+(1-a)H\left(\frac{b-a+\frac{x}{k}}{1-a}\right))} \\ \geq& 2^{k\mathcal{X}} \end{aligned} \tag{2.18}$$

where

$$\mathcal{X} = \max_x aH\left(\frac{x}{ak}\right) + (1-a)H\left(\frac{b-a+\frac{x}{k}}{1-a}\right) \tag{2.19}$$

subject to

$$k\max(0, a-b) \leq x \leq k\min(a, 1-b, \frac{1}{2}(a-b+c))$$

Note that (2.18) is true as $\binom{n}{k} = 2^{n(H(p)+o(1))}$ when $k \propto pn$.

Note that the function $\mathcal{X}$ is concave in x, so unconstrained optimization yields the two solutions below, each giving different values of $\min|N_{u,t}(d)|$:

$$x_1^* = ak - abk \text{ when } c \geq a + b(1-2a), \text{ yielding } \min|N_{u,t}(d)| = \binom{k}{d}$$

$$x_2^* = \frac{1}{2}k(a-b+c) \text{ when } c < a + b(1-2a), \text{ yielding } \min|N_{u,t}(d)| = \binom{k - \frac{2d}{3}}{\frac{d}{3}}$$

The resulting $\min|N_{u,t}(d)|$ are derived in Sections 2.9.1 and 2.9.2. As the second solution yields a smaller $\min|N_{u,t}(d)|$, we have an overall $\min|N_{u,t}(d)| = \binom{k-\frac{2d}{3}}{\frac{d}{3}}$. □

2.9.1 Solution 1: $c \geq a + b(1-2a)$

In this region, the solution to the unconstrained problem, $x_1^* = ak - abk$ gives us the maximal $\mathcal{X}$. Substituting in for the size of $N_{u,t}(d)$ and using the same entropy approximation as before, we have

$$\begin{aligned}|N_{u,t}(d)| &= 2^{k(aH\left(\frac{ak-abk}{ak}\right)+(1-a)H\left(\frac{b-a+\frac{ak-abk}{k}}{1-a}\right))} \\ &= 2^{k(aH(1-b)+(1-a)H(b))} = 2^{kH(b)} \approx \binom{k}{bk} = \binom{k}{d}.\end{aligned}$$

2.9.2 Solution 2: $c < a + b(1-2a)$

In this region, we choose one of the boundary points, $x_2^* = \frac{1}{2}k(a-b+c)$, as the solution to the maximization problem. Substituting this solution for x in $|N_{u,t}(d)|$, we obtain

$$|N_{u,t}(d)| = 2^{k(aH\left(\frac{a-b+c}{2a}\right)+(1-a)H\left(\frac{-a+b+c}{2(1-a)}\right))}$$

This gives us a function of a, b, c, so we want to find the worst case a, c that minimizes $|N_{u,t}(d)|$. The new optimization problem is thus

$$\begin{aligned} f(b) &= \min |N_{u,t}(d)| \\ &= \min_{a,c} aH\left(\frac{a-b+c}{2a}\right) + (1-a)H\left(\frac{-a+b+c}{2(1-a)}\right) \end{aligned} \tag{2.20}$$

Note that the bounds for this region are:

1. $a - b - c \leq 0$
2. $a - b + c \geq 0$
3. $c < a \leq 2c$
4. $0 \leq c \leq \frac{1}{2}$
5. $0 \leq a, b \leq 1$
6. $0 \leq 2 - a - b - c$
7. $0 \leq a + b - c$
8. $0 \leq a + b - c - 2ab$

where 1 and 2 come from the bounds on $d(u, v)$, 3 comes from the bounds on $\|u\|$, and 4 and 5 come from the ranges for j and the size of the network. Note that 1–5 are always true, not just in this region. 6, 7, and 8 come from the fact that our solution x_2^* is minimal in this region. Note that 8 implies 7.

Computing the Hessian of the function in (2.20) shows that it is concave in both a and b; the derivation is in 2.9.3. Since our function is concave, the $\min |N_{u,t}(d)|$ is found from the boundary points of Region 2. Rearranging the bounds from before in terms of a we have:

1. $a \leq b + c$
2. $a \geq b - c$

3. $a > c, a \leq 2c$

4. $c > 0, c \leq \frac{1}{2}$

5. $0 \leq a, a \leq 1$

6. $a \leq 2 - b - c$

7. $a \geq -b + c$

8. $a \geq \frac{c}{1-2b} - \frac{b}{1-2b}$ when $b \leq \frac{1}{2}$

9. $a \leq \frac{c}{1-2b} - \frac{b}{1-2b}$ when $b > \frac{1}{2}$

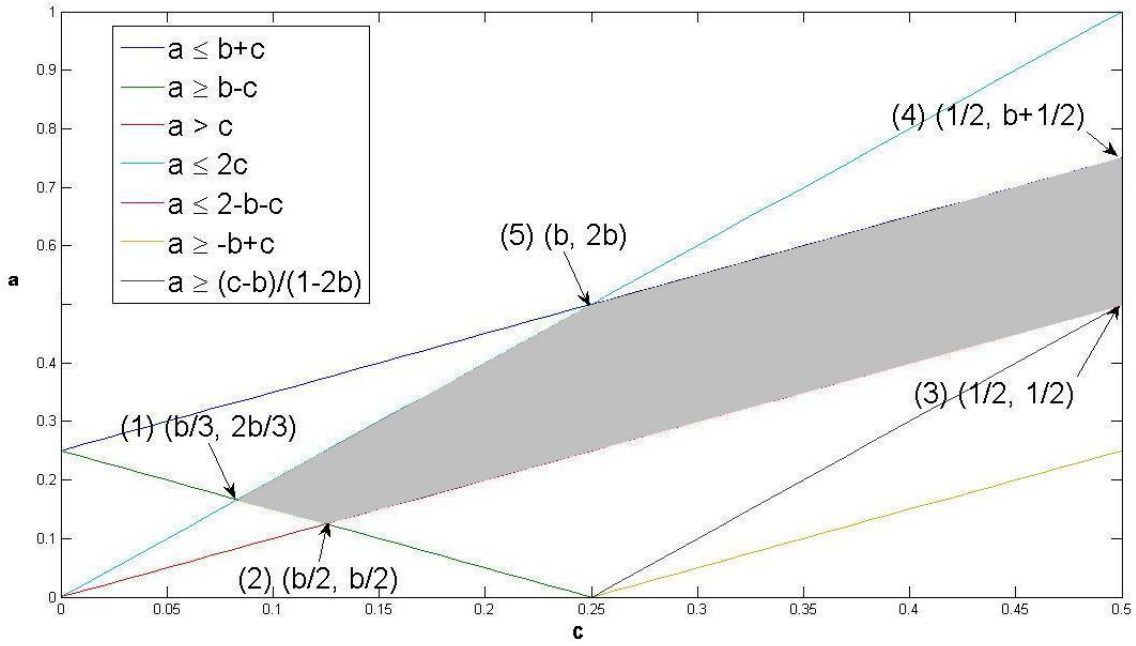

Figure 2.10: Boundaries of $f(b)$ when $b \leq \frac{1}{2}$

When $b \leq \frac{1}{2}$, only bounds (1,2,3,4) apply to $f(b)$, yielding 5 points that we need to examine, as shown in Figure 2.10. If $b \geq .115$, then $f(b)$ is minimal at point (1),

$(\frac{b}{3}, \frac{2b}{3})$, yielding

$$\begin{aligned} \min |N_{u,t}(d)| &= 2^{k(1-\frac{2b}{3})H\left(\frac{\frac{b}{3}}{1-\frac{2b}{3}}\right)} \\ &\approx \binom{k-\frac{2bk}{3}}{\frac{bk}{3}} \\ &= \binom{k-\frac{2d}{3}}{\frac{d}{3}} \end{aligned} \tag{2.21}$$

where (2.21) holds for large k, using the entropy approximation $\binom{n}{k} = 2^{n(H(p)+o(1))}$. If $b < 0.115$, then $f(b)$ is minimal at point (5), $(b, 2b)$, yielding

$$\min |N_{u,t}(d)| = 2^{k2b} = 4^d$$

When $b > \frac{1}{2}$, only bounds (2,3,4,and 8) apply to $f(b)$, yielding 4 points that we need to examine, as shown in Figure 2.11.

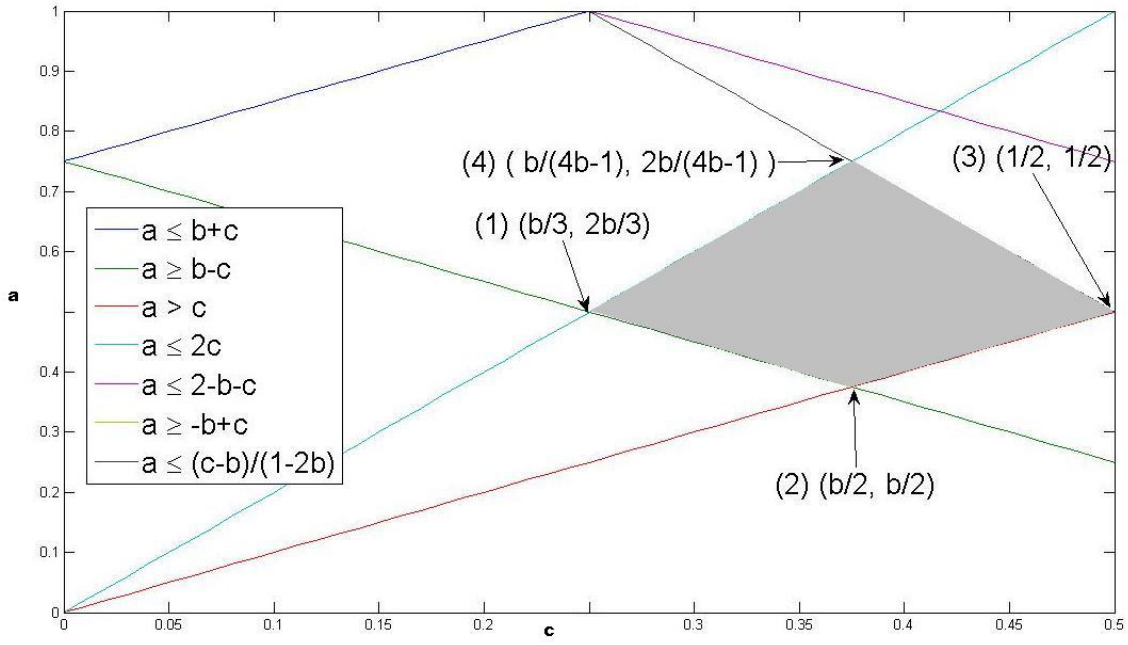

Figure 2.11: Boundaries of $f(b)$ when $b \geq \frac{1}{2}$

For this region, $f(b)$ is minimal at point (1), matching point (5) in the previous region, yielding

$$\begin{aligned}\min|N_{u,t}(d)| &= 2^{k(1-\frac{2b}{3})H\left(\frac{\frac{b}{3}}{1-\frac{2b}{3}}\right)} \\ &\approx \binom{k-\frac{2d}{3}}{\frac{d}{3}} \end{aligned} \tag{2.22}$$

where (2.22) holds for large k, using the entropy approximation $\binom{n}{k} = 2^{n(H(p)+o(1))}$. Thus, when $b < 0.115$, we have $\min|N_{u,t}(d)| = 4^d$, and when $b \geq 0.115$, we have $\min|N_{u,t}(d)| = \binom{k-\frac{2d}{3}}{\frac{d}{3}}$. Finally, we have that when $c < a + b(1-2a)$, we apply Solution 2, and we have $\min|N_{u,t}(d)| = \binom{k-\frac{2d}{3}}{\frac{d}{3}}$ when Solution 2 is valid. Comparing the Solution 1 with Solution 2, we have again that $\min|N_{u,t}(d)| = \binom{k-\frac{2d}{3}}{\frac{d}{3}}$.

2.9.3 Concavity of $f(a,b,c)$ for Solution 2

Lemma 2.6. *The function* $f(a,b,c) = aH\left(\frac{a-b+c}{2a}\right) + (1-a)H\left(\frac{-a+b+c}{2(1-a)}\right)$ *is concave in both* a *and* b.

Proof. To prove that the function is concave in both a and b, we need to see if the Hessian is negative definite. Let

$$f(a,b,c) = aH\left(\frac{a-b+c}{2a}\right) + (1-a)H\left(\frac{-a+b+c}{2(1-a)}\right)$$

Taking derivatives with respect to a, we find

$$\frac{\partial f}{\partial a} = \frac{1}{2}\left(-\log\frac{c+a-b}{2a} - \log\frac{b+a-c}{2a} + \log\frac{c-a+b}{2(1-a)} + \log\frac{2-a-b-c}{2(1-a)}\right)$$

and

$$\begin{aligned}\frac{\partial^2 f}{\partial a^2} &= \frac{-(c-b)^2}{a(c+a-b)(b+a-c)} + \frac{-(1-c-b)^2}{(1-a)(c-a+b)(2-a-b-c)} \\ &= \frac{1}{2}\left(\frac{-1}{a-b+c} + \frac{-1}{a+b-c} + \frac{2}{a} + \frac{-1}{-a+b+c} + \frac{-1}{2-a-b-c} + \frac{2}{1-a}\right)\end{aligned}$$

From the bounds for this region, we can see that the function is concave in a. Taking derivatives with respect to c, we find

$$\frac{\partial f}{\partial c} = \frac{1}{2}\left(-\log\left(c+a-b\right)+\log\left(a+b-c\right)-\log\left(c-a+b\right)+\log\left(2-a-b-c\right)\right)$$

and

$$\frac{\partial^2 f}{\partial c^2} = \frac{1}{2}\left(\frac{-1}{c+a-b}+\frac{-1}{a+b-c}+\frac{-1}{c-a+b}+\frac{-1}{2-a-b-c}\right)$$

From the bounds in this region, we can see that the function is concave in c. Taking derivatives with respect to both a and c, we find

$$\frac{\partial^2 f}{\partial c \partial a} = \frac{1}{2}\left(\frac{-1}{a-b+c}+\frac{1}{a+b-c}+\frac{1}{-a+b+c}+\frac{-1}{2-a-b-c}\right)$$

The Hessian H is

$$\begin{pmatrix} \frac{\partial^2}{\partial a^2} & \frac{\partial^2}{\partial a \partial c} \\ \frac{\partial^2}{\partial a \partial c} & \frac{\partial^2}{\partial c^2} \end{pmatrix}$$

We want to show that the Hessian is negative definite, i.e, that $H < 0$. We have already shown that $\frac{\partial^2}{\partial a^2} < 0$, so it remains to show that the second leading principal minor of H is positive definite. This is just the determinant of H

$$det[H] = \frac{\partial^2}{\partial a^2}\frac{\partial^2}{\partial c^2} - \left(\frac{\partial^2}{\partial a \partial c}\right)^2 > 0$$

We rewrite the second derivatives as

$$\begin{aligned}
\frac{\partial^2}{\partial a^2} &= \frac{1}{2}\left(f_1 + f_2 + \frac{2}{a} + \frac{2}{1-a}\right) \\
\frac{\partial^2}{\partial c^2} &= \frac{1}{2}\left(f_1 + f_2\right) \\
\frac{\partial^2}{\partial a \partial c} &= \frac{1}{2}\left(f_1 - f_2\right)
\end{aligned}$$

where, from above,

$$\begin{aligned} f_1 =& \frac{-1}{a-b+c} + \frac{-1}{2-a-b-c} < 0 \\ f_2 =& \frac{-1}{a+b-c} + \frac{-1}{-a+b+c} < 0 \end{aligned}$$

So, our determinant is now

$$\begin{aligned} det[H] &= \left(f_1 + f_2 + \frac{2}{a} + \frac{2}{1-a} \right) (f_1 + f_2) - (f_1 - f_2)^2 \\ &= \frac{1}{4}(f_1 + f_2)^2 + \frac{1}{4} \left(\frac{2}{a} + \frac{2}{1-a} \right) (f_1 + f_2) - \frac{1}{4}(f_1 - f_2)^2 \\ &= f_1 f_2 + \frac{(f_1 + f_2)}{2a(1-a)} \end{aligned}$$

Simplifying, this is just

$$det[H] = -(-a-b+c+2ab)^2[(a-b+c)(-2+a+b+c)(a+b-c)(a-b-c)a(a-1)]^{-1}$$

which, from our bounds, is positive. Since the determinant of H is positive, and since $\frac{\partial^2}{\partial a^2}$ is negative, we can say that H is negative definite, and the function is concave in both a and c. □

Chapter 3

Matching

3.1 Introduction

Many-to-one matching markets exist in numerous different forms, such as college admissions, matching medical interns to hospitals for residencies, assigning housing to college students, and the classic firms and workers market. These markets are widely studied in academia and also widely deployed in practice, and have been applied to other areas, such as FCC spectrum allocation and supply chain networks [9, 98]

In the conventional formulation, matching markets consist of two sets of agents, such as medical interns and hospitals, each of which have preferences over the agents to which they are matched. In such settings it is important that matchings are 'stable' in the sense that agents do not have incentive to change assignments after being matched. The seminal paper on matching markets was by Gale and Shapley [54], and following this work an enormous literature has grown, e.g., [77, 114, 115, 116] and the references therein. Further, variations on Gale and Shapley's original algorithm for finding a stable matching are in use today by the National Resident Matching Program (NRMP), which matches medical school graduates to residency positions at hospitals [113].

However, as often happens when translating theory to reality, problems arise when implementing the matching algorithms in the real world. For example, couples participating in the NRMP would often reject their matches and search outside the system,

so much so that eventually a separate couples matching market was set up to fix the problem. In housing assignment markets where college students are asked to list their preferences over housing options, there is often collusion among friends to list the same preference order for houses, in an attempt to be matched together. These two examples highlight that 'peer effects', whether just between two people or a more general set of friends, often play a significant role in many-to-one matchings. That is, agents care not only where they are matched, but also which other agents are matched to the same place. Similarly, 'complementarities' often play a role on the other side of the market. For example, hospitals and colleges care not only about which individual students are assigned to them, but also that the group has a certain diversity, e.g., of specializations, gender, etc.

As a result of the issues highlighted above, there is a growing literature studying many-to-one matchings with externalities (i.e., peer effects and complementarities) [43, 58, 73, 74, 106, 110, 8, 44, 120] and the research has found that designing matching mechanisms is significantly more challenging when externalities are considered, e.g. incentive compatible mechanism design is no longer possible. In fact, even determining the existence of stable matchings in the presence of externalities has been difficult.

The reason for the difficulty is that there is no longer a guarantee that a stable many-to-one matching will exist when agents care about more than their own matching [113, 115], and, if a stable matching does exist, it can be computationally difficult to find [112]. Consequently, most research has focused on identifying when stable matchings do and do not exist. Papers have proceeded by constraining the matching problem through restrictions of the possible preference orderings, [43, 58, 73, 74, 106, 110], and by considered variations on the standard notion of stability [8, 44, 120]. Our work also considers a modification of the model, described in the following.

The key idea is that *peer effects are often the result of an underlying social network*. That is, when agents care about where other agents are matched, it is often because they are friends. With this in mind, we construct a model in Section 3.2 that includes

a weighted, undirected social network graph and allows agents to have utility functions (which implicitly define their preference ordering) that depend on where neighbors in the graph are assigned. The model is motivated by [8], which also considers peer effects defined by a social network but focuses on one-sided matching markets rather than two-sided matching markets.

We focus on *two-sided exchange stable* matchings — see Section 3.2 for a detailed definition and a discussion for how this definition of stability differs from the traditional one in [54]. We note that this is a distinct notion of stability, but one that is relevant to many situations where agents can compare notes with each other, such as the housing assignment or medical matching problem. For example, in [8, 9, 50], "pairwise-stability" is considered since they consider models where agents exchange offices or licenses in FCC spectrum auctions. Further, consider a situation where two hospital interns prefer to exchange the hospitals allocated to them by the NRMP. If this is a traditional stable matching, the hospitals would not allow the swap, even though the interns are highly unsatisfied with the match. Such a situation has been documented in [66], and has led to a similar type of stability, exchange stability, as defined in [2, 30, 31, 66]. Our definition of stability incorporates both sides of the market, but considers only pairwise exchanges of agents.

Given our model of peer effects, the focus of the chapter is then on characterizing the set of two-sided exchange stable matchings. Our results concern (i) the existence of two-sided exchange stable matchings, (ii) algorithms for finding two-sided exchange stable matchings, and (iii) the efficiency of exchange stable matchings (in terms of social welfare).

With respect to the existence of stable matchings (Section 3.3), it is not difficult to show using a potential function argument that in our model two-sided exchange stable matchings always exist. Further, if students value houses according to the same rules, the matching that maximizes social welfare is guaranteed to be two-sided exchange stable. In fact, in this special case, the potential function of the game is exactly the social welfare function. Given the contrast to the negative results that are common for many-to-one matchings, e.g., [44, 112, 113], these results are perhaps

surprising. Upon closer examination, it becomes clear that the key ingredient for the existence of stable matchings is network symmetry — the social network must be undirected, as is required for many of the existence results in hedonic coalition formation [7, 21, 28], a related market.

Further, due to the similarity of the potential and social welfare functions, the results on characterizing the existence of stable matchings naturally suggest two simple algorithms for finding stable matchings, which we discuss in Section 3.4. To measure the performance of these algorithms, we look at two sample social networks: (1) a real-world social network among undergraduate students at the California Institute of Technology and (2) an on-line social network generated from voting patterns of Wikipedia members.

With respect to the efficiency of exchange stable matchings (Section 3.5), results are not as easy to obtain. In this context, we limit our focus to one-sided matching markets, but as a result we are able to attain bounds on the ratio of the welfare of the optimal matching to that of the worst stable matching, i.e., the 'price of anarchy'. In certain cases, we can show that the ratio of the welfare of the optimal matching to that of the best stable matching, i.e., the 'price of stability' is one. We can further show that the bound on the price of anarchy is tight. When considering only one-sided markets, our model becomes similar to hedonic coalition formation, but with several key differences, as highlighted in Section 3.5. Our results (Theorems 3.5 and 3.6) show that the price of anarchy does not depend on the number of, say, interns, but does grow with the number of, say, hospitals — though the growth is typically sublinear. Further, we observe that the impact of the structure of the social network on the price of anarchy happens only through the clustering of the network, which is well understood in the context of social networks, e.g., [67, 131]. Finally, it turns out that the price of anarchy has a dual interpretation in our context; in addition to providing a bound on the inefficiency caused by enforcing exchange stability, it turns out to also provide a bound on the loss of efficiency due to peer effects.

3.2 Model and notation

To begin, we define the model we use to study many-to-one matchings with peer effects and complementarities. There are four components to the model, which we describe in turn: (i) basic notation for discussing matchings; (ii) the model for agent utilities, which captures both peer effects and complementarities; (iii) the notion of stability we consider; and (iv) the notion of social welfare we consider.

To provide a consistent language for discussing many-to-one matchings, throughout this chapter we use the setting of matching incoming undergraduate students to residential houses. In this setting many students are matched to each house, and the students have preferences over the houses, but also have peer effects as a result of wanting to be matched to the same house as their friends. Similarly, the houses have preferences over the students, but there are additional complementarities due to goals such as maintaining diversity. It is clear that some form of stability is a key goal of this "housing assignment" problem.

Notation for many-to-one matchings. Using the language of the housing assignment problem, we define two finite and disjoint sets, $H = \{h_1, \ldots, h_m\}$ and $S = \{s_1, \ldots, s_n\}$ denoting the houses and students, respectively. For each house, there exists a positive integer *quota* q_h which indicates the number of positions a house has to offer. The quota for each house may be different.

A matching μ describes the assignment of students to houses such that students are matched to only one house, while houses are matched to multiple students. More formally:

Definition 2. *A* matching *is a subset* $\mu \subseteq S \times H$ *such that* $|\mu(s)| = 1$ *and* $|\mu(h)| = q_h$*, where* $\mu(s) = \{h \in H : (s,h) \in \mu\}$ *and* $\mu(h) = \{s \in S : (s,h) \in \mu\}$.[1]

Note that we use $\mu^2(s)$ to denote the set of student s's housemates (students also in house $\mu(s)$).

[1] If the number of students in $\mu(h)$, say r, is less than q_h, then $\mu(h)$ contains $q_h - r$ "holes" — represented as students with no friends and no preference over houses.

Friendship network. The friendship network among the students is modeled by a weighted graph, $G = (V, E, w)$ where $V = S$ and the relationships between students are represented by the weights of the edges connecting nodes. The strength of a relationship between two students s and t is represented by the weight of that edge, denoted by $w(s,t) \in \mathbb{R}^+ \cup \{0\}$. We require that the graph is undirected, i.e., the adjacency matrix is symmetric so that $w(s,t) = w(t,s)$ for all s, t.

Additionally, we define a few metrics quantifying the graph structure and its role in the matching. Let the total weight of the graph be denoted by $|E| := \frac{1}{2}\sum_{s\in S}\sum_{t\in S} w(s,t)$. Further, let the weight of edges connecting students assigned to houses h and g under matching μ be denoted by $E_{hg}(\mu) := \sum_{s\in\mu(h)}\sum_{t\in\mu(g)} w(s,t)$. Note that in the case of edges between students within the same house is defined slightly differently: $E_{hh}(\mu) := \frac{1}{2}\sum_{s\in\mu(h)}\sum_{t\in\mu(h)} w(s,t)$, to avoid double-counting edges. Finally, let the weight of all edges "captured" in a given matching μ (i.e., the edges between students in all of the houses for a given matching μ) be denoted by $E_{in}(\mu) := \sum_{h\in H} E_{hh}(\mu)$.

Agent utility functions. In our model, each agent derives some utility from a particular matching and an agent (student or house) always strictly prefers matchings that give a strictly higher utility and is indifferent between matchings that give equal utility. This setup differs from the traditional notion of 'preference orderings' [54, 115], but is not uncommon [6, 8, 9, 28, 50]. It is through the definitions of the utility functions that we model peer effects (for students) and complementarities (for houses).

Under our model, students derive benefit both from (i) the house they are assigned to and (ii) their peers that are assigned to the same house. We model each house h as having an desirability of $D_h^s \in \mathbb{R}^+ \cup \{0\}$ for student s. A similar model was first used in [8] and is meant to capture the physical characteristics of the house (amenities, size, etc.), independent of peer effects. If this value is different for different students, (i.e., $\exists s, t, h$ such that $D_h^s \neq D_h^t$), then students value the characteristics of the house differently. For example, some students might prefer a house with only private rooms, whereas other students value having a roommate. If, on the other

hand, $D_h^s = D_h^t \; \forall s \neq t$ (objective desirability), this value can be seen as representing something like the U.S. News college rankings or hospital rankings — something that all students would agree on. This leads to a utility for student s under matching μ of

$$U_s(\mu) := D^s_{\mu(s)} + \sum_{t \in \mu^2(s)} w(s,t) \tag{3.1}$$

where $w(s,t)$ is the weight of the edge between s and t in the friendship graph and D_h^s is utility derived by student s for house h, so that the total utility that a student derives from a match is a combination of how "good" a house is as well as how many friends they will have in that house.[23]

Similarly, the utility of a house h under matching μ is modeled by

$$U_h(\mu) := D^h_{\mu(h)}, \tag{3.2}$$

where D_σ^h denotes the desirability of a particular set of students σ for house h (the utility house h derives from being matched to the set of students σ). Note that this definition of utility allows general phenomena such as heterogeneous house preferences over groups of students.

Two-sided exchange stability. Under the traditional definition of stability, if a student and a house were to prefer each other to their current match (forming a blocking pair), the student is free to move to the preferred house and the house is free to evict (if necessary) another student to make space for the preferred student. In our model, however, we assume that students and houses cannot "go outside the system" and leave the university (neither can students remain unmatched), like what medical students and hospitals do when they operate outside of the NRMP. As a result, we restrict ourselves to considering swaps of students between houses, similar to [8, 9, 50].

[2]We note that the utility of any "holes" (such as what happens when a house's quota is not met), is simply $U_s(\mu) = 0$.

[3]Note also that if we remove D_h from the utility function and allow unlimited quotas, the matching problem becomes the coalitional affinity game from [28].

To define exchange stability, it is convenient to first define a *swap matching* μ_s^t in which students s and t switch places while keeping all other students' assignments the same.

Definition 3. *A* ***swap matching*** $\mu_s^t = \{\mu \setminus \{(s,h),(t,g)\}\} \cup \{(s,g),(t,h)\}$.

Note that the agents directly involved in the swap are the two students switching places and their respective houses — all other matchings remain the same. Further, one of the students involved in the swap can be a "hole" representing an open spot, thus allowing for single students moving to available vacancies. When two actual students are involved, this type of swap is a two-sided version of the "exchange" considered in [2, 30, 31, 66] — *two-sided* exchange stability requires that houses approve the swap. As a result, while an exchange stable matching may not exist in either the marriage or roommate problem, we show in Section 3.3 that a two-sided exchange stable matching will always exist for the housing assignment problem.

Definition 4. *A matching* μ *is* ***two-sided exchange stable (2ES)*** *if and only if there does not exist a pair of students* (s,t) *such that:*

(i) $\forall\, i \in \{s,t,\mu(s),\mu(t)\}$, $U_i(\mu_s^t) \geq U_i(\mu)$ *and*

(ii) $\exists\, i \in \{s,t,\mu(s),\mu(t)\}$ *such that* $U_i(\mu_s^t) > U_i(\mu)$

This definition implies that a swap matching in which all agents involved are indifferent is two-sided exchange stable. This avoids looping between equivalent matchings. Note that the above definition implies that if two students want to switch between two houses (or a single student wants to "switch" with a hole), the houses involved must "approve" the swap or if two houses want to switch two students, the students involved must agree to the swap (a hole will always be indifferent). Note that either houses or students can initiate the swap. This is natural for the house assignment problem and many other many-to-one matching markets, but would be less appropriate for some other settings, such as the college-admissions model.

Social welfare. One key focus of this chapter is to develop an understanding of the "efficiency loss" that results from enforcing stability of assignments in matching markets. We measure the efficiency loss in terms of the "social welfare", which we define as follows:

$$W(\mu) := \sum_{s \in S} U_s(\mu) + \sum_{h \in H} U_h(\mu)$$

Using this definition of social welfare, the efficiency loss can be quantified using the *Price of Anarchy* (PoA) and *Price of Stability* (PoS). Specifically, the PoA (PoS) is the ratio of the optimal social welfare over all matchings, not necessarily stable, to the minimum (maximum) social welfare over all stable matchings. Understanding the PoA and PoS is the focus of Section 3.5.

3.3 Existence of stable matchings

We begin by focusing on the existence of two-sided exchange stable matchings. In most prior work, matching markets with externalities do not have guaranteed existence of a stable matching. For example, in the presence of couples on the resident side of the hospital matching market, the NRMP algorithm may fail to have a stable outcome [113, 115], and even if a stable matching does exist, it may be NP-hard to find [112].

In contrast to the prior literature discussed above, we prove that a two-sided exchange stable matching always exists in the model considered in this chapter. We begin by proposing a potential function $\Phi(\mu)$ for the matching game:

$$\Phi(\mu) = \sum_{h \in H} U_h(\mu) + \sum_{s \in S} D^s_{\mu(s)} + \frac{1}{2} \sum_{s \in S} \left(\sum_{x \in \mu^2(s)} w(s, x) \right) \tag{3.3}$$

Due to the symmetry of the social network, every approved swap will result in a strict increase of the potential function. The analysis is straightforward and draws its key ideas from the work of [8], which considers only a one-sided market rather than the two-sided market considered here. Specifically,

Lemma 3.1. *Any swap matching μ_s^t for which (i) and (ii) below are satisfied, $\Phi(\mu_s^t) > \Phi(\mu)$.*

(i) $\forall\, i \in \{s, t, \mu(s), \mu(t)\}$, $U_i(\mu_s^t) \geq U_i(\mu)$, *and*

(ii) $\exists\, i \in \{s, t, \mu(s), \mu(t)\}$ *with* $U_i(\mu_s^t) > U_i(\mu)$

Proof. We begin by calculating the difference in the potential function for a swap matching using (3.3), assuming that $\mu(s) = h$ and $\mu(t) = g$:[4]

$$\begin{aligned}\Phi(\mu_s^t) - \Phi(\mu) = \sum_{h \in H} U_h(\mu_s^t) - U_h(\mu) + \sum_{s \in S} D^s_{\mu_s^t(s)} - D^s_{\mu(s)} \\ + \frac{1}{2}\sum_{s \in S}\left(\sum_{x \in \mu_s^t(s)} w(s,x)\right) - \frac{1}{2}\sum_{s \in S}\left(\sum_{x \in \mu(s)} w(s,x)\right) \end{aligned} \tag{3.4}$$

Expanding and canceling like terms, we have

$$\begin{aligned}\Phi(\mu_s^t) - \Phi(\mu) = U_h(\mu_s^t) - U_h(\mu) + U_g(\mu_s^t) - U_g(\mu) + D^s_g - D^t_g + D^t_h - D^s_h \\ + \frac{1}{2}\left[\left(\sum_{x \in \mu(g)} w(s,x) - w(s,t) + \sum_{x \in \mu(h)} w(t,x) - w(s,t)\right)\right. \\ \left. + \left(\sum_{x \in \mu(g)} w(x,s) - w(s,t) + \sum_{x \in \mu(h)} w(x,t) - w(s,t)\right)\right] \\ - \frac{1}{2}\left[\left(\sum_{x \in \mu(h)} w(s,x) + \sum_{x \in \mu(g)} w(t,x)\right) + \left(\sum_{x \in \mu(h)} w(x,s) + \sum_{x \in \mu(g)} w(x,t)\right)\right]\end{aligned} \tag{3.5}$$

[4]Note that we have a little abuse of notation here, for convenience. We are using $x \in \mu_s^t(s)$ to denote the the other students x that are in the same house as s under the swap matching μ_s^t. Similarly, $x \in \mu(s)$ denotes the other students that are in the same house as s under the original matching μ. We revert to the correct notation in (3.5).

which becomes, due to the symmetry of the social network,

$$\Phi(\mu_s^t) - \Phi(\mu) = U_h(\mu_s^t) - U_h(\mu) + U_g(\mu_s^t) - U_g(\mu) + D_g^s - D_g^t + D_h^t - D_h^s + \sum_{x \in \mu(g)} (w(s,x) - w(t,x)) + \sum_{x \in \mu(h)} (w(t,x) - w(s,x)) - 2w(s,t) \tag{3.6}$$

Note that if t is a "hole", this becomes

$$\Phi(\mu_s^t) - \Phi(\mu) = U_h(\mu_s^t) - U_h(\mu) + U_g(\mu_s^t) - U_g(\mu) + D_g^s - D_h^s + \sum_{x \in \mu(g)} (w(s,x)) - \sum_{x \in \mu(h)} (w(s,x)) \tag{3.7}$$

Now, consider a matching μ and a swap matching μ_s^t that satisfies (i) and (ii) from the lemma statement. Without loss of generality, assume that student s strictly improves. The other student could be either a "hole" or a real student that either improves or is indifferent to the swap. The other cases are symmetric. Define $\mu(s) = h$, and $\mu(t) = g$. The change in utility for student s is then

$$0 < U_s(\mu_s^t) - U_s(\mu) = D_g^s - D_h^s - \sum_{x \in \mu(h)} w(s,x) + \sum_{x \in \mu(g)} w(s,x) - w(s,t),$$

Similarly, for student t, we have

$$0 \leq U_t(\mu_s^t) - U_t(\mu) = D_h^t - D_g^t - \sum_{x \in \mu(g)} w(t,x) + \sum_{x \in \mu(h)} w(t,x) - w(s,t).$$

Adding the above inequalities, we obtain the following:

$$0 < D_g^s - D_g^t + D_h^t - D_h^s + \sum_{x \in \mu(g)} (w(s,x) - w(t,x)) + \sum_{x \in \mu(h)} (w(t,x) - w(s,x)) - 2w(s,t) := \delta_{s,t}$$

Note that we are using $\delta_{s,t}$ to denote the change in utilities for the two students, s

and t directly involved in the swap. On the house side of the market, we have

$$0 \leq U_h(\mu_s^t) - U_h(\mu) + U_g(\mu_s^t) - U_g(\mu) := \Delta_H$$

as only houses h and g are affected by the swap and the change in their utilities is nonnegative by assumption.

Thus, comparing (3.6) with the expressions for Δ_H and $\delta_{s,t}$ above, we see that

$$\Phi(\mu_s^t) - \Phi(\mu) = \Delta_H + \delta_{s,t} > 0. \tag{3.8}$$

Note that this holds even if t is a "hole." □

Note that the symmetry of the social network was key in proving Lemma 3.1. Without network symmetry, it is possible that no two-sided exchange stable matching will exist, as is the case in the example below.

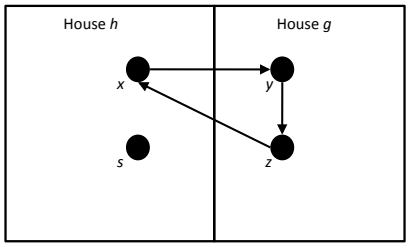

Figure 3.1: Asymmetry leads to nonexistence of stable matching

Example 4 (Nonexistence due to asymmetry)**.** *In this example, we have a* directed *social network, as shown in Figure 3.1. As a result, students will "chase" each other from house to house, assuming that* $D_h^s = D \ \forall \ h, s$*. For example, starting in the matching shown, student* z *will switch with student* s*, who does not care which house she is in, in order to be with* x*. Then,* x *will switch with* s *to be with* y*. Finally,* y *will switch with* s *to be with* z*, and we are effectively at the initial matching. Thus, in this "love-triangle" example, no stable matching exists.*

Using Lemma 3.1, it is now easy to prove the following theorem.

Theorem 3.2. *All local maxima of $\Phi(\mu)$ are two-sided exchange stable.*

Proof. Let matching μ be a local maximum of $\Phi(\mu)$. Assume, by way of contradiction, that μ is not two-sided exchange stable. Lemma 3.1 shows that any swap matching that is acceptable to all parties (i.e., satisfies conditions (i) and (ii)) strictly increases $\Phi(\mu)$. But this contradicts the assumption that μ is a local maximum. Thus, μ must be two-sided exchange stable. □

As the number of matches is finite, the global maximum of the potential function must be two-sided exchange stable, and, therefore, a two-sided exchange stable matching will always exist for every housing assignment market of this form.

3.3.1 Special case: Objective desirability

If we assume that there are no vacancies in any of the houses and students value houses according to the same rules (i.e., $D_h^s = D_h^t \; \forall \; s \neq t$), then each each approved swap will result in a strict increase in the *social welfare*. Specifically,

Lemma 3.3. *If house quotas are exactly met and $D_h^s = D_h^t \; \forall \; s \neq t$, then any swap matching μ_s^t for which*

(i) $\forall \, i \in \{s, t, \mu(s), \mu(t)\}$, $U_i(\mu_s^t) \geq U_i(\mu)$, *and*

(ii) $\exists \, i \in \{s, t, \mu(s), \mu(t)\}$ *with* $U_i(\mu_s^t) > U_i(\mu)$

has $W(\mu_s^t) > W(\mu)$.

Proof. Consider a matching μ and a swap matching μ_s^t that satisfies (i) and (ii) from the lemma statement. Note that due to the assumption that the house quotas are all met, the swap must be between two students, not a student and a "hole". Without loss of generality, assume that student s strictly improves. The other cases are symmetric. Define $\mu(s) = h$, and $\mu(t) = g$. The change in utility for student s is then

$$0 < U_s(\mu_s^t) - U_s(\mu) = D_g - D_h - \sum_{x \in \mu(h)} w(s, x) + \sum_{x \in \mu(g)} w(s, x) - w(s, t),$$

Similarly, for student t, we have

$$0 \leq U_t(\mu_s^t) - U_t(\mu) = D_h - D_g - \sum_{x \in \mu(g)} w(t,x) + \sum_{x \in \mu(h)} w(t,x) - w(s,t).$$

Adding the above inequalities, we obtain the following:

$$0 < \sum_{x \in \mu(g)} (w(s,x) - w(t,x)) + \sum_{x \in \mu(h)} (w(t,x) - w(s,x)) - 2w(s,t) := \delta_{s,t}$$

Continuing, the total change in utility for *all* students is:

$$\begin{aligned}
\Delta_S :=& \sum_{x \in S} U_x(\mu_s^t) - \sum_{x \in S} U_x(\mu) \\
&= \delta_{s,t} + \underbrace{\sum_{x \in \mu(g)} w(x,s) - w(s,t)}_{\text{gain from } s \text{ joining } g} - \underbrace{\sum_{x \in \mu(h)} w(x,s)}_{\text{loss from } s \text{ leaving } h} + \underbrace{\sum_{x \in \mu(h)} w(x,t) - w(s,t)}_{\text{gain from } t \text{ joining } h} - \underbrace{\sum_{x \in \mu(g)} w(x,t)}_{\text{loss from } t \text{ leaving } g} \\
&= 2\delta_{s,t} \qquad (3.9) \\
&> 0
\end{aligned}$$

where line (3.9) comes from the fact that we assume the social network graph is symmetric.

On the house side of the market, we have

$$0 \leq U_h(\mu_s^t) - U_h(\mu) + U_g(\mu_s^t) - U_g(\mu) := \Delta_H$$

as only houses h and g are affected by the swap and the change in their utilities is nonnegative by assumption. Thus, the total social welfare strictly increases:

$$W(\mu_s^t) - W(\mu) = \Delta_S + \Delta_H > 0$$

□

As before, it is now easy to prove the following theorem.

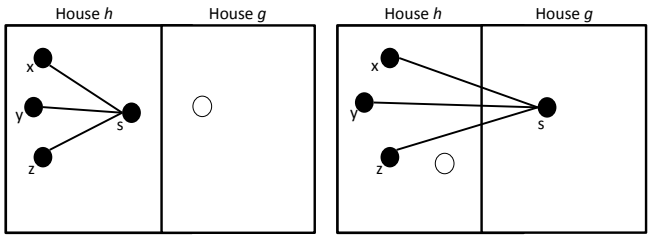

Figure 3.2: Forced swap increases social welfare

Theorem 3.4. *If house quotas are exactly met and* $D_h^s = D_h^t \ \forall \ s \neq t$*, all local maxima of* $W(\mu)$ *are two-sided exchange stable.*

Proof. Let matching μ be a local maximum of $W(\mu)$. Lemma 3.3 shows that any swap matching that is acceptable to all parties (i.e. satisfies conditions (i) and (ii)) strictly increases the total social welfare. But this contradicts the assumption that μ is a local maximum. Thus, μ must be stable. □

Note that this implies that the maximally efficient matching will be two-sided exchange stable.[5] However, not all two-sided exchange stable matchings are local maxima of $\Phi(\mu)$ or $W(\mu)$. Such a case arises when one student, for example, refuses a swap as her utility would decrease, but the other student involved stands to benefit a great deal from such a swap. If the swap were forced, the total potential function (or social welfare) could increase, but only at the expense of the first student. We show an example of this below.

Example 5 (Forced swap increases social welfare)**.** *For this example, let* $U_s(h) = 0$*,* $U_s(g) = 4$*,* $U_i(h) = U_i(g) = 0 \ \forall \ i \neq s$*, and* $U_h(\mu) = U_g(\mu) = 0 \ \forall \ \mu$*. In the first match (left side of Figure 3.2), student s is unhappy with her match, and the match is unstable because there is a hole in house g – an available spot for student s. However, the social welfare of this match is* $W(\mu_1) = 2 * 3 + 0 = 6$*. If student s moves to house g, as shown in the right side of Figure 3.2, the new social welfare will*

[5]Note that a local maximum of $W(\mu)$ is a matching μ for which there exists no matching μ' which is obtained from μ by swapping the assignment of exactly two students (or a student and an empty spot) and has $W(\mu') > W(\mu)$.

be $W(\mu_2) = 0 + 4 = 4$*. Note that this matching is stable, since* s *does not want to move from house* g*. If we force the* s *back to* h*, we can increase the social welfare.*

The contrast between Theorem 3.2 and results such as [113] and [115] can be explained by considering a few aspects of the model we study. In particular, we are using a distinct type of stability appropriate to our housing assignment market. Further, the assumption that the social network graph is symmetric is key to guaranteeing existence.

3.4 Finding stable matchings

In the previous section we have shown that a two-sided exchange stable matching will always exist and, moreover, that under certain assumptions, socially optimal matchings are two-sided exchange stable. In this section, we turn to the task of developing algorithms for finding two-sided exchange stable matchings. In particular, two natural algorithms follow immediately from our analysis. For simplicity, in this section we assume the conditions of Theorem 3.4; namely, that quotas are exactly met and students rate houses according to the same rules.[6]

Algorithm 1 (Greedy)

while $i \leq$ maxIterations **do**
  Search for "approved" swap μ_s^t
  $\mu \leftarrow \mu_s^t$
  $i \leftarrow i + 1$
end while

Algorithm 1 proceeds by greedily considering "approved" swaps among students/houses that improve the social welfare. Note that this algorithm can easily be implemented in a distributed manner, and loosely models the process by which individuals adjust a matching that is not stable. For example, consider starting at a random matching, and giving students a preset amount of time to talk amongst themselves and make

[6]We note that the results of this section extend to the more general case, using the potential function defined in Section 3.3 rather than the social welfare function.

swaps, obtaining the approval of their houses for each swap. Given enough time, such a distributed method will converge to a 2ES match.

Lemma 3.3 and Theorem 3.4 immediately give that Algorithm 1 will converge to a two-sided exchange stable matching, since the social welfare strictly improves with each iteration, and all local maxima of W are two-sided exchange stable matchings. Note that Algorithm 1 is not guaranteed to converge to the socially optimal stable matching; it will likely find just a local maxima of W. Also, note that each iteration of the algorithm above can involve searching many pairs of students (and houses) for an "approved" swap.

Algorithm 2 MCMC

while $i \leq$ maxIterations **do**
  Pick random pair of students $\{s, t\}$
  $P_T = \frac{1}{1+e^{-T(W(\mu_s^t)-W(\mu))}}$
  $\mu \leftarrow \mu_s^t$ with probability P_T
  if $(W(\mu_s^t) > W_{best})$ **then**
    $W_{best} = W(\mu_s^t)$
  end if
  $i \leftarrow i + 1$
end while

The second algorithm we consider again seeks to optimize W, this time using a MCMC heat bath. In this algorithm we start with a random initial matching and at each iteration swap a random pair of students with a probability that depends on the change in social welfare: a positive change yields a probability of swapping larger than 1/2 and vice versa. Algorithm 2 therefore can emerge from a local maximum. The algorithm keeps track of the "best" matching found so far, even as it moves to worse matchings. If Algorithm 2 is run sufficiently long (perhaps exponential time) it can find the optimal two-sided exchange stable matching [59]. However, there is no guarantee that the best matching encountered in finite time is even two-sided exchange stable, a situation that can be remedied by applying the greedy algorithm to this matching. Simulation results show the superiority of Algorithm 2 to Algorithm 1 in terms of welfare, at the expense of an increase in the number of computations. To illustrate the performance of these two algorithms, we use two social network data

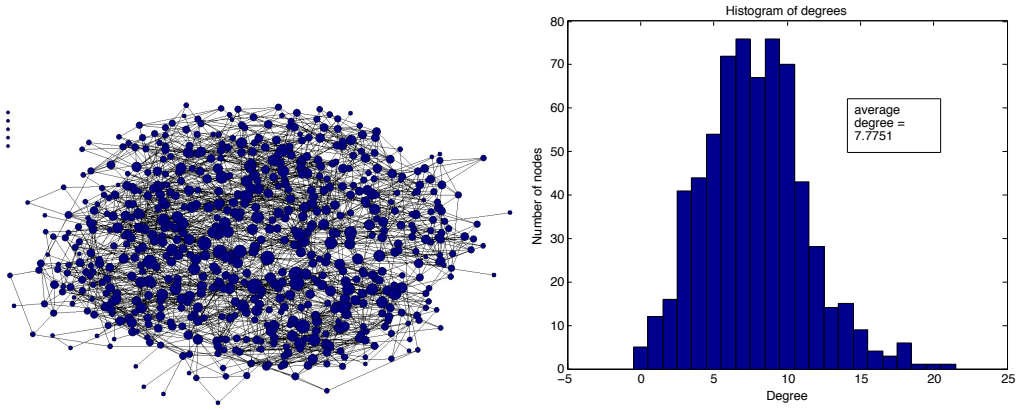

(a) Undirected Caltech social network (b) Caltech SN: Degree histogram

Figure 3.3: Caltech social network

sets, as follows.

3.4.1 Case study: Caltech social network

The first data set is from the Caltech Project [47]. The original data set is an directed graph representing the friendship links among the undergraduates at the California Institute of Technology in 2010, including approximately 900 nodes and 4700 directed edges. This graph was collected by surveying the undergraduates at Caltech and asking them to list up to 10 of their friends. The survey response rate was about 75%, resulting in $\sim$ 650 nodes with outgoing edges and $\sim$ 250 nodes with only incoming edges (these nodes represent students who were named as friends by other students but did not themselves take the survey). For the purposes of this chapter, we require an undirected network, so we first restrict the node set to only those that took the survey. We then use an OR rule to generate undirected edges in the final network, as follows. Let A be the adjacency matrix representing the generated undirected Caltech social network and $\hat{A}$ the collected directed network. Include an edge, $A(i,j) = 1$ if $\hat{A}(i,j) = 1$ or $\hat{A}(j,i) = 1$. After this process is complete, we are left with an undirected network consisting of 658 nodes and 2558 undirected edges. This network is shown in Figure 3.3a, along with its degree histogram, in Figure 3.3b.

For this example, we consider a *one-sided matching market*, to compare the per-

formance of the matching algorithms given above to the actual matching of students to houses at Caltech. Formally, we assume $D_h^s = D_h^t = 0 \ \forall \ s, t, \in S, \ h \in H$, and $U_h(\mu) = 0 \ \forall h \in H$. As a result, what we are considering is essentially a network partitioning problem, with the size of the partitions constrained by the actual number of slots available in each of the 9 Caltech houses. We calculate the value of the real Caltech housing assignment, $SW(\mu_{real})$, as $2E_{in}(\mu_{real}) = 3654$, and show its approximate value compared to what is found by the algorithms in Figure 3.4. Figure 3.4a shows the performance of the greedy matching algorithm, starting at a random match and in each iteration, searching for an acceptable swap (one that strictly improves at least one agent, no others are hurt). The algorithm terminates after a sufficient number of iterations in which no acceptable swap is found. Figure 3.4b shows the performance of the heat bath matching algorithm using the undirected Caltech social network as input. The y-axis in all figures shows the social welfare of the matching at each iteration. For both the Caltech social network and the WikiVote network in the next example, Algorithm 2 has longer running time than Algorithm 1, which converges quickly.[7] As expected, Algorithm 1 converges to a suboptimal matching for both networks, but this value is of the same order of magnitude as that found by Algorithm 2.

3.4.2 Case study: On-Line WikiVote network

The second data set we use is from voting records for admin promotion at Wikipedia [41]. Edges in the data-set represent votes for or against a user by another user. For simplicity, we treated the directed graph as undirected, using the same OR rule as before, resulting in approximately 7000 nodes and 100000 edges. To illustrate the performance of the algorithms on a *two-sided matching market*, we created 71 houses and assigned them desirability values uniformly distributed from 0 to 10. Formally, in this example $D_h^s \neq D_h^t$ for most s, t and h. For the other side of the market, each

[7] We note that in the greedy algorithm, an "iteration" can take much more time to complete than one "iteration" of the MCMC heat bath. Even with this effect, however, the MCMC takes longer than the greedy algorithm.

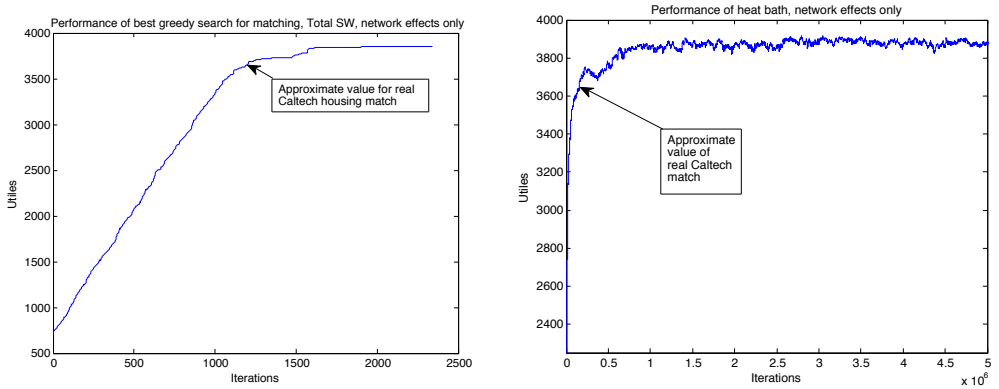

(a) Algorithm 1 (b) Algorithm 2

Figure 3.4: Illustration of the performance of Algorithms 1 and 2 on the Caltech social network

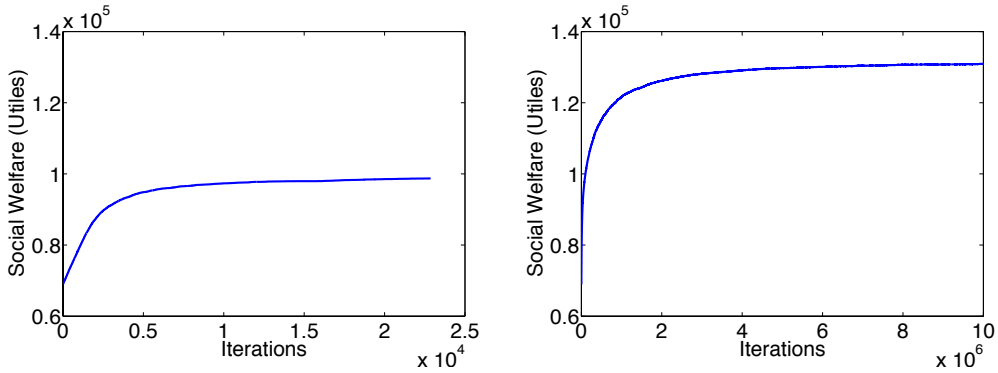

(a) Algorithm 1 (b) Algorithm 2

Figure 3.5: Illustration of the performance of Algorithms 1 and 2 on the Wikipedia voting network

user is assigned a score by each house, uniformly distributed from 0 to 10. As a result, the utility derived from house h for match μ becomes $U_h(\mu) = \sum_{s \in \mu(h)} U^h(s)$, a simple sum of the values that each house has for each student assigned to it. Both the greedy and heat bath algorithms are run using the same initial values, and the results are shown in Figure 3.5.

3.5 Efficiency of stable matchings

To this point, we have focused on the existence of two-sided exchange stable matchings and how to find them. In this section our focus is on the "efficiency loss" due to stability in a matching market and the role peer effects play in this efficiency loss.

We measure the efficiency loss in a matching market using the price of stability (PoS) and the price of anarchy (PoA) as defined in Section 3.2. Interestingly, the price of anarchy has multiple interpretations in the context of this chapter. First, as is standard, it measures the worst-case loss of social welfare that results due to enforcing exchange stability. For example, the authors in [6] bound the loss in social welfare caused by individual rationality (by enforcing stable matchings) for matching markets without externalities. Second, it provides a competitive ratio for Algorithm 1 for finding a stable matching, since Algorithm 1 provides no guarantee about which stable matching it will find. Third, we show later that the price of anarchy also has an interpretation as capturing the efficiency lost due to peer effects.

The results in this section all require one additional simplifying assumption to our model: *complementarities are ignored and only peer effects are considered.* Specifically, we assume, for all of our PoA results, $U_h(\mu) = 0$, and thus $W(\mu) = \sum_{s \in S} U_s(\mu)$. Under this assumption, the market is one-sided, with only students participating — as a result we are only considering exchange stability. This assumption is limiting, but there are still many settings within which the model is appropriate. Two examples are the housing assignment problem in the case when students can swap positions without needing house approval, and the assignment of faculty to offices as discussed in [8], as clearly the offices have no preferences over which faculty occupy them. In order to simplify the analysis, we also make use of the assumptions in Theorem 3.4: (i) $D_h^s = D_h^t \; \forall \; s \neq t$ and (ii) house quotas are exactly met.

3.5.1 Related models

When the housing assignment problem is restricted to a one-sided market involving only students, we note that it becomes very similar to both (i) a hedonic coalition

formation game with symmetric additively separable preferences, as described in [21], and (ii) a coalitional affinity game, as described in [28].

In hedonic coalition formation games, agents' preferences for a given coalition are based on the other members of that coalition [42]. Note that coalition games are necessarily one-sided — agents care about the coalitions but the coalitions cannot care about the agents. The most related work to ours in this area is [21], where the authors show that when agents' preferences over coalition are symmetric and additively separable (as the student utility functions in the housing assignment problem are), a Nash (and individually) stable coalition structure will always exist. This mimics the existence result proved in Section 3.3, however our result applies for a two-sided market. Further work on hedonic games looks at the complexity of finding stable coalition structures; see [7, 29, 46, 53, 95] for examples.

Coalitional affinity games consider the pairwise relationships between agents, as represented by a weighted graph [28], and are a special subclass of hedonic games. The most related result to the current work is [28], which proves a tight upper bound on the Price of Anarchy using the notion of core stability[8] when the weighted graph is symmetric.

While the one-sided housing assignment problem and hedonic coalition formation games appear to be very similar, there are a number of key differences. Most importantly, the housing assignment problem considers a *fixed* number of houses with a limited number of spots available; students cannot break away and form a new coalition/house, nor can a house have more students than its quota. In addition, our model considers exchange stability, which is closest to the Nash stability of [21], but is still significantly different in that it involves a pair of students willing and able to swap. Finally, each student gains utility from the house they are matched with, in addition to the other members of that house, which is different from the original formulation of hedonic coalition games.

[8] A coalition structure is core stable if no set of agents can break away and form a new coalition to improve their own utility.

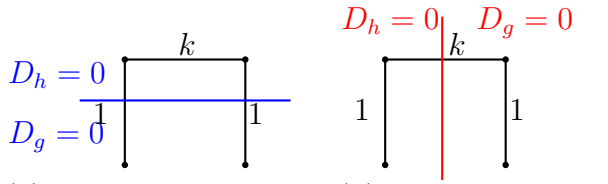

(a) optimal matching (b) stable matching

Figure 3.6: Arbitrarily bad exchange stable matching

3.5.2 Discussion of results

To begin the discussion of our results, note that, as discussed in Section 3.3, the price of stability is 1 for our model because any social welfare optimizing matching is stable.

However, the price of anarchy can be much larger than 1. In fact, depending on the social network, the price of anarchy can be unboundedly large, as illustrated in the following example.

Example 6 (Unbounded price of anarchy)**.** *Consider a matching market with 4 students and 2 houses, each with a quota of 2, and two possible matchings illustrated by Figure 3.6. As shown in Figure 3.6 (a) and (b), respectively, in the optimal matching μ^*, $W(\mu^*) = k$; whereas there exists a exchange stable matching with $W(\mu) = 2$. Thus, as k increases, the price of anarchy grows linearly in k.*

Despite the fact that, in general, there is a large efficiency loss that results from enforcing exchange stability, in many realistic cases the efficiency loss is actually quite small. The following two theorems provide insight into such cases.

A key parameter in these theorems is γ_m^* which captures how well the social network can be "clustered" into a *fixed* number of m groups and is defined as follows.

$$\gamma_m(\mu) := \frac{E_{in}(\mu)}{|E|} \tag{3.10}$$

$$\gamma_m^* := \max_{\mu} \gamma_m(\mu) \tag{3.11}$$

Thus, γ_m^* represents the maximum edges that can be captured by a partition satisfying the house quotas. Note that γ_m^* is highly related to other clustering metrics, such as

the conductance [70], [123] and expansion [107].

We begin by noting that due to the assumption that $\sum_{h\in H} U_h(\mu) = 0$, we can separate the social welfare function into two components:

$$W(\mu) = \sum_{s\in S} U_s(\mu) = \sum_{h\in H}\sum_{s\in\mu(h)}\left(D_h + \sum_{t\in\mu(h)} w(s,t)\right) = 2E_{in}(\mu) + \sum_{h\in H} q_h D_h.$$

Thus,

$$\frac{\max_\mu W(\mu)}{\min_{\mu \text{ is stable}} W(\mu)} = \frac{Q + \max_\mu \gamma_m(\mu)}{Q + \min_{\text{stable } \mu} \gamma_m(\mu)} \tag{3.12}$$

where

$$Q := \frac{\sum_{h\in H} q_h D_h}{2E}. \tag{3.13}$$

Note that the parameter Q is independent of the particular matching μ.

Our first theorem regarding efficiency is for the "simple" case of unweighted social networks with equal house quotas and/or equivalently valued houses.

Theorem 3.5. *Let $w(s,t) \in \{0,1\}$ for all students s,t and let $q_h \geq 2, D_h \in \mathbb{Z}^+ \cup \{0\}$ for all houses h. If $q_h = q$ for all h and/or $D_h = D$ for all h, then*

$$\min_{\text{stable } \mu} W(\mu) \geq \frac{\max_\mu W(\mu)}{1 + 2(m-1)\gamma_m^*}$$

The bound in Theorem 3.5 is tight, as illustrated by the example below.

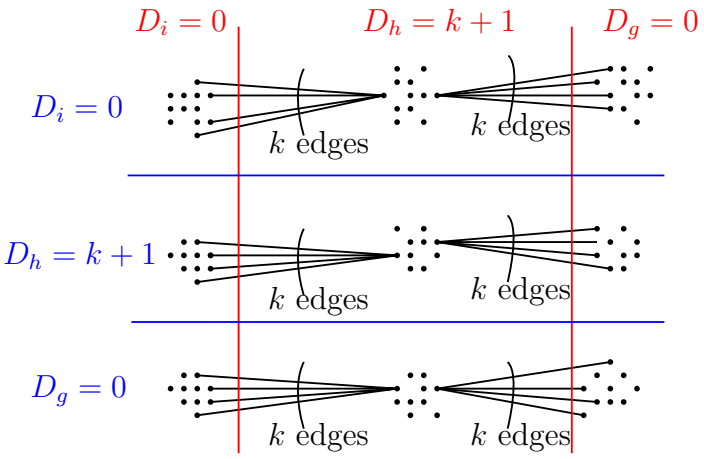

Figure 3.7: Network that achieves PoA bound.

Example 7 (Tightness of Theorem 3.5)**.** *Consider a setting with m houses and $q_h = mk$ for all $h \in H$. Students are grouped into clusters of size $k > 2$, as shown for $m = 3$ in Figure 3.7. The houses have $D_h = k + 1$ and $D_g = D_i = 0$. Each student in the middle cluster in each row has k edges to the other students outside of their cluster (but none within), as shown.*

The worst-case stable exchange-matching is represented by the vertical red lines. Note that since $D_h = k + 1$, this matching is stable, even though all edges are cut. Thus $\min_{\mu \text{ stable}} \gamma_m(\mu) = 0$. The optimal matching is represented by the horizontal blue lines in the figure; note that $\gamma_m^* = 1$. To calculate the price of anarchy, we start from equations (3.12) *and* (3.13) *and calculate*

$$Q = \frac{\sum_{h \in H} q_h D_h}{2|E|} = \frac{mk(k+1)}{2mk(m-1)k} = \frac{k+1}{2(m-1)k},$$

which gives,

$$\frac{\max_\mu W(\mu)}{\min_{\text{stable } \mu} W(\mu)} = \frac{Q + \gamma_m^*}{Q + \min_{\mu \text{ stable}} \gamma_m(\mu)} = 1 + 2(m-1)\left(\frac{k}{k+1}\right).$$

Notice that as k becomes large, this approaches the bound of $1 + 2(m-1)\gamma_m^*$.

We note that the requirement $q_h = q$ for all h and/or $D_h = D$ for all h is key to the proof of Theorem 3.5 and in obtaining such a simple bound; otherwise, Theorem 3.6 applies. We omit the proofs of these theorems here for brevity; see Section 3.7 for the details.

Our second theorem removes the restrictions in the theorem above, at the expense of a slightly weaker bound. Define $q_{max} = \max_{h \in H} q_h$, $w_{max} = \max_{s,t \in S} w(s,t)$ and $D_\Delta = \min_{h,g \in H}(D_h - D_g)$, assuming that the houses are ordered in increasing values of D_h.

Theorem 3.6. *Let $w(s,t) \in \mathbb{R}^+ \cup \{0\}$ for all students s, t and $D_h \in \mathbb{R}^+ \cup \{0\}$, $q_h \in \mathbb{Z}^+$ for all houses h, then*

$$\min_{\text{stable } \mu} W(\mu) \geq \frac{\max_\mu W(\mu)}{1 + 2(m-1)\left(\gamma_m^* + \frac{q_{max} w_{max}}{D_\Delta}\right)}$$

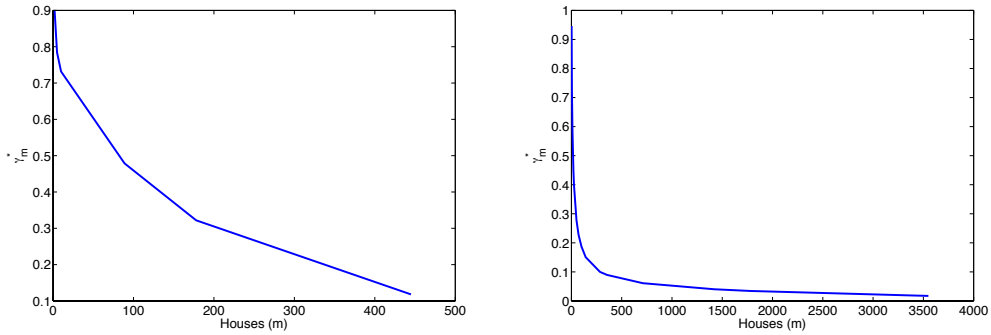

(a) Caltech γ_m^* (b) Wikipedia γ_m^*

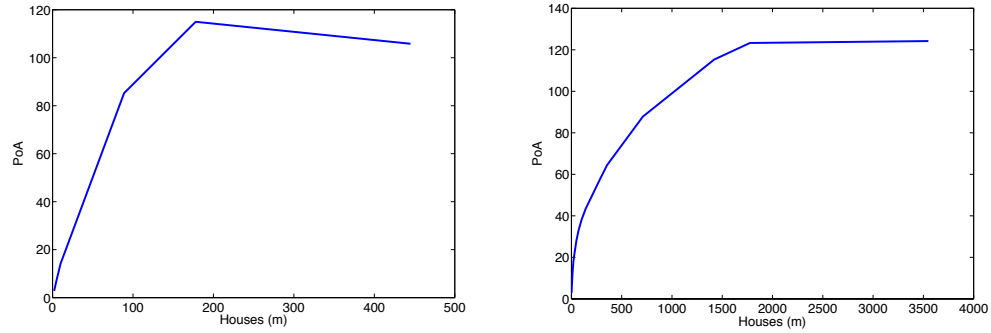

(c) Caltech PoA (d) Wikipedia PoA

Figure 3.8: Illustration of γ_m^* and price of anarchy bounds in Theorem 3.5 for Caltech and Wikipedia networks.

Though Theorem 3.5 is tight, it is unclear at this point whether Theorem 3.6 is also tight. However, a slight modification of the above example does show that it has the correct asymptotics, i.e., there exists a family of examples that have price of anarchy $\Theta(m\gamma_m^* q_{max} w_{max} D_\Delta^{-1})$.

A first observation one can make about these theorems is that the price of anarchy has no direct dependence on the number of students. This is an important practical observation since the number of houses is typically small, while the number of students can be quite large (similar phenomena hold in many other many-to-one matching markets). In contrast, the theorems highlight that the degree of heterogeneity in quotas, network edge weights, and house valuations all significantly impact inefficiency.

A second remark about the theorems is that the only dependence on the social

network is through γ_m^*, which measures how well the graph can be "clustered" into m groups. An important note about γ_m^* is that it is highly dependent on m, and tends to shrink quickly as m grows. We give an illustration of this effect in Figures 3.8a and 3.8b using the two social network data sets described in Section 3.4. A consequence of this behavior is that the price of anarchy is not actually linear in m in Theorems 3.5 and 3.6, as it may first appear, it turns out to be sublinear. This is illustrated in the context of real social network data in Figures 3.8c and 3.8d. We note that as we are increasing m, what we are in fact doing is creating finer allowable partitions of the network.

Next, let us consider the impact of peer effects on the price of anarchy. Considering the simple setting of Theorem 3.5, we see that if there were no peer effects, this would be equivalent to setting $w(s,t) = 0$ for all s, t. This would imply that $\gamma_m^* = 0$, and so the price of anarchy is one. Thus, another interpretation of the price of anarchy in Theorem 3.5 is the efficiency lost as a result of peer effects.

3.6 Concluding remarks

In this chapter we have focused on many-to-one matchings with peer effects and complementarities. Typically, results on this topic tend to be negative, either proving that stable matchings may not exist, e.g., [113, 115], or that stable matchings are computationally difficult to find, e.g., [112]. Our goal has been to provide positive results. To this end, we focus on the case when peer effects are the result of an underlying social network, and this restriction on the form of the peer effects allows us to prove that a two-sided exchange-stable matching always exists and that socially optimal matchings are always stable. Further, we provide bounds on the maximal inefficiency (price of anarchy) of any exchange-stable matching and show how this inefficiency depends on the clustering properties of the social network graph. Interestingly, in our context the price of anarchy has a dual interpretation as characterizing the degree of inefficiency caused by peer effects.

There are numerous examples of many-to-one matchings where the results in this

chapter can provide insight; one of particular interest to us is the matching of incoming undergraduates to residential houses which happens yearly at Caltech and other universities. Currently incoming students only report a preference order for houses, and so are incentivized to collude with friends and not reveal their true preferences. For such settings, the results in this chapter highlight the importance of having students report not only their preference order on houses, but also a list of friends with whom they would like to be matched. In particular, our simulations in Section 3.4 clearly show an improvement in social welfare by considering the social network in the matching mechanism. Using a combination of these factors the algorithms and efficiency bounds presented in this chapter provide a promising approach, for this specific market as well as any general market where peer effects change the space of stable matchings.

Our current results represent only a starting point for research into the interaction of social networks and many-to-one matchings. There are a number of simplifying assumptions in this work which would be interesting to relax. For example, the efficiency bounds we have proven consider only a one-sided market, where houses do not have preferences over students, students rate houses similarly, and quotas are exactly met. These assumptions are key to providing simpler bounds, and they certainly are valid in some matching markets; however relaxing these assumptions would broaden the applicability of the work greatly.

3.7 Appendix: Proofs of Theorems 3.5 and 3.6

We note that these proofs hold for the one-sided market; i.e., when $U_h(\mu) = 0 \; \forall h \in H$, where the quotas for the houses are *exactly* satisfied; i.e., there are no "holes", and students value houses according to the same rules; i.e., $D_h^s = D_h^t \; \forall \; s \neq t, \; h \in H$. Also note that for ease of notation, we use E instead of $|E|$ to represent the total edge weight of the graph in this section.

3.7.1 Proof of Theorem 3.5

Throughout the proof we assume that the houses are ordered: i.e., if $g < h$ then $D_g < D_h$. An important tool that we use throughout the proof is a rephrasing of the definition of exchange stability *in the one-sided market case* in terms of a function α as follows.

Definition 5. *Let $\alpha_\mu(s, g)$ be a function representing the benefit a student s gains by moving to house g under matching μ:*

$$\alpha_\mu(s, g) = D_g - D_{\mu(s)} + \sum_{x \in \mu(g)} w(s, x) - \sum_{x \in \mu^2(s)} w(s, x) \tag{3.14}$$

Notice that using the definition above, given a specific swap matching μ_s^t where $t \in \mu(g)$, we can calculate the difference in utility for the involved student s as

$$U_s(\mu_s^t) - U_s(\mu) = \alpha_\mu(s, g) - w(s, t)$$

because $\sum_{x \in \mu_s^t(g)} w(s, x) = \sum_{x \in \mu(g)} w(s, x) - w(s, t)$.

The definition of α also provides a useful new phrasing of the definition of exchange stability, which is equivalent to that of Definition 4 when the market is one-sided, i.e, when $U_h(\mu) = 0 \; \forall h \in H$. Note that we are only considering the Price of Anarchy for the one-sided market here – we plan to generalize these results for the two-sided case in future work.

Definition 6. *A matching μ is **exchange stable (ES)** in the one-sided (students-only) housing assignment market if and only if for all pairs of students $s \in \mu(h)$ and $t \in \mu(g)$, at least one of the following conditions holds:*

(Condition 1) s doesn't want to swap, i.e., $\alpha_\mu(s, g) < w(s, t)$.

(Condition 2) t doesn't want to swap, i.e., $\alpha_\mu(t, h) < w(s, t)$.

(Condition 3) s and t are indifferent, i.e., $\alpha_\mu(s, g) = \alpha_\mu(t, h) = w(s, t)$.

Using the above rephrasing of the definition of exchange stability, we now continue with the proof of Theorem 3.5. In order to prove an upper bound on the price of anarchy, we prove a lower bound on $\gamma_m(\mu)$ when μ is stable. To prove this lower bound, we first prove an upper bound on the number of cross edges ($E_{hg} = E_{gh}$) in the following lemma.

Lemma 3.7. *Let $w(s,t) \in \{0,1\}$ for all students s,t and let $q_h \geq 2, D_h \in \mathbb{Z}^+ \cup \{0\}$ for all h. Let $q_h = q$ for all h and/or $D_h = D$ for all h. If a matching μ is stable, then for all houses h and g,*

$$E_{hg} \leq \max(q_h(D_h - D_g), q_g(D_g - D_h)) + 2(E_{hh} + E_{gg}) \tag{3.15}$$

Proof. Using the conditions of stability from Definition 6 and Lemmas 3.11 and 3.12 as summarized below and proved in Section 3.8, we have

Case 1: If there exists $s \in \mu(h)$ such that $\alpha_\mu(s,g) > 1$ then, by Lemma 3.11, if μ is stable it follows that

$$E_{gh} \leq q_g(D_g - D_h) + 2E_{gg}$$

Case 2: If there exists $t \in \mu(g)$ such that $\alpha_\mu(t,h) > 1$ then, by Lemma 3.11, if μ is stable it follows that

$$E_{hg} \leq q_h(D_h - D_g) + 2E_{hh}$$

Case 3: If there does not exist $s \in \mu(h)$ such that $\alpha_\mu(s,g) > 1$ and there does not exist $t \in \mu(g)$ such that $\alpha_\mu(t,h) > 1$ then, by Lemma 3.12, if μ is stable it follows that

$$E_{hg} \leq \max(q_h(D_h - D_g), q_g(D_g - D_h)) + 2(E_{hh} + E_{gg})$$

Given any matching μ in the student-only market, it must fall into one of the three cases above. Thus, if μ is stable, it follows that one of the three bounds above holds. Because the edges are undirected, $E_{hg} = E_{gh}$, we can combine the three bounds to

conclude that if μ is stable,

$$E_{hg} \leq \max(q_h(D_h - D_g), q_g(D_g - D_h)) + 2(E_{hh} + E_{gg})$$

□

Next, we use the above to prove a lower bound on $\gamma_m(\mu)$.

Lemma 3.8. *Let $w(s,t) \in \{0,1\}$ and let $q_h \geq 2, D_h \in \mathbb{Z}^+ \cup \{0\}$ for all h. Let $q_h = q$ for all h and/or $D_h = D$ for all h. If a matching μ is stable, then*

$$\gamma_m(\mu) \geq \max\left(\frac{E - \sum_{g<h} q_h(D_h - D_g)}{(2m-1)E}, 0\right) \tag{3.16}$$

Proof.

$$\begin{aligned} E_{in}(\mu) &= E - \sum_{g<h} E_{gh} \\ &\geq E - \sum_{g<h} (q_h(D_h - D_g) + 2(E_{hh} + E_{gg})) \qquad (3.17) \\ &= E - 2(m-1)E_{in}(\mu) - \sum_{g<h} (q_h(D_h - D_g)) \end{aligned}$$

where we have used the assumption that the houses are ordered in line (3.17). Solving for $E_{in}(\mu)$ gives

$$E_{in}(\mu) \geq \frac{E - \sum_{g<h} q_h(D_h - D_g)}{2m-1}.$$

Thus,

$$\gamma_m(\mu) = \frac{E_{in}(\mu)}{E} \geq \frac{E - \sum_{g<h} q_h(D_h - D_g)}{(2m-1)E}.$$

Note that the above bound is only useful when the numerator is positive; otherwise, the bound becomes negative. However, it is immediate to see that $\gamma_m(\mu) \geq 0$ always, as $E_{in}(\mu)$ and E are nonnegative, which completes the proof. □

Finally, we can complete the proof of Theorem 3.5 using the above lemmas. There are two cases to consider, depending on the value of E :

Case 1: $E > \sum_{g<h} q_h(D_h - D_g)$

Plugging the bound from Lemma 3.8 into (3.12) gives

$$\frac{\max_\mu W(\mu)}{\min_{\mu \text{ is stable}} W(\mu)} = \frac{Q + \gamma_m^*}{Q + \gamma_m(\mu)} \leq \frac{\frac{\sum_{h\in H} q_h D_h}{2E} + \gamma_m^*}{\frac{\sum_{h\in H} q_h D_h}{2E} + \frac{E - \sum_{g<h} q_h(D_h - D_g)}{(2m-1)E}}$$
$$= \frac{(2m-1)\sum_{h\in H} q_h D_h + 2(2m-1)E\gamma_m^*}{(2m-1)\sum_{h\in H} q_h D_h + 2E - 2\sum_{g<h} q_h(D_h - D_g)}$$

Using Lemma 3.13 to substitute for $\sum_{h\in H} q_h D_h$ is then enough to complete the proof in this case, after some algebra using the fact that $\gamma_m^* \leq 1$.

Case 2: $E \leq \sum_{g<h} q_h(D_h - D_g)$

In this case, Lemma 3.8 states that $\gamma_m(\mu) \geq 0$. Using this bound and plugging into (3.12) gives

$$\frac{\max_\mu W(\mu)}{\min_{\mu \text{ is stable}} W(\mu)} = \frac{Q + \gamma_m^*}{Q + \gamma_m(\mu)} \leq 1 + \frac{\gamma_m^*}{Q} \tag{3.18}$$

Note that $Q > 0$ as long as $E > 0$ because we are given that $E \leq \sum_{g<h} q_h(D_h - D_g)$ in this case. Further, note that the case of $E = 0$ is trivial because all matchings have the same welfare and so the price of anarchy is 1.

Using $E \leq \sum_{g<h} q_h(D_h - D_g)$ we have

$$Q \geq \frac{\sum_{h\in H} q_h D_h}{2\sum_{g<h} q_h(D_h - D_g)}. \tag{3.19}$$

Combining (3.18) and (3.19) and again using Lemma 3.13 is then enough to complete the proof in this case, after some algebra.

One final remark about this proof is that in the special case of $D_h = 0$ a tighter bound holds. Specifically, the price of anarchy is bounded by $(2m-1)\gamma_m^*$ in this case.

3.7.2 Proof of Theorem 3.6

The proof of Theorem 3.6 follows the same structure as the proof of Theorem 3.5, with a few added complexities that cause the bound to become weaker.

To begin, we again derive a bound on the cross-edges.

Lemma 3.9. *Let $w(s,t) \in \mathbb{R}^+ \cup \{0\}$ for all students s,t and let $D_h \in \mathbb{R}^+ \cup \{0\}$ for all houses h. If a matching μ is stable, then for all houses h and g,*

$$E_{hg} \leq \max(q_h(D_h - D_g), q_g(D_g - D_h)) + 2(E_{hh} + E_{gg}) + q_{max}w_{max}.$$

Proof. Using the conditions of stability from Definition 6 for the one-sided market and Lemmas 3.14 and 3.15 from Section 3.8, we have three cases.

Case 1: If there exists $s \in \mu(h)$ such that $\alpha_\mu(s,g) > w(s,t)$ for all $t \in \mu(g)$ then, by Lemma 3.14, if μ is stable, it follows that

$$E_{gh} \leq q_g(D_g - D_h) + 2E_{gg} + q_g w_{max}.$$

Case 2: If there exists $t \in \mu(g)$ such that $\alpha_\mu(t,h) > w(s,t)$ for all $s \in \mu(h)$ then, by Lemma 3.14, if μ is stable, it follows that

$$E_{hg} \leq q_h(D_h - D_g) + 2E_{hh} + q_h w_{max}.$$

Case 3: If there does not exist $s \in \mu(h)$ such that $\alpha_\mu(s,g) > w(s,t)$ and there does not exist $t \in \mu(g)$ such that $\alpha_\mu(t,h) > w(s,t)$, for all $t \in \mu(g), s \in \mu(h)$ respectively, then, by Lemma 3.15, if μ is stable, it follows that

$$E_{hg} \leq \max(q_h(D_h - D_g), q_g(D_g - D_h)) + 2(E_{hh} + E_{gg}) + q_{max}w_{max}.$$

Given any matching μ, it must fall into one of the three cases above. Thus, if μ is exchange stable, it follows that one of the three bounds above holds. Because the edges are undirected, $E_{hg} = E_{gh}$, we can combine the three bounds to conclude that,

if μ is stable,

$$E_{hg} \leq \max(q_h(D_h - D_g), q_g(D_g - D_h)) + 2(E_{hh} + E_{gg}) + q_{max}w_{max}$$

□

Next, we use the above to prove a lower bound on $\gamma_m(\mu)$.

Lemma 3.10. *Let $w(s,t) \in \mathbb{R}^+ \cup \{0\}$. If a matching μ is stable, then*

$$\gamma_m(\mu) \geq \max\left(\frac{E - \sum_{g<h} q_h(D_h - D_g) - \binom{m}{2} q_{max}w_{max}}{(2m-1)E}, 0\right)$$

Proof.

$$\begin{aligned} E_{in}(\mu) &= E - \sum_{g<h} E_{gh} \\ &\geq E - \sum_{g<h} (q_h(D_h - D_g) + 2(E_{hh} + E_{gg}) + q_{max}w_{max}) \qquad (3.20) \\ &= E - 2(m-1)E_{in}(\mu) - \sum_{g<h} (q_h(D_h - D_g)) - \binom{m}{2} q_{max}w_{max} \end{aligned}$$

where line (3.20) follows from the assumption that the houses are ordered.

Solving for $E_{in}(\mu)$ gives

$$E_{in}(\mu) \geq \frac{E - \sum_{g<h} q_h(D_h - D_g) - \binom{m}{2} q_{max}w_{max}}{2m-1},$$

and thus

$$\gamma_m(\mu) = \frac{E_{in}(\mu)}{E} \geq \frac{E - \sum_{g<h} q_h(D_h - D_g) - \binom{m}{2} q_{max}w_{max}}{(2m-1)E}.$$

This bound is only relevant when $E > \sum_{g<h} q_h(D_h - D_g) + \binom{m}{2} q_{max}w_{max}$. Otherwise, the bound becomes negative, in which case we use the fact that $\gamma_m(\mu) \geq 0$ always, as $E_{in}(\mu)$ and E are nonnegative. □

Finally, we can complete the proof of Theorem 3.6 using the lemmas above. There are two cases to consider, depending on the value of E.

Case 1: $E > \sum_{g<h} q_h(D_h - D_g) + \binom{m}{2} q_{max} w_{max}$

Plugging the bound from Lemma 3.10 into (3.12) gives

$$\frac{\max_\mu W(\mu)}{\min_{\mu \text{ is stable}} W(\mu)} = \frac{Q + \gamma_m^*}{Q + \gamma_m(\mu)} \leq \frac{\frac{\sum_{h \in H} q_h D_h}{2E} + \gamma_m^*}{\frac{\sum_{h \in H} q_h D_h}{2E} + \frac{E - \sum_{g<h} q_h(D_h - D_g) - \binom{m}{2} q_{max} w_{max}}{(2m-1)E}}$$
$$= \frac{(2m-1)\sum_{h \in H} q_h D_h + 2(2m-1)E\gamma_m^*}{(2m-1)\sum_{h \in H} q_h D_h + 2E - 2\sum_{g<h} q_h(D_h - D_g) - 2\binom{m}{2} q_{max} w_{max}}$$

Using Lemma 3.13 to substitute for $\sum_{h \in H} q_h D_h$, the bound becomes, after some algebra,

$$\frac{\max_\mu W(\mu)}{\min_{\mu \text{ is stable}} W(\mu)} \leq (1 + 2(m-1)\gamma_m^*) \left(\frac{2(m-1)E + \sum_{g<h} q_h(D_h - D_g)}{2(m-1)E + \sum_{g<h} q_h(D_h - D_g) - 2(m-1)\binom{m}{2} q_{max} w_{max}} \right).$$

Using $E \geq \sum_{g<h} q_h(D_h - D_g) + \binom{m}{2} q_{max} w_{max}$, we have, after some algebra,

$$\frac{\max_\mu W(\mu)}{\min_{\mu \text{ is stable}} W(\mu)} \leq (1 + 2(m-1)\gamma_m^*) \left(1 + \frac{2(m-1)\binom{m}{2} q_{max} w_{max}}{(2m-1)\sum_{g<h} q_h(D_h - D_g)} \right).$$

Case 2: $E \leq \sum_{g<h} q_h(D_h - D_g) + \binom{m}{2} q_{max} w_{max}$

In this case, Lemma 3.10 states that $\gamma_m(\mu) \geq 0$. Using this bound and plugging into (3.12), we have

$$\frac{\max_\mu W(\mu)}{\min_{\mu \text{ is stable}} W(\mu)} = \frac{Q + \gamma_m^*}{Q + \gamma_m(\mu)} \leq 1 + \frac{\gamma_m^*}{Q}.$$

Using $E \leq \sum_{g<h} q(D_h - D_g) + \binom{m}{2} q_{max} w_{max}$ we have

$$Q \geq \frac{\sum_{h \in H} q_h D_h}{2\sum_{g<h} q_h(D_h - D_g) + 2\binom{m}{2} q_{max} w_{max}}.$$

and so the price of anarchy becomes, again using Lemma 3.13,

$$\frac{\max_\mu W(\mu)}{\min_{\mu \text{ is stable}} W(\mu)} \leq 1 + 2(m-1)\gamma_m^* + \frac{2\binom{m}{2} q_{max} w_{max}}{\sum_{h \in H} q_h D_h}.$$

We can combine the two cases into one (looser) bound,

$$\frac{\max_\mu W(\mu)}{\min_{\mu \text{ is stable}} W(\mu)} \leq 1 + 2(m-1)\gamma_m^* + \frac{2(m-1)q_{max}w_{max}}{D_\Delta}.$$

3.8 Appendix: Technical lemmas

This section includes the lemmas used in the proofs of Theorems 3.5 and 3.6.

Lemma 3.11. *Let $w(s,t) \in \{0,1\}$ for all students s,t and let $D_h \in \mathbb{Z}^+ \cup \{0\}$ for all h. Let μ be a stable matching. If there exists a student $s \in \mu(h)$ such that $\alpha_\mu(s,g) > 1$ for some other house g, then $E_{gh} \leq q_g(D_g - D_h) + 2E_{gg}$.*

Proof. Since μ is stable, then for all $t \in \mu(g)$, (s,t) must satisfy at least one of the three conditions stated in the definition of exchange stability (Definition 6). However, for all $t \in \mu(g)$,

$$\alpha_\mu(s,g) > 1 \geq w(s,t).$$

Thus, (s,t) cannot satisfy conditions 1 or 3. Therefore, it must satisfy condition 2, which implies that for all $t \in \mu(g)$

$$\alpha_\mu(t,h) < w(s,t) \leq 1.$$

Since $D_h, w(s,t) \in \mathbb{Z}^+ \cup \{0\}$ we have that $\alpha_\mu(t,h) \in \mathbb{Z}^+ \cup \{0\}$, and so

$$\alpha_\mu(t,h) < 1 \implies \alpha_\mu(t,h) \leq 0, \ \forall\, t \in \mu(g).$$

Summing over all $t \in \mu(g)$ gives

$$\sum_{t \in \mu(g)} \alpha_\mu(t,h) \leq 0.$$

Using the definition of α, we have

$$\sum_{t \in \mu(g)} \left(D_h - D_g + \sum_{x \in \mu(h)} w(t,x) - \sum_{x \in \mu(g)} w(t,x) \right) \leq 0.$$

Simplifying the above yields

$$q_g(D_h - D_g) + E_{gh} - 2E_{gg} \leq 0,$$

from which the desired bound follows. □

Lemma 3.12. *Let $w(s,t) \in \{0,1\}$ for all students s,t, and let $D_h \in \mathbb{Z}^+ \cup \{0\}$ for all houses h. Let μ be a stable matching and let $q_h = q \geq 2$ and/or $D_h = D \in \mathbb{Z}^+ \cup \{0\}$ for all h. If (i) there does not exist an $s \in \mu(h)$ such that $\alpha_\mu(s,g) > 1$ and (ii) there does not exists $a \in \mu(g)$ such that $\alpha_\mu(t,h) > 1$, then*

$$E_{hg} \leq \max(q_h(D_h - D_g), q_g(D_g - D_h)) + 2(E_{hh} + E_{gg})$$

Proof. It follows from the assumptions in the theorem statement that the students in houses h and g can be partitioned into 6 sets based on their house and α values (either 1, 0, or negative), as shown in Figure 3.9.

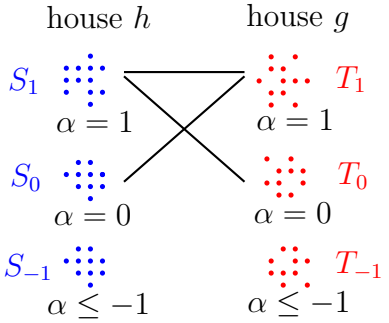

Figure 3.9: Partition of students based on α function

Let S_0, S_1, and S_{-1} denote the set of students in house h such that $\alpha_\mu(s,g) = 0$, $\alpha_\mu(s,g) = 1$, and $\alpha_\mu(s,g) \leq -1$, respectively. For convenience, we use the same notation for the set and the number of students in the set, e.g., $|S_1| = S_1$ The same

conventions apply to the T variables and students in house g. Two sets are connected with a black line in Figure 3.9 if all students in one set must be connected to all students in the other set. These connections follow from the conditions of stability in Definition 6. This gives us 3 constraints:

1. if $\alpha_\mu(s, g) = 1$ and $\alpha_\mu(t, h) = 1$ then $w(s, t) = 1$
2. if $\alpha_\mu(s, g) = 1$ and $\alpha_\mu(t, h) = 0$ then $w(s, t) = 1$
3. if $\alpha_\mu(s, g) = 0$ and $\alpha_\mu(t, h) = 1$ then $w(s, t) = 1$

These constraints give us a lower bound on the edges between houses h and g.

$$\sum_{t \in \mu(g)} \sum_{x \in \mu(h)} w(t, x) \geq S_1 T_1 + S_1 T_0 + S_0 T_1 \tag{3.21}$$

To prove the theorem, we want to find an upper bound on the cross edges, E_{hg}, so we relate the edges in the graph to the sum of the α values using the definition of the α function.

$$\sum_{s \in \mu(h)} \alpha_\mu(s, g) = q_h(D_g - D_h) + E_{hg} - 2E_{hh} \tag{3.22}$$

Since the students in each house are partitioned by their α values, we can bound this sum as:

$$\sum_{s \in \mu(h)} \alpha_\mu(s, g) \leq S_1 - S_{-1} \tag{3.23}$$

Combining (3.22) and (3.23) gives

$$E_{hg} \leq q_h(D_h - D_g) + 2E_{hh} + S_1 - S_{-1} \tag{3.24}$$

To continue, we need to find an upper bound on the quantity $S_1 - S_{-1}$. To do this, we start by lower bounding E_{gg}.

$$2E_{gg} = \sum_{t \in \mu(g)} \sum_{x \in \mu(g)} w(t, x)$$

Recalling the definition of α in (3.14) gives

$$\sum_{x\in\mu(g)} w(t,x) = D_h - D_g + \sum_{x\in\mu(h)} w(t,x) - \alpha_\mu(t,h).$$

Combining the previous two equations yields

$$\begin{aligned} 2E_{gg} =& \sum_{t\in\mu(g)} \left(D_h - D_g + \sum_{x\in\mu(h)} w(t,x) - \alpha_\mu(t,h) \right) \\ =& q_g(D_h - D_g) + \sum_{t\in\mu(g)} \sum_{x\in\mu(h)} w(t,x) - \sum_{t\in\mu(g)} \alpha_\mu(t,h). \end{aligned}$$

Using inequalities (3.21) and (3.23) gives

$$S_1T_1 + S_1T_0 + S_0T_1 - (T_1 - T_{-1}) \leq 2E_{gg} + q_g(D_g - D_h) \tag{3.25}$$

We can now use the above to find an upper bound on $S_1 - S_{-1}$. To do this, we relate the left-hand side of the above inequality to $S_1 - S_{-1}$.

Specifically, let $f(S_1, S_0, S_{-1}, T_1, T_0, T_{-1}) = S_1T_1 + S_1T_0 + S_0T_1 - T_1 + T_{-1} - (S_1 - S_{-1})$. It is possible to show using elementary techniques that this function is nonnegative, and thus that

$$S_1 - S_{-1} \leq S_1T_1 + S_1T_0 + S_0T_1 - T_1 + T_{-1} \tag{3.26}$$

We omit the details for brevity. Note, however that the inequality in (3.26) holds only for the case where $q_h = q$ for all $h \in H$. In the case where the quotas are not equal but $D_h = D$ for all $h \in H$, the proof technique differs slightly, but still yields $S_1 - S_{-1} \leq 2E_{gg}$, from which the result follows.

Finally, combining (3.25) and (3.26) gives

$$\begin{aligned} S_1 - S_{-1} &\leq S_1T_1 + S_1T_0 + S_0T_1 - T_1 + T_{-1} \\ &\leq 2E_{gg} + q_g(D_g - D_h) \end{aligned}$$

To complete the proof we now plug the above into (3.24) to get

$$\begin{aligned} E_{hg} \leq & q_h(D_h - D_g) + 2E_{hh} + 2E_{gg} + q_g(D_g - D_h) \\ & \leq \max(q_h(D_h - D_g), q_g(D_g - D_h)) + 2(E_{hh} + E_{gg}). \end{aligned}$$

where the final step follows from noting that at most one of $D_h - D_g$ and $D_g - D_h$ is strictly positive. □

Lemma 3.13.

$$\frac{\sum_{g<h\in H} q_h(D_h - D_g)}{\sum_{h\in H} q_h D_h} \leq m - 1$$

Proof. Without loss of generality assume the houses are ordered so that if $g < h$, then $D_g < D_h$. The following inequalities hold simply because q_h, q_g, D_h, D_g are all nonnegative values.

$$\begin{aligned} \frac{\sum_{g<h\in H} q_h(D_h - D_g)}{\sum_{h\in H} q_h D_h} &\leq \frac{\sum_{g<h\in H}(q_h D_h + q_g D_g)}{\sum_{h\in H} q_h D_h} \\ &\leq \frac{\sum_{h\in H}\sum_{g\neq h\in H} q_h D_h}{\sum_{h\in H} q_h D_h} \\ &= \frac{\sum_{h\in H}(m-1) q_h D_h}{\sum_{h\in H} q_h D_h} \\ &= m - 1 \end{aligned}$$

□

The remaining lemmas parallel the above lemmas, but are used for proving Theorem 3.6, and thus apply in more-general settings.

Lemma 3.14. *Let $w(s,t) \in \mathbb{R}^+ \cup \{0\}$ for all students s, t, and let $D_h \in \mathbb{R}^+ \cup \{0\}$ for all $h \in H$. Consider a stable matching μ. If there exists an $s \in \mu(h)$ such that $\alpha_\mu(s,g) > w(s,t)$ for all $t \in \mu(g)$, then $E_{gh} < q_g(D_g - D_h) + 2E_{gg} + q_g w_{max}$.*

Proof. By assumption, there exists a student in h that strictly wants to swap with any student in house g. It then follows from the stability of μ that *all* students in g

must strictly oppose the swap (i.e., $\alpha_\mu(t,h) < w(s,t)$). This gives

$$D_h - D_g + \sum_{x \in \mu(h)} w(t,x) - \sum_{x \in \mu(g)} w(t,x) < \ w(s,t) < \ w_{max},$$

for all $t \in \mu(g)$. Summing the above equation over $t \in \mu(g)$ then yields

$$q_g(D_h - D_g) + E_{gh} - 2E_{gg} < q_g w_{max}$$

Rearranging the previous equation completes the proof. □

Lemma 3.15. *Let $w(s,t) \in \mathbb{R}^+ \cup \{0\}$ for all students s,t, and let $D_h \in \mathbb{R}^+ \cup \{0\}$ for all $h \in H$. Consider a stable matching μ. If (i) there does not exist an $s \in \mu(h)$ such that $\alpha_\mu(s,g) > w(s,t)$ for all $t \in \mu(g)$ and (ii) there does not exist $t \in \mu(g)$ such that $\alpha_\mu(t,h) > w(s,t)$ for all $s \in \mu(h)$, then*

$$E_{hg} \leq \max(q_h(D_h - D_g), q_g(D_g - D_h)) + 2(E_{hh} + E_{gg}) + q_{max} w_{max}$$

Proof. Conditions (i) and (ii) are equivalent to requiring

$$\forall s \in \mu(h), D_g - D_h + \sum_{x \in \mu(g)} w(s,x) - \sum_{x \in \mu(h)} w(s,x) \leq w(s,t) \ \forall t \in \mu(g)$$

and

$$\forall t \in \mu(g), D_h - D_g + \sum_{x \in \mu(h)} w(t,x) - \sum_{x \in \mu(g)} w(t,x) \leq w(s,t) \ \forall s \in \mu(h)$$

To complete the proof we simply sum these two bounds using $w(s,t) \leq w_{max}$ and $E_{gh} = E_{hg}$. □

Chapter 4

Epidemics

4.1 Introduction

Epidemic models attempting to quantify how diseases are transmitted have been extensively studied since the Kermack-McKendrick SIR (Susceptible-Infectious-Recovered) model was proposed in 1927 [72]. Though initially these models were proposed to understand the spread of contagious diseases, the insights learned from them apply to many other settings where something spreads through a population of agents. For example, applications such as (i) network security, where the goal is to understand and limit the spread of computer viruses [34], [129], [37] (ii) viral advertising, where the goal is to create an epidemic to propagate interest in a product [104], [111], and (iii) information propagation, where the goal is to understand how quickly new ideas propagate through a network [65], [68], [32], can all be understood through the lens of epidemic models. See [67] and [39] for comprehensive surveys of prior results.

Most epidemic models focus on determining the existence and stability of system equilibria for various diseases, applying Lyapunov's stability theory to the SIS (Susceptible-Infected-Susceptible) infection model. Early models assume a well-mixed population [4]; i.e., any node can infect any other node. In practice, however, this is rarely the case, motivating the study of epidemics where the interaction of the agents is limited to a network, such as [102, 100, 101, 24, 12, 130, 33]. Some of this work examines possible containment or immunization schemes to minimize the final number of infected nodes, or eradicate the disease entirely. See [33, 103, 34, 90] for

some of these results. Other work applies techniques from percolation theory to the SIR model, attempting to answer whether an infection can start from a random node in a network and infect a giant component of the graph, e.g., [91, 92, 71]. Regardless of the infection model, most of this work focusses on the long-term behavior of the system.

Though understanding the extent to which an infection spreads is an important question in itself, these models can be even more useful in understanding the *cost* of an epidemic. Within the medical community, there is a growing trend to quantify the cost of an epidemic by looking at the direct and indirect medical costs to both the hospitals and doctors treating and immunizing a population for specific diseases, as well as the cost to individuals in the population paying for medical care. See [27] and [117] for two examples of such studies. This interest in cost, both the cost of disease and the cost of immunization, is the motivation for the current paper. There is little existing work in the modeling community studying this cost, since any such calculation depends on the transient behavior of the epidemic model that is often hard to analyze mathematically. This paper attempts to fill this void.

In this paper, we assume an SIS model of infection, as in [130], [33], and [103], on a random network that is a variant of the generalized Erdös-Rényi random graph with arbitrary degree distributions [35, 94] and define the cost or the economic impact of such an epidemic. Our main contribution is the derivation of (i) the exact cost of an epidemic in the large graph limit (Theorem 4.1) and (ii) bounds on this cost for a given graph (Theorem 4.3). We further provide an optimal scheme for random one-time vaccination, minimizing the total cost of the epidemic, including both disease and immunization costs. All our results are validated through extensive simulations.

In the derivation of our results, we make use of several techniques from random matrix theory. We refer the reader to [45, 3] for further details on this subject. Random matrix theory has found applications in wireless communications [126] and in the analysis of random graphs [128]. In this paper, we apply ideas from the Stieltjes transform [126, 125] to analyze the epidemic process on a random network. To the best of our knowledge, our approach using random matrices is novel to the study of

epidemic processes and we hope to extend it in further research.

The paper is organized as follows. We introduce a random network model in Section 4.2 and the infection process in Section 4.3. Using this framework, we define and compute the cost of an epidemic in Section 4.4. In Section 4.5, we verify the assumptions of our model and results through extensive simulations. Finally, we discuss extensions and conclude in Sections 4.6 and 4.7, respectively.

4.2 Network model

There are two major components to the model studied in this paper: the model of the underlying network and the model of the infection process. We discuss the model of the network here and then move to the model of the infection process in the next section.

Our network model is related to the "configuration" model in [94] and the "general random graph" model from [35]; however, the model we use is slightly more general than each.

In particular, let A be an $n \times n$ adjacency matrix corresponding to the network, where there are n nodes in the population and $A_{ij} = 1$ if there exists a relationship from node i to node j. For the purposes of this paper, we only consider undirected graphs; i.e., $A_{ij} = A_{ji}$. We assume that the network is drawn from a general class of random graphs, $\mathcal{G}$. For example, the network represented by A could be a realization of an Erdös-Rényi random graph, $G_{n,p}$, which would correspond to allowing each edge to exist independently with probability p.

The construction of the graph proceeds as follows. First, define a degree distribution $p(\cdot)$, and obtain n i.i.d. samples $w = (w_1, \ldots, w_n)$. From this vector, generate a random graph given by the adjacency matrix:

$$A_{ij} = A_{ji} = \begin{cases} 1 & \text{w.p. } w_i w_j \rho \\ 0 & \text{w.p. } 1 - w_i w_j \rho \end{cases} \quad \text{where } \rho = \frac{1}{\sum_i w_i}. \tag{4.1}$$

Note that the expected degree of node i is $\sum_j w_i w_j \rho = w_i$. Since this model is fully determined by one degree distribution $p_n(\cdot)$, for ease of reference, we call it $G_{n,p_n(\cdot)}$.

Example 8. *To generate the Erdös-Rényi random graph $G_{n,p}$, let $p_n(w) = \delta(w - np)$, where $\delta(\cdot)$ is the Dirac δ-function. Thus, $w = (np, np, \ldots, np)$ and for all nodes i and j, $A_{ij} = 1$ with probability p. With our notation, we denote the graph $G_{n,\delta(w-np)}$. Two example networks generated according to our model are shown in Figure 4.1. The p is chosen just beyond the threshold for connectivity.*

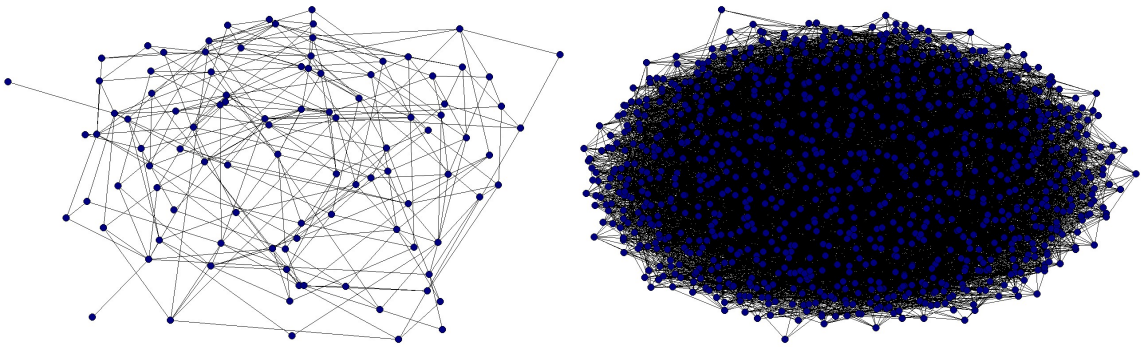

(a) $n = 100, p = 0.0561$ (b) $n = 1000, p = 0.0169$

Figure 4.1: Sample Erdös-Rényi random graphs

Example 9. *To generate a random graph with an exponential degree distribution, let $p(w) = \lambda e^{-\lambda w}$. Following the construction outlined above, the resulting graph will have n nodes with average degree λ^{-1}. Example graphs with 100 and 1000 nodes and mean degree 6 ($\lambda = 1/6$) are shown in Figure 4.2.*

Example 10. *To generate a random graph with a power-law degree distribution, (specifically, a Pareto distribution), let $p(w) = \frac{\theta}{w^{\theta+1}}$. Following the construction outlined above, the resulting graph will have n nodes with average degree $\frac{\theta}{\theta-1}$. Two example graphs with $\alpha = 1.5$ (mean degree 3) are shown in Figure 4.3.*

Clearly the $G_{n,p_n(\cdot)}$ model is quite general. To relate this model to the configuration model [94] and the general random graph model [35], note that in the case of the configuration model the degree sequence is enforced deterministically and that in the

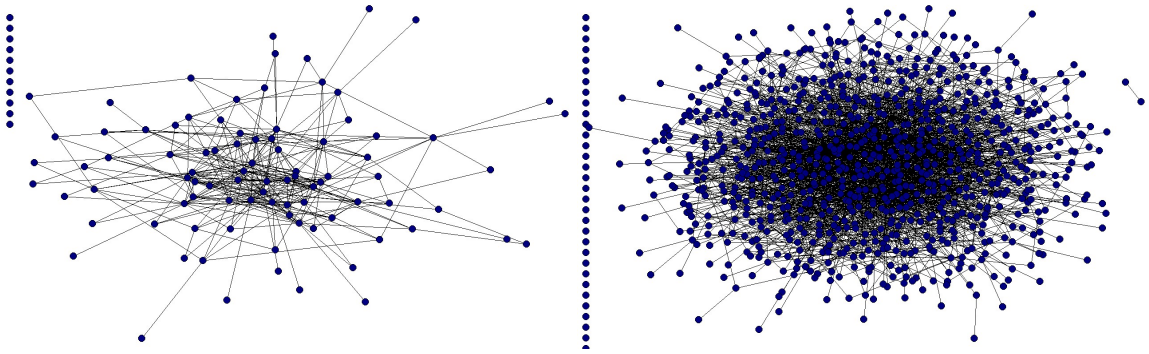

(a) $n = 100$ (b) $n = 1000$

Figure 4.2: Sample exponential random graphs with $\lambda = \frac{1}{6}$

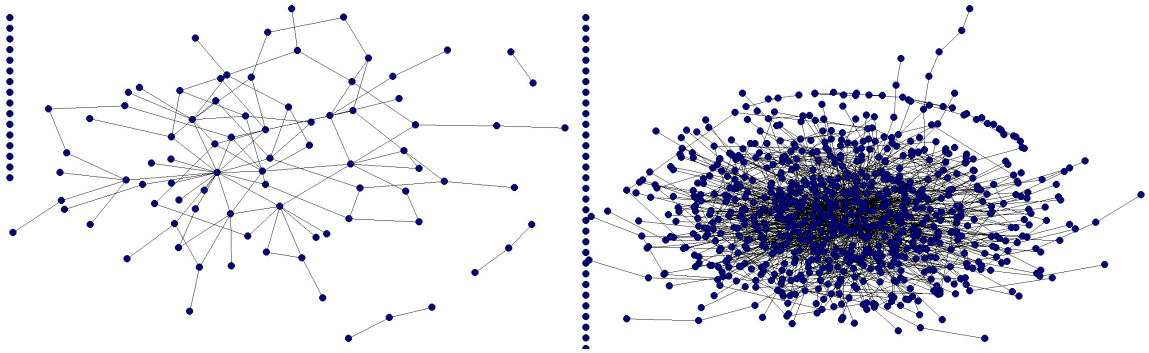

(a) $n = 100$ (b) $n = 1000$

Figure 4.3: Sample power law (Pareto, $\theta = 1.5$) random graphs

general random graph model the expected degree sequence is fixed rather than the distribution. However, note (like the two models it generalizes) the model we consider here does not exhibit clustering.

4.3 Infection model

In this section, we describe the infection process that is the focus of this paper. It is based on the SIS (Susceptible-Infected-Susceptible) epidemic model. In this formulation, each node in the population transitions between two possible states, i.e., *susceptible* and *infected*. The process is characterized by two parameters, i.e., δ and β that represent the recovery rate and the infection rate, respectively. Time is taken to be discrete and events proceed in each time-step as follows:

1. If node i is infected, it recovers with probability δ. Note that it cannot be infected in the same time-step in which it recovers.

2. If node i is susceptible, it becomes infected by each of its neighbors with i.i.d. probability β.

In its full generality, this model of SIS infection spread on a network is difficult to analyze. Thus, it is imperative that we make simplifying approximations to arrive at a mathematically tractable formulation. To that end, we study a linear infection spread model commonly used in the literature that was first derived in [130]. We also describe in detail the sequence of approximations used to derive the linear spread.

First, let us introduce some notation. Consider a graph G on n nodes over which the epidemic process runs. Let $A_{n\times n}$ denote its adjacency matrix. Note that the graph can be one sample of the random graph model presented in the previous section or it might just be a fixed graph. Define the $n \times 1$ vector $P(t)$ where $P_i(t)$ denotes the probability that node i is infected at time t. Using this notation, the linear dynamics of the infection process are given as:

$$P(t+1) = \left[\underbrace{(1-\delta)I}_{:=M_1} + \underbrace{\beta A}_{:=M_2} \right] P(t). \tag{4.2}$$

where I is the $n \times n$ identity matrix. The probability of infection at time $t+1$ has contributions from two terms, i.e., $M_1P(t)$ and $M_2P(t)$. The first term is the contribution from the nodes that are infected at time t and do not recover in the next time-step with probability $1-\delta$. Infected neighbors contributes to the second term $M_2P(t)$ through the adjacency matrix of the graph. Define the *system matrix* of the epidemic process as:

$$M = (1-\delta)I + \beta A \tag{4.3}$$

Note that in the special case when the infection begins with α-fraction of the nodes infected at time $t = 0$, we have $P(0) = \alpha 1$, where '1' denotes an $n \times 1$ vector

of all ones. Thus, $P(t)$ can be rewritten as:

$$P(t) = M^t P(0) = \alpha M^t 1. \tag{4.4}$$

The above linear system is a commonly adopted approximation for the SIS model and, has been used in the literature, e.g., in [33, 103, 130].

In this paper, we consider a discrete-time model of the infection process. However, there is also a large literature that considers continuous-time models, e.g., [101, 102, 24, 12]. Interestingly, the mean field equation describing the system dynamics in the continuous-time setting is an exact analog of (4.8) and hence the results of our analysis can be generalized to the continuous-time case.

We now provide a derivation of (4.2) that clearly delineates all the approximations involved in going from the networked SIS model to the linear system model in (4.2).

Let $\mathcal{N}_i$ be the set of neighbors of the i-th node. Consider a sample path s of the disease propagation. In the sample path s, let $P_i^{(s)}(t)$ denote the probability of node i being infected at time t in s. We analyze the quantity $P_i^{(s)}(t+1)$ by conditioning it on the state of the node i at time t in s. Define the random variable $X_i^{(s)}(t)$ as the number of infected neighbors of i if it is not infected at t in s. If node i is infected at t in s, we set $X_i^{(s)}(t) = 0$. We conclude from the infection spreading process that the probability that node i does not get infected at $t+1$, given that it was susceptible at the last time-step, is $(1-\beta)^{X_i^{(s)}(t)} \approx 1 - \beta X_i^{(s)}(t)$. This approximation is valid, assuming β is small. Thus we can write an expression for $P_i^{(s)}(t+1)$ as:

$$P_i^{(s)}(t+1) = (1-\delta)P_i^{(s)}(t) + \beta X_i^{(s)}(t)(1 - P_i^{(s)}(t)). \tag{4.5}$$

We take expectation over all sample paths in (4.5) and make use of the fact that $P_i(t)$ is the expectation of $P_i^{(s)}(t)$ over all sample paths to obtain:

$$P_i(t+1) = (1-\delta)P_i(t) + \beta\, \mathbb{E}_s \left[\left(1 - P_i^{(s)}(t)\right) \cdot X_i^{(s)}(t) \right] \tag{4.6}$$

Now, we approximate by assuming the terms inside the expectation in (4.6) to be independent:

$$P_i(t+1) \approx (1-\delta)P_i(t) + \beta(1-P_i(t)) \cdot \mathbb{E}_s[X_i^s(t)]. \tag{4.7}$$

Of course the terms inside the expectation in (4.6) are not generally independent. But, such an approximation may be "reasonable" when the deviations of $X_i^{(s)}(t)$ are not too far from its expectation over all sample paths. One may expect this to be true for light-tailed degree distributions, but not for heavy-tailed degree distributions.

Now, we evaluate $\mathbb{E}_s[X_i^{(s)}(t)]$. Note that it is the sum of the probabilities of the neighbors of node i being infected given that node i itself is susceptible at time t in s. We approximate this quantity by dropping the conditioning on node i being susceptible at t in s. This approximation is again valid if the number of infected neighbors is not too different for nodes that have different degrees. If the degree distribution is not too heavy-tailed, we expect this to be "reasonable." Thus, we have $\mathbb{E}_s[X_i^{(s)}(t)] \approx \sum_{j \in \mathcal{N}_i} P_j(t)$. Combining this, we get the following nonlinear recursion:

$$P_i(t+1) \approx (1-\delta)P_i(t) + \beta(1-P_i(t)) \sum_{j \in \mathcal{N}_i} P_j(t) \tag{4.8}$$

We linearize this and express it in matrix-vector form as:

$$P(t+1) \approx \left[(1-\delta)I + \beta A\right] P(t),$$

Note that the approximations made in the derivation above highlight that we should not expect the linear system in (4.3) to accurately model SIS infection spread in all settings. However, it should be a good approximation when the infection rate is small and when the degree distribution is light-tailed. We should expect the accuracy to degrade as the infection rate grows or the tail of the degree distribution becomes heavier. In Section 4.5, we provide simulations to better understand the relationship of the accuracy of approximation with these parameters of the epidemic model.

4.4 Epidemic cost

Given the network and infection models described previously, we can now discuss the *cost* of an epidemic on a network. As mentioned previously, a key contribution of this paper is to provide analytic results characterizing the cost of an epidemic over its entire lifetime. This includes the effects of the *transient* behavior of the epidemic, which is typically difficult to study.

To determine the cost of a disease, we consider a simple model where c_d is defined as the cost of an individual being infected during a single time-step. Thus, c_d can capture both the direct costs to the individual for medication, doctor visits, etc., as well as secondary costs such as missed work. We note that this model leaves open the question of how exactly to determine the parameter c_d. This is ongoing work within the medical community; see [27, 117] for example studies in this area. In future work we expect to incorporate these results to obtain a more accurate cost of various diseases, but for the purposes of this paper, we leave it as a general parameter of the model. Note also that this section only concerns the cost of the disease; it does not include the cost of any strategy to contain or control the epidemic, such as immunization. In Section 4.6 we discuss minimizing the total cost of both the disease and the given containment strategy.

Given this model for the cost of disease to an individual, we can formalize the total social cost of an epidemic. To begin, assume some fraction $\alpha < 1$ of the nodes are infected at time $t = 0$. Denote the epidemic process on a network by the 5-tuple $(G, \delta, \beta, \alpha, c_d)$, where G is the network, δ, β and α define the infection parameters, and c_d defines the cost parameter. Define $C_D(n)$, the "disease cost", as the expected (averaged over the random spread of the disease) per-node disease cost of an epidemic *during its entire course*. Since the infection propagation is stochastic in nature, the cost for a given tuple $(G, \delta, \beta, \alpha, c_d)$ will be a random variable, and $C_D(n)$ denotes the expected value of this quantity when averaged over all infection propagation paths. To express it in closed form, note that the expected per-node disease cost in a *given time-step* t is simply $\frac{1^T P(t)}{n}$. Furthermore, since $P(0) = \alpha \mathbf{1}$ and $P(t) = M^{t-1}P(0)$,

we can express the disease cost per-node as

$$C_D(n) := \frac{1}{n}\left[\mathbf{1}^T\left(\sum_{t=0}^{\infty} M^t\right)\mathbf{1}\alpha c_d\right]. \tag{4.9}$$

When the infinite sum converges, i.e., when $||M|| < 1$, the disease will eventually die out, and we have

$$C_D(n) = \frac{1}{n}\alpha c_d[\mathbf{1}^T(I-M)^{-1}\mathbf{1}]. \tag{4.10}$$

We emphasize that the above expression is averaged over all possible infection propagation paths, but is a random variable when the underlying network is a random graph. However, we show that this cost converges almost surely to a deterministic constant when the network is drawn randomly according to our model (under certain conditions) and can be explicitly computed.

In Section 4.4.1, we explore the cost in (4.10) in the asymptotic regime, i.e., in the large graph limit as $n \to \infty$, letting the degree distribution and the infection rate to vary with the population size. Specifically, the degree distribution for a population of size n is $p_n(\cdot)$ and the infection rate is β_n. We compute $C_D(n)$ associated with the epidemic process defined by $\left(G_{n,p_n(\cdot)}, \delta, \beta_n, \alpha, c_d\right)$. Note that a fixed n is a special case; i.e., the case where the degree distribution and infection rate do not scale with n is subsumed in our result. In Section 4.4.3, we provide a bound for the cost of the disease over a fixed graph. Further, in Section 4.5, we illustrate these results through extensive simulations.

4.4.1 Asymptotic cost of disease over random graph

In this section, we compute the cost of the epidemic process $\left(G_{n,p_n(\cdot)}, \delta, \beta_n, \alpha, c_d\right)$, presenting our result formally in Theorem 4.1.

Let $w_{n\times 1}$ be n independent samples drawn according to the degree distribution $p_n(\cdot)$ and $W = \text{diag}(w)$. Consider the vector $v := \beta_n w$. Assume that $p_n(\cdot)$ and β_n scale such that the vector v behaves as n independent samples drawn from a scale invariant distribution $p(\cdot)$ that has a support $[v_{min}, \infty)$, where $v_{min} > 0$.

Define the following quantities:

$$\begin{aligned} V &:= \operatorname{diag}(v) = \beta_n W, \\ \mu &:= \left(\sum_{i=1}^{n} v_i \right)^{-1}, \\ \bar{v} &:= \mathbb{E}\, v = \int_{v_{min}}^{\infty} v p(v) dv, \\ \kappa &:= \frac{1}{\delta \sqrt{\bar{v}}} \lim_{n \to \infty} \sqrt{\beta_n}. \end{aligned}$$

Note that if $p_n(\cdot)$ and β_n do not vary with n then $\kappa > 0$. If $\beta_n \to 0$ as $n \to \infty$, then $\kappa = 0$.

Recall that for the random graph model described in Section 4.2, the off-diagonal entries of the adjacency matrix has mean and variance:

$$\begin{aligned} \mathbb{E}\, A_{ij} =& \rho w_i w_j, \\ \text{Var } A_{ij} =& \rho w_i w_j - (\rho w_i w_j)^2 \approx \rho w_i w_j. \end{aligned}$$

where $\rho = (1^T w)^{-1}$. Define the following $n \times n$ matrix C:

$$C := \frac{1}{\sqrt{n\rho}} W^{-1/2} \left(A - \rho w w^T \right) W^{-1/2} \tag{4.11}$$

$$= \sqrt{\frac{\beta_n}{n\mu}} V^{-1/2} \left(A - \frac{\mu v v^T}{\beta_n} \right) V^{-1/2}. \tag{4.12}$$

It can be verified that C is a standard Wigner matrix [125] where each off-diagonal

entry has mean zero and variance $\frac{1}{n}$. Now define the following $n \times n$ matrices:

$$Y_n^{(1)} := \frac{1}{n}\left(V^{-1} - \sqrt{\frac{\beta_n}{\delta^2 \bar{v}}}C\right)^{-1}, \tag{4.13}$$

$$Y_n^{(2)} := \frac{1}{n}\left[I - \sqrt{\frac{\beta_n}{\delta^2 \bar{v}}}V^{1/2}CV^{1/2}\right]^{-1} \tag{4.14}$$

$$Y_n^{(3)} := \frac{1}{n}\left[V^{1/2}\left(V^{-1} - \sqrt{\frac{\beta_n}{\delta^2 \bar{v}}}C\right)^{-1}V^{1/2}\right]. \tag{4.15}$$

Using these expressions, we present the technical assumption required for the proof:

Assumption 1. *For $k = 1, 2, 3$, suppose the following holds.*

$$\lim_{n\to\infty}\left[1^T\left(Y_n^{(k)}\right)1 - \mathbb{E}\,\mathrm{tr}\,Y_n^{(k)}\right] = 0 \quad a.s. \tag{4.16}$$

This essentially means that the sum of the off-diagonal entries of the matrices $Y_n^{(1)}, Y_n^{(2)}$ and $Y_n^{(3)}$ vanishes in the limit $n \to \infty$.

With this assumption and the notation presented above, we can now state the main result of this paper that calculates the disease cost $C_D(n)$:

Theorem 4.1. *For $\left(G_{n,p_n(\cdot)}, \delta, \beta_n, \alpha, c_d\right)$, if $p_n(\cdot)$ has finite variance, the system matrices are almost surely stable for all n, and Assumption 1 holds then*

$$\lim_{n\to\infty} C_D(n) = \begin{cases} \frac{\alpha c_d}{\delta}\left(1 - \frac{\bar{v}^2}{\mathbb{E}\,v^2 - \delta\bar{v}}\right) & a.s \quad \text{if } \kappa = 0, \\ \frac{\alpha c_d}{\delta}\left(1 + \kappa^2 F^2 - \frac{\kappa^2 F^2}{1 - \bar{v}/F - \delta\kappa^2\bar{v}}\right) & a.s \quad \text{if } \kappa \neq 0. \end{cases}$$

$$\text{where } F = \int_{v_{min}}^{\infty} \frac{p(v)}{v^{-1} - \kappa^2 F} dv.$$

Before we present the proof, we briefly remark on the assumptions required for the result to hold. The system matrix $M = \delta I - \beta_n A$ is assumed to be almost surely stable. Essentially, this means that the disease dies out with high probability as the epidemic process proceeds on the random network. If this assumption does not hold, the cost $(C_D(n))$ is infinite. We also assume the distribution $p_n(\cdot)$ has finite variance.

To elucidate this assumption, suppose $\beta_n = \beta$ for all n and the degree distribution $p_n(\cdot)$ is scale invariant. Thus $\kappa > 0$. In this regime, most degree distributions that do not have finite variance are heavy-tailed. It is well known [100] that over most networks with heavy-tailed degree distributions, there does not exist an infection threshold in the large-graph limit, i.e., there is no positive ratio of δ/β for which the infection dies out in these networks. Thus, since we require stability, we need not consider such networks. However, when the infection and network parameters scale with n, the connection between stability and finite variance is more involved; hence, we require the assumption of both finite variance and stability.

For the remainder of this section, we focus on the proof of Theorem 4.1.

4.4.2 Proof of Theorem 4.1

The disease cost in (4.10) can be written as

$$\begin{aligned}
\lim_{n\to\infty} C_D(n) &= \lim_{n\to\infty} \frac{\alpha}{c_d}\left[1^T(I-M)^{-1}1\right] \\
&= \lim_{n\to\infty} \frac{\alpha c_d}{n}\left[1^T\left(\delta I - \beta A\right)^{-1}1\right] \\
&= \lim_{n\to\infty} \frac{\alpha c_d}{n}\left[1^T\left(\delta I - \beta_n\sqrt{n\rho}W^{1/2}CW^{1/2} - \beta\rho w w^T\right)^{-1}1\right] \\
&= \lim_{n\to\infty} \frac{\alpha c_d}{n}\left[1^T\left(\underbrace{\delta I - \sqrt{n\beta_n\mu}V^{1/2}CV^{1/2}}_{:=X} - \mu v v^T\right)^{-1}1\right] \\
&= \lim_{n\to\infty} \frac{\alpha c_d}{n}\left[1^T\left(X - \mu v v^T\right)^{-1}1\right].
\end{aligned}$$

Applying the Matrix Inversion Lemma [64], we get

$$\begin{aligned}
\lim_{n\to\infty} C_D(n) &= \lim_{n\to\infty} \frac{\alpha c_d}{n}\left[1^T\left(X^{-1} - \frac{X^{-1}vv^TX^{-1}}{-\frac{1}{\mu} + v^TX^{-1}v}\right)1\right] \\
&= \alpha c_d \lim_{n\to\infty}\left[\left(\frac{1}{n}1^TX^{-1}1\right) - \frac{\left(\frac{1}{n}1^TX^{-1}v\right)^2}{-\frac{1}{n\mu} + \left(\frac{1}{n}v^TX^{-1}v\right)}\right]. \qquad (4.17)
\end{aligned}$$

From the Strong Law of Large Numbers, we have $\lim_{n\to\infty} n\mu = 1/\bar{v}$ almost surely. To proceed, we show that each of the terms in (4.17), i.e., $\frac{1}{n}(1^TX^{-1}1)$, $\frac{1}{n}(1^TX^{-1}v)$, and

$\frac{1}{n}(v^T X^{-1} v)$, almost surely self-average under certain technical conditions (Assumption 1) and can be computed easily using $p_n(\cdot)$, κ and δ. The result of this computation is summarized as follows:

Lemma 4.2. *If Assumption 1 holds, then*

$$(a)\ \lim_{n\to\infty} \frac{1}{n} 1^T X^{-1} v = \frac{F}{\delta} \quad a.s. \tag{4.18}$$

$$(b)\ \lim_{n\to\infty} \frac{1}{n} 1^T X^{-1} 1 = \frac{1+\kappa^2 F^2}{\delta} \quad a.s. \tag{4.19}$$

$$(c)\ \lim_{n\to\infty} \frac{1}{n} v^T X^{-1} v = \begin{cases} \mathbb{E}\, v^2 \quad a.s. & \text{if } \kappa = 0, \\ \frac{1}{\delta\kappa^2}\left(1 - \frac{\bar{v}}{F}\right) \quad a.s. & \text{if } \kappa \neq 0. \end{cases} \tag{4.20}$$

where F is the solution of the following fixed point equation:

$$F = \int_{v_{min}}^{\infty} \frac{p(v)}{v^{-1} - \kappa^2 F} dv. \tag{4.21}$$

We defer the proof of Lemma 4.2 to Appendix 4.8. Using this lemma and the fact that $\lim_{n\to\infty} n\mu = \frac{1}{\bar{v}}$ a.s. in (4.17), we have, for $\kappa \neq 0$:

$$\begin{aligned} \lim_{n\to\infty} C_D(n) &= \alpha c_d \lim_{n\to\infty} \left[\left(\frac{1}{n} 1^T X^{-1} 1 \right) - \frac{\left(\frac{1}{n} 1^T X^{-1} v\right)^2}{-\frac{1}{n\mu} + \left(\frac{1}{n} v^T X^{-1} v\right)} \right] \\ &= \alpha c_d \left(\frac{1+\kappa^2 F^2}{\delta} - \frac{\frac{F^2}{\delta^2}}{-\bar{v} + \frac{1}{\delta\kappa^2}\left(1 - \frac{\bar{v}}{F}\right)} \right) \quad \text{a.s.} \\ &= \frac{\alpha c_d}{\delta} \left(1 + \kappa^2 F^2 - \frac{\kappa^2 F^2}{1 - \bar{v}/F - \delta\kappa^2 \bar{v}} \right) \quad \text{a.s.} \end{aligned}$$

Similarly, the case for $\kappa = 0$ follows by substituting the relevant expressions from Lemma 4.2 in (4.17), which completes the proof.

4.4.3 Bounds for a fixed network

Previously we considered the asymptotic regime for the epidemic process $\left(G_{n,p_n(\cdot)}, \delta, \beta_n, \alpha, c_d\right)$ and computed the cost exactly for a specific scaling of the parameters. In this section, we fix the graph and compute the cost of the epidemic process $(G, \delta, \beta, \alpha, c_d)$. Since

the bound applies to any specific instance of the graph, it also applies to a family of graphs generated according to the random graph model in Section 4.2.

Theorem 4.3. *For $(G, \delta, \beta, \alpha, c_d)$, with a stable system matrix $M = (1-\delta)I - \beta A$, the cost of disease per-node satisfies*

$$C_D(n) \leq \frac{\alpha c_d}{1 - \lambda_{max}(M)}$$

where $\lambda_{max}(.)$ denotes the maximum eigenvalue of the corresponding matrix.

Proof. Similarly, let $\lambda_{min}(.)$ denote the mainimum eigenvalue of a matrix. From Perron-Frobenius theorem, it follows that

$$-1 < -\lambda_{max}(M) \leq \lambda_{min}(M) \leq \lambda_{max}(M) = |\lambda_{max}(M)| < 1 \tag{4.22}$$

Note that $(I - M)^{-1}$ is a positive definite matrix since all eigenvalues are positive. From (4.22), we have

$$\frac{1}{1 - \lambda(M)} \leq \frac{1}{1 - \lambda_{max}(M)}$$

and

$$1^T (I - M)^{-1} 1 \leq 1^T \left(\frac{I}{1 - \lambda_{max}(M)} \right) 1 \tag{4.23}$$

This follows from the fact that if M_1 and M_2 are positive definite matrices with eigenvalues $\lambda_{M_1} \leq \lambda_{M_2}$ for all eigenvalues λ_{M_1} and λ_{M_2}, then $x^T M_1 x \leq x^T M_2 x$ for all $x \in \mathbb{R}^n$. The bound follows. □

We note that the necessary and sufficient condition required for the disease to die out and the social cost to converge are the same, i.e., $\lambda_{max}(M) < 1$. Also, note that the bound only depends on $\lambda_{max}(M)$ from the disease propagation model, which is popularly known as the disease threshold. It is interesting that the same parameter of the disease plays the central role in both the tapering off of the disease and its total cost.

4.4.4 Illustration with Erdös-Rényi network

In this section, we illustrate our results using a specific type of network — the Erdös-Rényi random graph. As described in Example 8, in this type of network, an edge exists between each pair of nodes with uniform probability p. To generate this graph using our network model, the degree distribution $p_n(\cdot)$ is a delta function at np. It is well known that such graphs are connected with high probability if $p > \log n/n$ in the large-graph regime [35]. We study the cost of disease in this type of network when the infection rate β_n scales such that $\beta_n np$ is a constant. Since we are interested in the regime $np \to \infty$, the infection rate satisfies $\beta_n \to 0$ and $\kappa = 0$ in this case. The scale invariant distribution $p_n(\cdot)$ satisfies:

$$\begin{aligned} p(v) &= \delta(v - \beta_n np), \\ \mathbb{E}\, v &= \bar{v} = \beta_n np, \\ \mathbb{E}\, v^2 &= (\beta_n np)^2. \end{aligned}$$

We refer to the constant $\beta_n np$ as $\bar{v}$. Using this notation, Theorem 4.1 yields

$$\begin{aligned} \lim_{n\to\infty} C_D(n) &= \frac{\alpha c_d}{\delta}\left(1 - \frac{\bar{v}^2}{\mathbb{E}\, v^2 - \delta\bar{v}}\right) \quad \text{a.s.} \\ &= \frac{\alpha c_d}{\delta}\left(1 - \frac{\bar{v}^2}{\bar{v}^2 - \delta\bar{v}}\right) \quad \text{a.s.} \\ &= \frac{\alpha c_d}{\delta - \bar{v}} \quad \text{a.s.} \end{aligned} \tag{4.24}$$

Note that this is essentially the same result as in [17], but applied to the case where the network and infection parameters scale with n and using slightly different notation.

Now we illustrate the bound in Theorem 4.3 using this class of networks. Consider a randomly sampled Erdös-Rényi graph with a reasonably large population size n and edge-forming probability p. To ensure connectedness with high probability, p is chosen to be greater than $\log n/n$. The infection parameters δ and β are selected such that $\delta > \beta np$. As a result, the maximum eigenvalue of the adjacency matrix of this graph

($\lambda_{max}[A]$) is np [35]. Thus we have

$$\lambda_{max}(M) = 1 - \delta + \beta np \quad \text{w.h.p.}$$

where w.h.p. denotes "with high probability." Note that the choice of $\delta > \beta np$ ensures that M is stable w.h.p. Using Theorem 4.3, we then have

$$C_D(n) \leq \frac{\alpha c_d}{\delta - \beta np} \quad \text{w.h.p.} \tag{4.25}$$

It is interesting that for an Erdös-Rényi network of large population size the exact cost in (4.24) as calculated from Theorem 4.1 coincides exactly with the bound in (4.25) as calculated from Theorem 4.3. This can be explained as follows. For an Erdös-Rényi network, the adjacency matrix has a large maximum eigenvalue (np) as compared to the rest of the spectrum that is concentrated in the interval $[-2\sqrt{np}, 2\sqrt{np}]$ (from Wigner's Semicircle Law [125]). The system matrix M has an eigen-spectrum that is a translation and stretch of the eigen-spectrum of A. Thus it also has the property that $\lambda_{max}(M) \gg \lambda(M)$, where $\lambda(M)$ is a randomly sampled eigenvalue of M. The calculations from Theorem 4.1 and 4.3 coincide since the largest eigenvalue dominates over the other eigenvalues. We illustrate the closeness of the disease cost as predicted by the two theorems for an Erdös-Rényi network using simulations in the next section.

4.5 Simulation and discussion

In this section we use simulations to illustrate our results in the previous sections. We first present simulations in Section 4.5.1 to explore how accurate the linearized model of epidemic process in (4.2) is when contrasted with the actual disease propagation. According to our simulations, when the infection rate β is small enough and the degree distribution $p_n(.)$ is not too heavy in its tail, the cost computed via the linear model of infection spread is a good estimate of the actual disease cost. In the second part of this section, we illustrate Theorems 4.1 and 4.3 in Section 4.5.2, simulating

the disease on both random and real-world networks and comparing the results to the predictions of our theorems.

4.5.1 Evaluation of assumptions

To analyze the parameter regimes for which the linear disease propagation model is accurate, first consider an Erdös-Rényi network with $n = 1000$. Assume the recovery rate is $\delta = 0.6$ and the initial fraction of infected nodes is $\alpha = 0.2$. We evaluate two quantities: (i) $\alpha c_d[1^T(I - M)^{-1}1]$ and (ii) actual cost by summing up the number of infected nodes at each time until the disease dies out, normalizing to obtain the average per-node cost. We calculate the relative error between the linear model and the actual cost, averaged over 100 runs. To determine the parameter regimes for which our model is accurate, we simulate with various values of the infection rate β and edge probability p. Our results are presented in Figure 4.4. Note that in the case of an Erdös-Rényi random network, stability of the system matrix requires that $\delta > \beta np$; this bound is shown in 4.4. Outside of this bound, when both β and p are large, the disease does not die out. Hence we determine regions that guarantee error percentages within certain ranges. Note that much of the region within the stability region has relative error less than 10%, indicating that the approximation is good in regimes where the disease dies out.

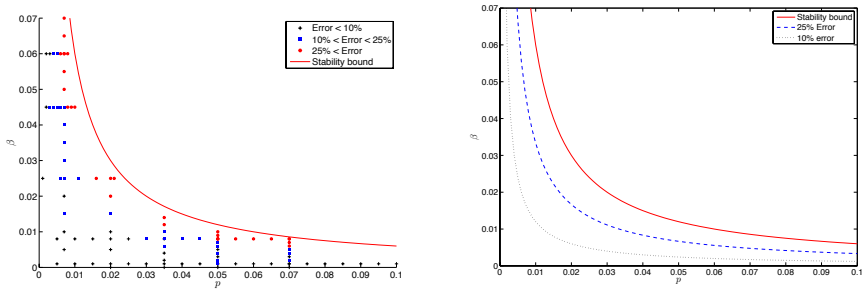

(a) Percent Error (b) Estimated bounds for percent error

Figure 4.4: Percent error between simulated cost and linearized model (4.10) for ER network

Now consider a 1000-node network with a Pareto degree distribution, as described

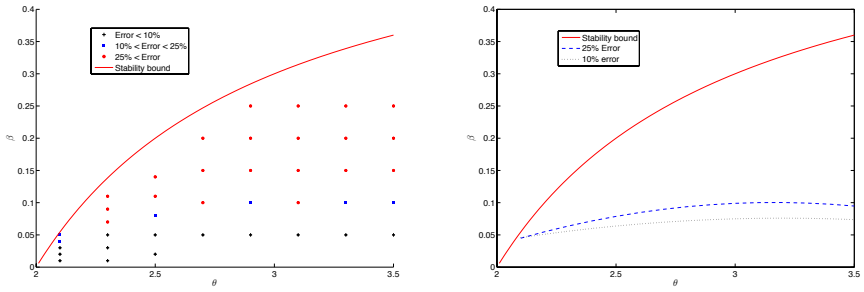

(a) Percent Error (b) Estimated bounds for percent error

Figure 4.5: Percent error between simulated cost and linearized model (4.10) for Pareto network

in Example 10. Note that this is a heavy-tailed distribution and only has finite variance for $\theta > 2$. Again, we test various network and infection parameters (in this case, β and θ) to determine the relative error between our linearized model and the actual epidemic process. The results are presented in Figure 4.5. As expected, a heavier tail (smaller θ) results in a larger relative error. Similarly, a higher infection rate β results in a larger error. However, there does exist a decent sized region within which the linear model is a good approximation.

Note that Erdös-Rényi random network and a network with a heavy-tailed distribution represent the extreme cases, in terms of degree distribution. Whereas an Erdös-Rényi network has a degree distribution is concentrated around the mean, the heavy-tailed Pareto distribution is characterized by large deviations in the degrees of each node. Our simulations show that under reasonable assumptions on the graph parameters and the infection rate, the linear model is quite accurate wherever the disease dies out (inside the stability region) and thus validating our choice of using it to compute the costs in Theorems 4.1 and 4.3.

4.5.2 Illustration of theorems

In this section we compare our different expressions for the disease cost, from Equation (4.10) to Theorem 4.1 and the bound of Theorem 4.3 for various types of random and real-world graphs. We show through simulations that despite the approximations

made in calculating the closed-form solution in Theorem 4.1, it is very close to the original expression of the disease cost from (4.10), as well to the simulated spread of the the disease. Further, for some types of graphs, the bound in Theorem 4.3 is also rather tight. Note that in all cases, and n grows, our approximations become tighter.

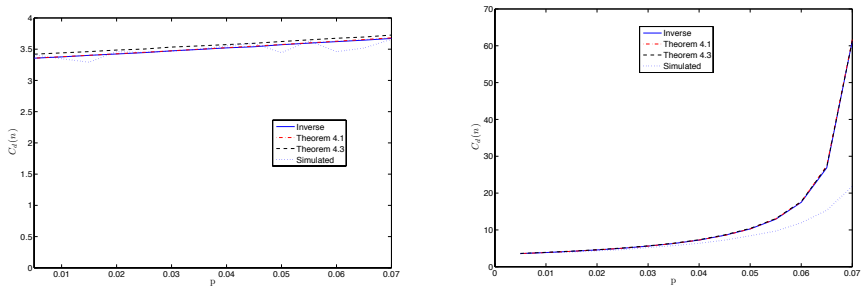

(a) $n = 100$ (b) $n = 1000$

Figure 4.6: Simulated and calculated disease cost on ER network

As expected, the Erdös-Rényi random network has the closest agreement between Theorems 4.1 and 4.3 and the linear model, from (4.10). Similar to the accuracy regimes described above, as the expected degree grows, the gap between the linear model and the actual simulation increases, as shown in Figure 4.6.

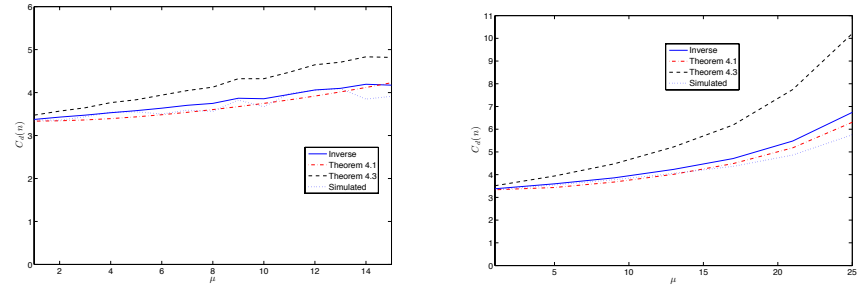

(a) $n = 100$ (b) $n = 1000$

Figure 4.7: Simulated and calculated disease cost on exponential network

For a network with an exponential degree distribution, as shown in Figure 4.7, we see fairly close agreement between Theorem 4.1, the linear model (4.10), and the actual simulation. However, the upper bound from Theorem 4.3 is looser than in the Erdös-Rényi case.

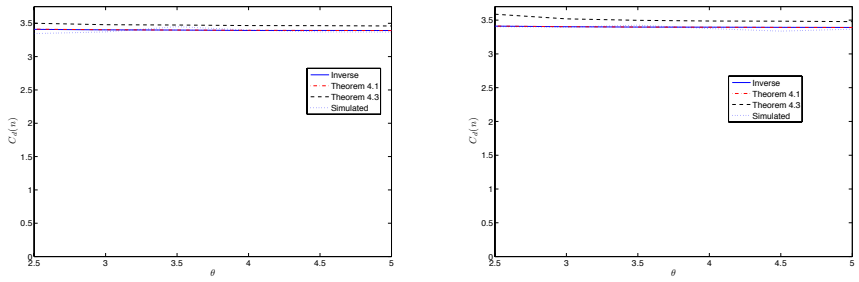

(a) $n = 100$ (b) $n = 1000$

Figure 4.8: Simulated and calculated disease cost on Pareto network

The network with a Pareto degree distribution has similar results to one with an exponential degree distribution. Again, we see close agreement between the linear model and Theorem 4.1. However, due to the increased variance in node degrees, the simulated cost of diseases varies more than in the networks with a more concentrated degree distribution.

4.5.3 Disease cost case studies

To illustrate our results on actual networks, we present two case studies here, evaluating Theorem 4.3 and simulating the disease on each. The first real-world network we examine is a social network of undergraduates at the California Institute of Technology (Caltech) [47]. This data was gathered via a survey in 2010, asking participating students to list up to 10 of their friends. Participation was about 72% of the undergraduate student body, resulting in at least partial network information for about 95% of te students. We generate an undirected network for our simulations by making each directed edge undirected. The final network has about 900 nodes and 3500 edges. Both the network and its degree distribution (the CCDF in a log log plot) are shown in Figure 4.9.

The second network we look at is gathered from voting records in Wikipedia [41]. This network has about 7000 nodes and 100000 edges. The network and its degree distribution (the CCDF in a log log plot) are shown in Figure 4.10. Though this is not an actual social network, it is a good representation of a larger data set with

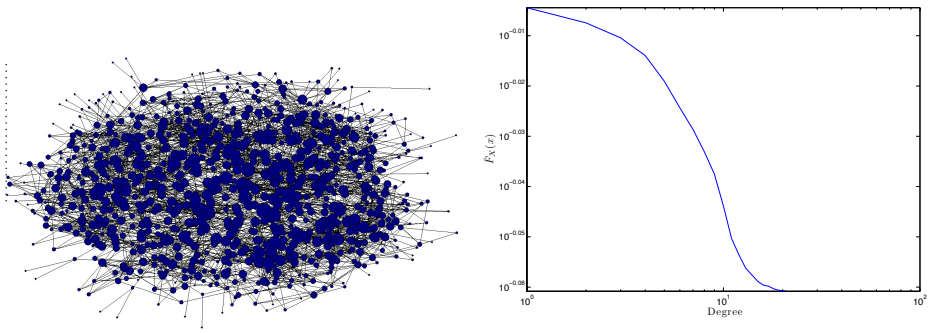

(a) Network (b) Degree CCDF

Figure 4.9: Caltech social network

similar characteristics to social networks.

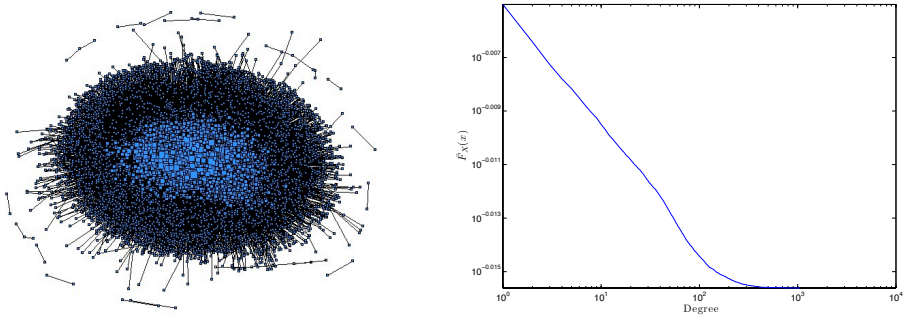

(a) Network (b) Degree CCDF

Figure 4.10: Wikipedia voting network

Simulating the disease cost on both of these networks, similarly to the method used for the random networks in the previous section, we see that our model and upper bound are relatively close to the simulated cost. See Figure 4.11 for the performance on both the Caltech and Wikipedia social networks. As we do not have access to a $p(\cdot)$ for either of these real networks, we focused on the difference between the upper bound (Theorem 4.3) and the actual simulation of the disease. Since the Wikipedia network was rather large, we only plot the upper bound, using the maximum eigenvalue of the system matrix, for that network.

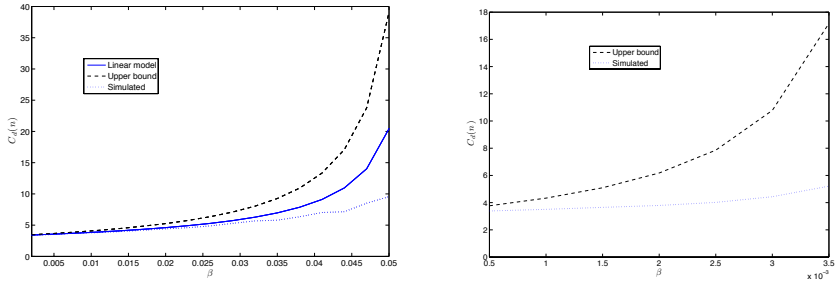

(a) Caltech (b) Wikipedia

Figure 4.11: Simulated disease on Caltech and Wikipedia social networks

4.6 Extensions

As described in [17], one of the key benefits of the relatively simple expressions of the disease cost in Section 4.4 is the ability to calculate and minimize the total "social cost" of an epidemic, defined as the sum of the disease cost and the cost of whatever containment or immunization scheme is being considered. As a first step, we examine a one-shot immunization scheme. In this scenario, nodes are immunized at $t = 0$ and remain immune for all time, incurring a single immunization cost. This cost could represent the monetary cost of a vaccine to an individual, the cost of quarantining, or a normalized development and administration cost. For simplicity, we assume that these costs can all be represented by a single quantity, c_v.

It is relatively easy to incorporate the immunization process into the random graph model from Section 4.2. Recall that to generate a network with n nodes according to this model, the degree distribution $p_n(\cdot)$ is sampled n times. Consider a randomized immunization procedure where πn nodes are chosen uniformly at random at $t = 0$ to be immunized. The resulting network is formed by sampling $p_n(\cdot)$ only for the nodes that remain after the immunization. The immunized nodes are removed from the adjacency matrix A and the corresponding system matrix M, yielding $\tilde{A}$ and $\tilde{M}$, with $\mathbb{E}[\dim \tilde{M}] = (1 - \pi)n := \tilde{n}$. To model a degree-based immunization scheme, we can simply truncate the degree distribution $p_n(\cdot)$ and sample to generate the network

as before. In either case, the social cost of an epidemic can be defined as

$$S(M, \tilde{M}) := \frac{1}{n}\left[(\dim M - \dim \tilde{M})c_v + \left(1^T(I - \tilde{M})^{-1}1\right)\alpha c_d\right]. \tag{4.26}$$

The second half of the above expression represents the disease cost on the immunized network and can be calculated using the results in Section 4.4.

In general, any one-shot immunization scheme simply results in a transformation of $p_n(\cdot)$ and the disease cost calculations in Section 4.4 all still apply.

4.6.1 Optimal random immunization

For example, consider the random immunization discussed above. Define the expected per-node social cost $S_{\mathcal{G}}(\pi)$ on a class of graphs $\mathcal{G}$ as a function of the fraction π of immunized nodes as

$$S_{\mathcal{G}}(\pi) = \pi c_v + (1 - \pi)C_D\left(n(1 - \pi)\right) \tag{4.27}$$

Thus, applying the results from Section 4.4, we can obtain results for $S_{\mathcal{G}}(\pi)$. We illustrate this with an Erdös-Rényi random network. Using (4.24) from Section 4.4.4 for $\mathcal{G} = G_{n,\delta(w-np)}$, we have that, as $n \to \infty$,

$$S_{\mathcal{G}}(\pi) = \pi c_v + \frac{(1 - \pi)\alpha c_d}{\delta - \beta n(1 - \pi)p} \text{ w.h.p.} \tag{4.28}$$

We can now determine the optimal fraction of nodes to immunize by minimizing (4.28). For convenience, we normalize $c_d = 1$ and $c_v = C$, and define $a = \frac{\alpha}{\delta}$ and $b = \frac{\alpha\delta}{(\delta - \beta np)^2}$. The optimal fraction of nodes to immunize is then

$$\pi_{opt} = \begin{cases} 1 & C \le a < b \\ 1 - \frac{\delta - \sqrt{\delta\alpha/C}}{\beta np} & a < C < b \\ 0 & a < b \le C \end{cases}$$

To illustrate the above, we simulate a disease propagating on an Erdös-Rényi graph, with $n = 100000$, $p = 1.27 \times 10^{-4}$, $\alpha = 0.2$, $\beta = 0.02$, and $\delta = 0.39$, according to the infection model described in Section 4.3. We use a low $C = 0.1282$, medium $C = 1$, and high $C = 18.46$. The simulated cost as a function of π is shown in Figure 4.12, together with the approximate calculated cost as given in (4.28). The optimal immunization probability in each case is highlighted with a red circle.

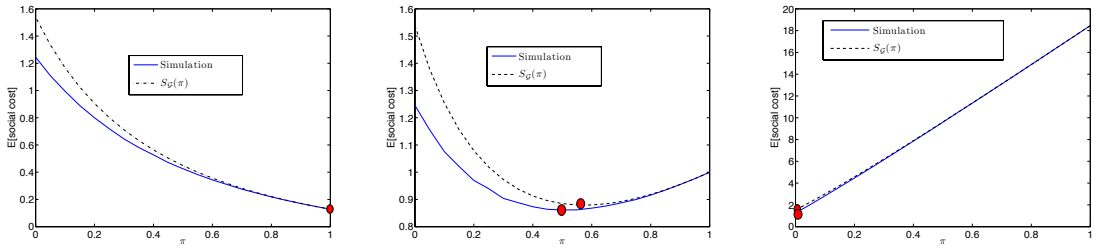

(a) Small C (b) Medium C (c) Large C

Figure 4.12: Social cost simulations on Erdös-Rényi network as a function of π

4.7 Conclusion

In this chapter we have used a random matrix approach to quantify the economic impact of an epidemic on a complex network. Using a linearized dynamical system based on the popular SIS model and a random graph as the underlying network, we calculate the cost of the disease in the large graph limit and derive bounds for the disease cost for a given graph (Theorems 4.1 and 4.3). This cost depends on the entire transient behavior of the system and hence this analysis differs from previous work that focuses on the steady-state equilibrium. Our calculation shows that the disease cost depends on the entire eigen-distribution of the system matrix, whereas the upper bound depends only on the largest eigenvalue. Despite its simpler form, the upper bound appears to be tight, as shown by our simulations. Our analysis makes use of ideas and techniques from random matrix theory, differentiating this work from previous work on the spread of epidemics. We apply our results in a brief analysis of optimal immunization strategies. We also carefully analyze the assumptions made in

our linear model and show graph regimes where our assumptions are valid. To the best of our knowledge, our approach using random matrices is novel to the study of epidemic processes and we hope to extend it in further research.

To extend this work, we would like to investigate both theoretical and practical refinements of our model. We can consider more sophisticated epidemic models (SIR, etc.) as well as immunization based on the strategic behavior of agents. Moreover, a case study with real data from communicable diseases like influenza or herpes would provide more insight into the accuracy and predictive power of these models in real-world scenarios, as well as help refine the cost of disease which we have assumed is a single parameter, c_d.

Our random network approach is a promising direction to tackle the problem of epidemic spread on network – our simulations show that at least under certain infection and graph parameters, our results are fairly accurate, giving us hope to quantify the cost of an epidemic on real-world networks. Our approach and the random matrix tools we use are fairly general; we hope to extend the tools, techniques and ideas in this chapter to further study complex processes on complex networks.

4.8 Appendix: Proof of Lemma 4.2

In this section, we prove Lemma 4.2, computing the terms $\frac{1}{n}(1^T X^{-1} v)$, $\frac{1}{n}(1^T X^{-1} 1)$, and $\frac{1}{n}(v^T X^{-1} v)$ in terms of δ, κ and $p(v)$. The calculation relies on techniques from Random Matrix Theory, specifically the Stieltjes Transform [125]. For the proof, we require a technical result (Lemma 4.4) that we state and prove in Appendix 4.9. The computation for the first term, i.e., $\frac{1}{n}(1^T X^{-1} v)$ follows directly from Lemma 4.4. For the other terms, we follow the proof technique of the same lemma and use its result to finish the proof. Throughout this section, Assumption 1 is supposed to be true.

4.8.1 Lemma 4.2 (a)

First we prove that

$$\lim_{n\to\infty} \frac{1}{n} 1^T X^{-1} v = \frac{F}{\delta} \quad \text{a.s.}, \tag{4.29}$$

provided the following condition holds:

$$\lim_{n\to\infty} \frac{1}{n}\left[1^T \left(V^{-1} - \sqrt{\frac{\beta_n}{\delta^2 \bar{v}}} C\right)^{-1} 1\right] - \frac{1}{n}\mathbb{E}\,\mathrm{tr}\left(V^{-1} - \sqrt{\frac{\beta_n}{\delta^2 \bar{v}}} C\right)^{-1} \quad \text{a.s..} \tag{4.30}$$

Note that this is the first assumption in Assumption 1. Recall that

$$F = \int_{v_{min}}^{\infty} \frac{p(v)}{v^{-1} - \kappa^2 F} dv.$$

where

$$\kappa = \lim_{n\to\infty} \sqrt{\frac{\beta_n}{\delta^2 \bar{v}}}.$$

As before, the Strong Law of Large Numbers gives us $\lim_{n\to\infty} \frac{1}{n\mu} = \bar{v}$ almost surely. Substituting the following expression for X in (4.29):

$$X = \delta I - \sqrt{n\beta_n \mu} V^{1/2} C V^{1/2}, \tag{4.31}$$

where C is a Wigner matrix and $V = diag(v)$, we obtain

$$\begin{aligned}
\lim_{n\to\infty} \frac{1}{n} 1^T X^{-1} v &= \lim_{n\to\infty} \frac{1}{n} [1^T X^{-1} V 1] \\
&= \lim_{n\to\infty} \frac{1}{n} \left[1^T (\delta I - \sqrt{n\beta_n \mu} V^{1/2} C V^{1/2})^{-1} V 1 \right] \\
&= \lim_{n\to\infty} \frac{1}{n} \left[1^T (\delta V^{-1} - \sqrt{n\beta_n \mu} V^{-1/2} C V^{1/2})^{-1} 1 \right] \\
&= \lim_{n\to\infty} \frac{1}{n} \left[1^T (\delta V^{-1} - \sqrt{n\beta_n \mu} C)^{-1} 1 \right] \\
&= \frac{1}{\delta} \lim_{n\to\infty} \frac{1}{n} \left[1^T \left(V^{-1} - \sqrt{\frac{\beta_n}{\delta^2 \bar{v}}} C \right)^{-1} 1 \right] \\
&= \frac{1}{\delta} \lim_{n\to\infty} \frac{1}{n} \mathbb{E} \operatorname{tr} \left(V^{-1} - \sqrt{\frac{\beta_n}{\delta^2 \bar{v}}} C \right)^{-1} \quad \text{a.s.} \\
&= \frac{F}{\delta} \quad \text{a.s.},
\end{aligned}$$

where the last step follows Lemma 4.4. This completes the proof of Lemma 4.2 (a).

4.8.2 Lemma 4.2 (b)

Now we turn to computing the term $\frac{1}{n} 1^T X^{-1} 1$. We prove that

$$\lim_{n\to\infty} \frac{1}{n} 1^T X^{-1} 1 = \frac{1 + \kappa^2 F^2}{\delta} \quad \text{a.s.} \tag{4.32}$$

Substituting the expression for X, we have

$$\begin{aligned}
\lim_{n\to\infty} \frac{1}{n} 1^T X^{-1} 1 &= \lim_{n\to\infty} \frac{1}{n} \left[1^T \left(\delta I - \sqrt{n\beta_n \mu} V^{1/2} C V^{1/2} \right)^{-1} 1 \right] \\
&= \frac{1}{\delta} \lim_{n\to\infty} \frac{1}{n} \left[1^T \left(I - \sqrt{\frac{\beta_n}{\delta^2 \bar{v}}} V^{1/2} C V^{1/2} \right)^{-1} 1 \right] \quad \text{a.s.} \\
&= \frac{1}{\delta} \lim_{n\to\infty} \frac{1}{n} \mathbb{E} \operatorname{tr} \left(I - \sqrt{\frac{\beta_n}{\delta^2 \bar{v}}} V^{1/2} C V^{1/2} \right)^{-1} \quad \text{a.s.}
\end{aligned}$$

where the last step follows from Assumption 1. Now, we use the same block matrix decomposition of C and V as in the proof of Lemma 4.4. The definition is restated

here.

$$V = \begin{bmatrix} v_1 & 0 \\ 0 & V_2 \end{bmatrix} \quad \text{and} \quad C = \begin{bmatrix} c_{11} & C_{21}^T \\ C_{21} & C_{22} \end{bmatrix},$$

where v_1 and c_{11} are scalars and the rest are matrices of appropriate sizes. Writing the matrix using these expressions, we have

$$\left(I - \sqrt{\frac{\beta_n}{\delta^2 \bar{v}}} V^{1/2} C V^{1/2} \right)^{-1} = \begin{bmatrix} 1 - \sqrt{\frac{\beta_n}{\delta^2 \bar{v}}} v_1 c_{11} & -\sqrt{\frac{\beta_n}{\delta^2 \bar{v}}} \sqrt{v_1} C_{21}^T V_2^{1/2} \\ \underbrace{-\sqrt{\frac{\beta_n}{\delta^2 \bar{v}}} \sqrt{v_1} V_2^{1/2} C_{21}}_{:=y} & \underbrace{I - \sqrt{\frac{\beta_n}{\delta^2 \bar{v}}} V_2^{1/2} C_{22} V_2^{1/2}}_{:=D} \end{bmatrix}^{-1}.$$

Applying the Matrix Inversion Lemma and continuing, we have

$$\begin{aligned}
&\lim_{n\to\infty} \mathbb{E} \operatorname{tr} \frac{1}{n} \left(I - \sqrt{\frac{\beta_n}{\delta^2 \bar{v}}} V^{1/2} C V^{1/2} \right)^{-1} \\
&\qquad = \lim_{n\to\infty} \mathbb{E} \left[1 - \sqrt{\frac{\beta_n}{\delta^2 \bar{v}}} v_1 c_{11} - y^T D^{-1} y \right]^{-1} \\
&\qquad = \lim_{n\to\infty} \mathbb{E} \left[1 - \sqrt{\frac{\beta_n}{\delta^2 \bar{v}}} v_1 c_{11} - \frac{\beta_n}{\delta^2 \bar{v}} v_1 C_{21}^T \left(V_2^{-1} - \sqrt{\frac{\beta_n}{\delta^2 \bar{v}}} C_{22} \right)^{-1} C_{21} \right]^{-1} \\
&\qquad = \lim_{n\to\infty} \mathbb{E} \left[1 - \frac{\beta_n}{\delta^2 \bar{v}} v_1 C_{21}^T \left(V_2^{-1} - \sqrt{\frac{\beta_n}{\delta^2 \bar{v}}} C_{22} \right)^{-1} C_{21} \right]^{-1} \\
&\qquad = \mathbb{E} \left(1 - \kappa^2 v_1 F \right)^{-1} \quad \text{a.s.} \qquad (4.33) \\
&\qquad = \int_{v_{min}}^{\infty} \frac{v^{-1} p(v)}{v^{-1} - \kappa^2 F} dv \quad \text{a.s..}
\end{aligned}$$

where we have applied Lemma 4.4 in (4.33). For convenience, define

$$S_1 := \int_{v_{min}}^{\infty} \frac{v^{-1} p(v)}{v^{-1} - \kappa^2 F} dv. \qquad (4.34)$$

Consider the following relation:

$$\begin{aligned} S_1 - \kappa^2 F^2 &= \int_{v_{min}}^{\infty} \frac{v^{-1}p(v)}{v^{-1} - \kappa^2 F} dv - \kappa^2 \int_{v_{min}}^{\infty} \frac{Fp(v)}{v^{-1} - \kappa^2 F} dv \\ &= \int_{v_{min}}^{\infty} p(v) dv \\ &= 1. \end{aligned}$$

Rearranging and solving for S_1 in terms of F, we see that $S_1 = 1 + \kappa^2 F^2$ and

$$\lim_{n\to\infty} \frac{1}{n} 1^T X^{-1} 1 = \frac{S_1}{\delta} = \frac{1 + \kappa^2 F^2}{\delta} \quad \text{a.s.},$$

This proves Lemma 4.2 (b).

4.8.3 Lemma 4.2 (c)

Now we move onto the last term, i.e., we prove that

$$\lim_{n\to\infty} \frac{1}{n} v^T X^{-1} v = \begin{cases} \mathbb{E}\, v^2 \quad \text{a.s.} & \text{if } \kappa = 0, \\ \frac{1}{\delta\kappa^2}\left(1 - \frac{\bar{v}}{F}\right) \quad \text{a.s.} & \text{if } \kappa \neq 0. \end{cases} \tag{4.35}$$

For brevity, we outline the steps involved.

$$\begin{aligned} \lim_{n\to\infty} \frac{1}{n} v^T X^{-1} v &= \lim_{n\to\infty} \frac{1}{n} \left[1^T V \left(\delta I - \sqrt{n\beta_n \mu} V^{1/2} C V^{1/2} \right)^{-1} V 1 \right] \\ &= \frac{1}{\delta} \lim_{n\to\infty} \frac{1}{n} \left[1^T V^{1/2} \left(V^{-1} - \sqrt{\frac{\beta_n}{\delta^2 \bar{v}}} C \right)^{-1} V^{1/2} 1 \right] \\ &= \frac{1}{\delta} \lim_{n\to\infty} \frac{1}{n} \mathbb{E}\,\mathrm{tr} \left[V^{1/2} \left(V^{-1} - \sqrt{\frac{\beta_n}{\delta^2 \bar{v}}} C \right)^{-1} V^{1/2} \right] \quad \text{a.s.} \end{aligned}$$

where the last step follows from Assumption 1. Using the block-decomposition of C and V as above, and proceeding as before to expand the above expression, we get

$$\begin{aligned}
&\lim_{n\to\infty} \frac{1}{n} \mathbb{E}\,\mathrm{tr}\left[V^{1/2} \left(V^{-1} - \sqrt{\frac{\beta_n}{\delta^2 \bar{v}}} C \right)^{-1} V^{1/2} \right] \\
&\quad = \lim_{n\to\infty} \mathbb{E}\, v_1 \left[v_1^{-1} - \sqrt{\frac{\beta_n}{\delta^2\bar{v}}} c_{11} - \frac{\beta_n}{\delta^2 \bar{v}} C_{21}^T \left(V_2^{-1} - \sqrt{\frac{\beta_n}{\delta^2\bar{v}}} C_{22} \right)^{-1} C_{21} \right]^{-1} \\
&\quad = \lim_{n\to\infty} \mathbb{E}\, v_1 \left[v_1^{-1} - \frac{\beta_n}{\delta^2 \bar{v}} C_{21}^T \left(V_2^{-1} - \sqrt{\frac{\beta_n}{\delta^2\bar{v}}} C_{22} \right)^{-1} C_{21} \right]^{-1} \\
&\quad = \mathbb{E}\left[v_1 \left(v_1^{-1} - \kappa^2 F \right)^{-1} \right] \quad \text{a.s.} \qquad (4.36) \\
&\quad = \int_{v_{min}}^{\infty} \frac{v p(v)}{v^{-1} - \kappa^2 F} dv \quad \text{a.s..}
\end{aligned}$$

where we have again applied Lemma 4.4 in (4.36). For convenience, define

$$S_2 := \int_{v_{min}}^{\infty} \frac{v p(v)}{v^{-1} - \kappa^2 F} dv. \qquad (4.37)$$

If $\kappa = 0$, then

$$S_2 = \int_{v_{min}}^{\infty} v^2 p(v) dv = \mathbb{E}\, v^2.$$

For the case where $\kappa \neq 0$, consider the following relation:

$$\begin{aligned}
F - \kappa^2 S_2 F &= \int_{v_{min}}^{\infty} \frac{p(v)}{v^{-1} - \kappa^2 F} dv - \int_{v_{min}}^{\infty} \frac{\kappa^2 v F p(v)}{v^{-1} - \kappa^2 F} dv \\
&= \int_{v_{min}}^{\infty} v p(v) dw \\
&= \bar{v}.
\end{aligned}$$

Rearranging and solving for S_2 in terms of F, we finally have

$$\lim_{n\to\infty} \frac{1}{n} v^T X^{-1} v = \begin{cases} \mathbb{E}\, v^2 & \text{if } \kappa = 0, \\ \frac{1}{\delta\kappa^2}\left(1 - \frac{\bar{v}}{F}\right) & \text{if } \kappa \neq 0. \end{cases}$$

This proves Lemma 4.2 (c).

4.9 Appendix: Technical proofs

Here we state and prove a technical result used in proving Lemma 4.2. This result is very similar to the derivation of Wigner's Semicircle Law using Stieltjes transform in Random Matrix Theory [125]. Our proof technique requires the following concentration inequality that we state without proof here:

Theorem. *Talagrand's Concentration Inequality: Let $K > 0$, and let $Y_1, \ldots, Y_n$ be independent variables with $|Y_i| \leq K$ for all $1 \leq i \leq n$. Let $F : \mathbb{R}^n \to \mathbb{R}$ be a 1-Lipschitz conveV function. Then there exists positive constants B, b such that for any λ,*

$$\begin{aligned} \Pr\left[|F(Y) - \mathbb{M}\, F(Y)| \geq \lambda K\right] &\leq B\exp(-b\lambda^2) \quad a.s., \\ \Pr\left[|F(Y) - \mathbb{E}\, F(Y)| \geq \lambda K\right] &\leq B\exp(-b\lambda^2) \quad a.s., \end{aligned}$$

where $\mathbb{M}$ denotes the median.

We first introduce the notation. Let $v_{n\times 1}$ be a vector of n independent samples from a distribution $p(.)$ that has support $[v_{min}, \infty)$. Define the $n \times n$ matrix $V := \mathrm{diag}(v)$. Also, let $C_{n\times n}$ be a Wigner matrix [125] such that all the off-diagonal entries have mean zero and variance $1/n$. Now, consider a sequence $\{k_n\}_{n=1}^{\infty}$ such that it has a limit, i.e.,

$$\lim_{n\to\infty} k_n = k,$$

where k is some constant. Using this notation, we present the result:

Lemma 4.4. *Let $Z_{n\times 1}$ be a vector with independent entries that satisfy $\mathbb{E}\, Z_k = 0$, $\mathbb{E}\, Z_k^2 = 1$ and the distribution of Z_k has bounded support. Then,*

$$\lim_{n\to\infty} \frac{1}{n}\left[Z^T\left(V^{-1} - k_n C\right)^{-1} Z\right] - \frac{1}{n}\,\mathbb{E}\,\mathrm{tr}\left(V^{-1} - k_n C\right)^{-1} = 0 \tag{4.38}$$

and

$$\lim_{n\to\infty} \frac{1}{n} \mathbb{E} \operatorname{tr} \left(V^{-1} - k_n C\right)^{-1} = T(k) \tag{4.39}$$

where $T(k)$ satisfies the following implicit equation:

$$T(k) = \int_{v_{min}}^{\infty} \frac{p(v)dv}{v^{-1} - T(k)}.$$

We prove this result through the rest of this section. To begin define the following function for complex number z:

$$T_n(z) := \frac{1}{n} \mathbb{E} \operatorname{tr} \left(V^{-1} - zC\right)^{-1}. \tag{4.40}$$

We first prove that:

$$T_n(z) - T_{n-1}(z) = \mathcal{O}\left(\frac{1}{n}\right).$$

Now, we prove the claim in (4.38). Note that for a deterministic positive semidefinite matrix $A_{n\times n}$ with operator norm $\mathcal{O}(1)$, the function $F(V) = \|A^{1/2}V\|$ is convex and Lipshitz continuous. Then Talagrand's inequality implies that there exists positive constants B, b such that for any $\lambda > 0$,

$$\Pr\left[\left|(V^T AV)^{1/2} - \mathbb{M}(V^T AV)^{1/2}\right| \geq \lambda\right] \leq B\exp(-b\lambda^2) \quad \text{a.s.}$$

Thus

$$(V^T AV)^{1/2} = \mathbb{M}(V^T AV)^{1/2} + \mathcal{O}(1) \quad \text{a.s..} \tag{4.41}$$

Now, $\|V\| = O(\sqrt{n})$ and hence $\mathbb{M}(V^T AV)^{1/2} = \mathcal{O}(\sqrt{n})$ a.s. On squaring and rearranging (4.41), we have

$$\Pr\left[\left|V^T AV - \mathbb{M}\, V^T AV\right| \geq \lambda\sqrt{n}\right] \leq B'\exp(-b'\lambda^2)$$

for some positive constants B', b'. Replacing the median by the expectation, we get

$$\Pr\left[\left|V^T AV - \mathbb{E}\, V^T AV\right| \geq \lambda\sqrt{n}\right] \leq B' \exp(-b'\lambda^2) \tag{4.42}$$

If A is a general $n \times n$ matrix with operator norm $\mathcal{O}(1)$, we can repeatedly use triangle inequality in (4.42) on the eigen-decomposition of A to get

$$\Pr\left[\left|V^T AV - \mathbb{E}\, V^T AV\right| \geq \lambda\sqrt{n}\right] \leq B' \exp(-b'\lambda^2)$$

Now, $\mathbb{E}\, V = 0$ and the entries are independent. Thus, $\mathbb{E}\, V^T AV = \operatorname{tr}(A)$. For a random matrix A independent of V, we can condition on A to get $\mathbb{E}\, V^T AV = \mathbb{E}\operatorname{tr}(A) = nT_n(z)$. Hence,

$$\Pr\left[\left|\frac{1}{n}\left[Z^T\left(V^{-1} - k_n C\right)^{-1} Z\right] - T_n(k_n)\right| \geq \frac{\lambda}{\sqrt{n}}\right] \leq B' \exp(-b'\lambda^2).$$

This gives us

$$\frac{1}{n}\left[Z^T\left(V^{-1} - k_n C\right)^{-1} Z\right] = T_n(k_n) + \mathcal{O}\left(\frac{1}{\sqrt{n}}\right). \tag{4.43}$$

In addition, an application of Borel-Cantelli lemma gives:

$$\lim_{n\to\infty} \frac{1}{n}\left[Z^T\left(V^{-1} - k_n C\right)^{-1} Z\right] - T_n(k_n) = 0. \quad \text{a.s.} \tag{4.44}$$

This proves the first claim (4.38) in Lemma 4.4. Now we move to the proof of (4.39). First, we show that $T_n(k_n)$ satisfies an implicit equation and then take limit as $n \to \infty$. We start with the block matrix decomposition of V and C. Let

$$V = \begin{bmatrix} v_1 & 0 \\ 0 & V_2 \end{bmatrix} \quad \text{and} \quad C = \begin{bmatrix} c_{11} & C_{21}^T \\ C_{21} & C_{22} \end{bmatrix}, \tag{4.45}$$

where v_1 and c_{11} are scalars and the rest are matrices of appropriate sizes. From the

Matrix Inversion Lemma [64], it follows that

$$T_n(k_n) = \frac{1}{n}\,\mathbb{E}\,\mathrm{tr}\begin{bmatrix} v_1^{-1} - k_n c_{11} & -k_n C_{21}^T \\ -k_n C_{21} & \underbrace{V_2^{-1} - k_n C_{22}}_{=D} \end{bmatrix}^{-1}$$
$$= \frac{1}{n}\,\mathbb{E}\,\mathrm{tr}\begin{bmatrix} \Delta^{-1} & -\Delta^{-1} C_{21}^T D^{-1} \\ -D^{-1} C_{21} \Delta^{-1} & D^{-1} + D^{-1} C_{21} \Delta^{-1} C_{21}^T D^{-1} \end{bmatrix}. \tag{4.46}$$

where Δ is the Schur complement of D defined as

$$\Delta = v_1^{-1} - k_n c_{11} - k_n^2 C_{21}^T D^{-1} C_{21}. \tag{4.47}$$

Note that all the diagonal entries of the matrix $(V^{-1} - k_n C)^{-1}$ are identically distributed. Thus we have

$$\begin{aligned} T_n(k_n) &= \mathbb{E}\,\Delta^{-1} \\ &= \mathbb{E}\left[v_1^{-1} - k_n c_{11} - k_n^2 C_{21}^T D^{-1} C_{21}\right]^{-1} \\ &= \mathbb{E}\left[v_1^{-1} - C_{21}^T \left(V_2^{-1} - k_n C_{22}\right)^{-1} C_{21} + \mathcal{O}\left(\frac{1}{n}\right)\right]^{-1}. \end{aligned}$$

since c_{11} has mean zero and variance $1/n$. Note that $C_{22}\sqrt{\frac{n}{n-1}}$ is a Wigner matrix of size $(n-1)\times(n-1)$. Using $Z := C_{21}\sqrt{\frac{n}{n-1}}$ in (4.43), we get

$$\begin{aligned} C_{21}^T \left(V_2^{-1} - k_n C_{22}\right)^{-1} C_{21} &= \left(\frac{n}{n-1}\right)^{3/2} T_{n-1}\left(k_n\sqrt{\frac{n}{n-1}}\right) + \mathcal{O}\left(\frac{1}{\sqrt{n}}\right) \quad \text{a.s.} \\ &= \left(\frac{n}{n-1}\right)^{3/2} T_n\left(k_n\sqrt{\frac{n}{n-1}}\right) + \mathcal{O}\left(\frac{1}{\sqrt{n}}\right) \quad \text{a.s.} \\ &= T_n\left(k_n\right) + \mathcal{O}\left(\frac{1}{\sqrt{n}}\right) \quad \text{a.s..} \end{aligned}$$

Thus,

$$T_n(k_n) = \mathbb{E}\left[\frac{1}{v_1^{-1} - k_n^2 T_n(k_n)}\right] + \mathcal{O}\left(\frac{1}{\sqrt{n}}\right)$$

Note that the expectation is over v_1 that is drawn according to the distribution $p(.)$. Taking limit as $n \to \infty$ on both sides

$$T(k) = \mathbb{E}\,\frac{1}{v^{-1} - k^2 T(k)}. \tag{4.48}$$

The rest follows from (4.44).

Chapter 5

Vaccination

5.1 Introduction

Vaccinations are one of the most cost effective ways of preventing disease and promoting health. Yet, vaccination rates for several diseases remains low despite significant government intervention to promote vaccination coverage. Although some of the low rates of vaccinations especially in developing countries might be explained by restricted supply or poor availability of health care, lack of demand for vaccinations also plays an important role ([40]). Recent vaccine scares and subsequent drops in vaccination uptake highlight the importance of this issue in the US and other developed countries. There is also emerging evidence that individuals might not fully appreciate the costs and benefits of vaccinations when deciding whether or not to vaccinate ([57, 119, 36, 127, 96, 134, 69, 83]). In addition, in our increasingly networked world with instant access to information and the opinions of others, individuals do not operate in a vacuum; friends', family, and even strangers' decisions might influence our behavior. Therefore, it is imperative to understand how individuals make decisions regarding vaccinations and the implications of alternate decision models or processes on the design of efficient public health policy to maximize vaccination coverage and reduce the burden of vaccine preventable diseases.

In this chapter, we consider two alternate models of the decision to vaccinate. The models differ in how individuals decision to vaccinate are influenced by the decision of peers to vaccinate. In particular, we consider two types of peer effects. In the

first, rational agents desire to free-ride on the vaccination decisions of their peers. For example, as an individual sees the overall vaccination coverage of her peers increasing, she has less desire to vaccinate herself, as there is less and less chance that she will herself be infected. In this case, peer effects are *nonconforming* — an increase in the vaccination coverage by peers leads to a decrease in an individual's probability of vaccinating. In the second type of peer effect, agents desire to copy what their peers are doing, through the simple desire to avoid being different. For example, consider an agent surrounded by peers who choose not to vaccinate, believing that the vaccine in question carries a very high risk. Such an agent could face an enormous amount of peer pressure to conform. As a result, one would expect the desire to copy others' behavior to play a large role in the vaccination decision-making process. In this case, peer effects are *conforming* — an increase in vaccination by peers leads to an increase in an individual's probability of vaccinating, and vice versa.

The economics literature on standard models of decision making and discussions of vaccination decisions consider the positive and normative implications of nonconforming peer effects or free-riding ([105]). However, the role of conforming peer effects has largely been ignored despite a vast literature documenting the existence of conforming peer effects in a variety of contexts, such as unhealthy behaviors, academic achievement and productivity ([118, 84, 48, 55]). In particular, some recent studies have documented the presence of conforming peer effects in vaccination decisions; see ([60, 61, 87, 99, 109, 121, 124]) for details. In particular, [109] looked at flu vaccination decisions made by undergraduates at a large private university and examined the role of the social network in health beliefs and vaccination choices. The authors determine that social effects play a large role in changing people's perceptions of the benefits of immunization. Taking advantage of the random assignment of students to housing, they were further able to show that the clustering of decisions in a social network were not simply due to homophily, but rather due to positive peer effects on individuals' decisions.

In this chapter, we develop a theoretical model based on the standard economic models of decision-making and incorporate both nonconforming and conforming peer

effects. Using this model, we examine how the introduction of peer effects affects our understanding of the decision to vaccinate and the role of public health policy in vaccination markets. We note two important related papers here: [52, 14], both of which model how imitation influences the dynamics of epidemics and vaccination uptake. In [52], individuals estimate the costs and benefits of vaccination by learning from others in the population. As agents imitate successful strategies, overall vaccination coverage drops below even the individual optimum. In [14], the authors propose a dynamic model in which individuals adopt strategies by imitating others while considering the current disease prevalence. This model leads to regimes in which the vaccination uptake oscillates, as is often seen in vaccine scares. The model we propose in this chapter explicitly examines the role of conforming and nonconforming peer effects in determining individually optimal strategies. We further build on these papers and others mentioned above by looking at the role of these peer effects in the effectiveness of various public health policies.

Overall, our results demonstrate that adding conforming peer effects to the traditional model of vaccination decisions can have important implications. In the traditional economic model, agents free-ride on the decisions of others and as a result the privately optimal vaccination rate is always below the socially optimal vaccination rate. In contrast, in the model with conforming peer effects privately optimal vaccination rates can be above or below the social optimal. In the fact the model produces several evolutionary stable equilibria including no vaccination coverage, full vaccination coverage and a mixed strategy equilibrium. Traditional models also imply that vaccine subsidies are always optimal and even large subsidies cannot achieve disease eradication. In contrast, in the model with conforming peer effects subsidies for vaccination are not always optimal. However, in certain cases, depending on disease and vaccine parameters, even small subsidies can achieve disease eradication.

To give a brief overview of this chapter, in Section 5.2, we develop a standard model of vaccination decisions, where rational economic agents maximize expected utility or payoffs. We carefully examine the difference between the individually optimal strategy and the socially optimal level of vaccination coverage, showing how

the parameters of the model will affect the gap between them. We also highlight the effect of government subsidies on vaccination uptake and how their effectiveness depends on the cost and risk of the vaccine and disease in question. In Section 5.3 we add conforming peer effects to the standard model and describe the changes in the individually optimal strategy. With the addition of conforming peer effects, the individually optimal strategy may lead to a higher level of vaccination coverage that what is socially optimal — we discuss the implications of this result and its effect on public policy in the second half of Section 5.3.

5.2 Standard economic model with nonconforming peer effects

In this section we develop a standard economic model of vaccination decisions, where rational economic agents maximize expected utility or payoffs, based on the models in [13, 15]. Vaccination confers immunity against an infectious disease but also may have adverse health side effects as well as monetary costs. In this model individual vaccination decisions are linked to decisions of the group as the benefit of vaccination depends on the prevalence of the infectious disease, which in turn depends on the group's likelihood of vaccination. For example, an increase in vaccination rate among peers would reduce disease prevalence which in turn would reduce individual incentives to vaccinate. Thus, in the standard economic model, peer effects are *nonconforming* — individual decisions are inversely related to group decisions. In Section 5.3 we add *conforming peer effects* to the standard model, where an increase in the group's likelihood to vaccinate leads to an increase in the individual's likelihood to vaccinate. Next, we contrast the normative and positive implications of the two models.

5.2.1 Payoffs

We start with a model of risk-neutral agents with additively separable utility in health and consumption. Under this model the expected utility from vaccination is given by

$$E_{vac} = h(H - d_v) + u(C - m) \tag{5.1}$$

where H is an individual's health endowment, C is consumption, d_v is the morbidity cost of side effects, and m is the marginal cost of producing the vaccine. If agents are risk-neutral, then the functions $h(\cdot)$ and $u(\cdot)$ are linear and the payoff from vaccination can be expressed as

$$E_{vac} = H - d_v + \theta(C - m) \tag{5.2}$$

where θ is the marginal utility of consumption in health units.

In the standard economic model with nonconforming peer effects the payoff for not vaccinating varies only with the infection probability, which depends on the total vaccination coverage. If agents are risk-neutral, the payoff from not vaccinating can be expressed as follows,

$$E_{nv}(p) = (H - d_i)w(p) + H(1 - w(p)) + \theta C \tag{5.3}$$

$$= H - d_i w(p) + \theta C \tag{5.4}$$

where d_i represents the morbidity cost of infection and $w(p)$ is the probability of being infected when the vaccination coverage is p. We assume that $w(p)$ is strictly decreasing in p for all $p \leq p_{crit}$. For $p \geq p_{crit}$, $w(p) = 0$, that is, p_{crit} is the critical vaccination threshold above which herd immunity is achieved and the disease eradicated. Note that in this model, the cost of not vaccinating only involves a cost of infection; individuals are fully insured against medical expenses related to treatment of vaccine preventable disease and face no other monetary or psychological costs of not vaccinating.

The expected payoff for playing a mixed strategy P (vaccinating with probability

P) when the vaccination coverage level is p is

$$\hat{E}[P,p] = P[H + \theta(C-m) - d_v] + (1-P)[H + \theta C - d_i w(p)] \tag{5.5}$$

$$= H + \theta C - P[\theta m + d_v] - (1-P)[d_i w(p)] \tag{5.6}$$

By defining the *relative cost* as

$$r = (\theta m + d_v)/d_i, \tag{5.7}$$

this expected payoff can be expressed as

$$E[P,p] = \frac{\hat{E}[P,p]}{d_i} = \frac{H + \theta C}{d_i} - rP - (1-P)[w(p)] \tag{5.8}$$

where the multiplicative constant d_i will not make any difference in our proofs or calculations. With the assumption that $0 \leq \theta m + d_v \leq d_i$, we have $0 \leq r \leq 1$.

5.2.2 Equilibria

In the vaccination game with nonconforming peer effects, individuals seek to maximize their expected payoff given the current vaccination coverage p. If $p \geq p_{crit}$, this payoff function becomes

$$E[P,p] = H + \theta C + P[-d_v - \theta m] \tag{5.9}$$

which is clearly decreasing in P. As a result, if the current vaccination coverage is above the critical threshold, individuals will always choose to never vaccinate ($P = 0$). Assuming that the game is played repeatedly (or at least that individuals make decisions assuming that it is so), this will decrease the total vaccination coverage until $p < p_{crit}$ and the probability of infection becomes nonzero.

If $p < p_{crit}$, then the expected payoff is given in (5.8). If the payoff function is decreasing in P, individuals will choose to never vaccinate; if it is increasing in P, individuals will choose to always vaccinate. Examining the first case, we see that the

payoff function is decreasing in P if $r > w(p)$,

$$\frac{\partial E[P,p]}{\partial P} = -r + w(p) < 0. \tag{5.10}$$

As a result, when $r > w(p)$ individuals will always choose to not vaccinate ($P = 0$), decreasing the total vaccination coverage p, and increasing $w(p)$ until the point p^* where the total vaccination coverage satisfies $w(p^*) = r$. Note, however, that if $r > w(0)$, this process will continue to the point where nobody will vaccinate, $p = 0$. This is an example of the classic "free-rider" problem, where individuals rationally choose a strategy where they benefit while not contributing to society, leading to the point where everyone follows the same strategy and nobody benefits.

In the second case, we see that the payoff function is increasing in P if $r < w(p)$,

$$\frac{\partial E[P,p]}{\partial P} = -d_v - \theta m + d_i w(p) > 0, \tag{5.11}$$

As a result, if the relative cost is sufficiently small, individuals will always choose to vaccinate ($P = 1$), increasing the vaccination coverage and increasing $w(p)$ until the point p^* where the total vaccination coverage satisfies $w(p^*) = r$. See Figure 5.1 for an illustration of this solution. This strategy is stable, as stated formally in Lemma 5.1; we leave the detailed proof of this lemma to 5.6.

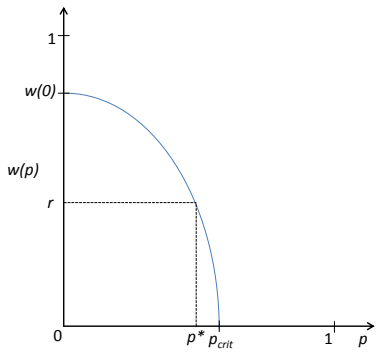

Figure 5.1: Solving $r = w(p^*)$

Lemma 5.1. *The mixed strategy p^* that satisfies $w(p^*) = r$ is a weak Nash Equilibrium and an Evolutionarily Stable Strategy in the vaccination game with nonconforming peer effects if $r = \frac{\theta m + d_v}{d_i} < w(0)$. If $r > w(0)$, the pure strategy $P = 0$ is a strict Nash Equilibrium and Evolutionarily Stable Strategy.*

5.2.3 Social welfare and individually optimum strategies

In many games the equilibrium reached by rational agents may not be the socially optimal value. In our case, we define the social welfare as the normalized total utility of the population,

$$W(p) = pE_{vac} + (1-p)E_{nv}(p) \tag{5.12}$$

and using our payoff functions from Section 5.2.1, we have

$$W(p) = p[H + \theta(C-m) - d_v] + (1-p)[H + \theta C - d_i w(p)]. \tag{5.13}$$

For a general infection probability function $w(p)$ with vaccination threshold p_{crit}, the socially optimal vaccination coverage p_{opt} is the vaccination level that maximizes the social welfare, i.e.,

$$p_{opt} = \underset{0 \le p \le 1}{\operatorname{argmax}} W(p) \tag{5.14}$$

The social welfare function is decreasing for $p > p_{crit}$:

$$\frac{\partial W(p)}{\partial p} = -\theta m - d_v < 0 \tag{5.15}$$

where (5.15) uses the fact that $w(p) = 0$ for $p > p_{crit}$. For $p > p_{crit}$, increasing vaccination rates reduces the social welfare, as the disease is already eradicated and increasing vaccinations provide no benefit but individuals incur the monetary costs of the vaccine.

For $p < p_{crit}$, differentiating with respect to p, we have

$$\frac{\partial W(p)}{\partial p} = -\theta m - d_v + d_i \left[w(p) - (1-p)\frac{\partial w(p)}{\partial p} \right] \tag{5.16}$$

where $\frac{\partial w(p)}{\partial p} < 0$ for $0 < p < p_{crit}$. As a result, the social welfare function is increasing in p for $p \leq p_{crit}$ if

$$\theta m + d_v < d_i \left[w(p) - (1-p)\frac{\partial w(p)}{\partial p} \right] \tag{5.17}$$

or equivalently, if

$$r < w(p) - (1-p)\frac{\partial w(p)}{\partial p}. \tag{5.18}$$

If this condition is met, the maximum social welfare will be achieved at $p_{opt} = p_{crit}$, the point at which the disease is eradicated. If this condition is not met, we have $p_{opt} \leq p_{crit}$, since the social welfare function is always decreasing beyond p_{crit}.

Remark 1. *Note that from a policy perspective, often the desired vaccination level is one that achieves herd immunity or disease eradication, so $p_{opt} = p_{crit}$, regardless of wherever the minimum of the social welfare function might be. For example, in 1977 the World Health Organization (WHO) successfully eradicated smallpox through a worldwide vaccination program [49]. The rationale is that disease eradication benefits not only the current generation but also future generations. The social welfare function we consider in this chapter only models the welfare of the current generation and therefore within the context of our model p_{opt} can be lower than p_{crit}.*

Remark 2. *As a running example throughout this chapter, we will consider the infection probability $w(p)$ as the steady-state infection probability in a SIR (Susceptible-Infected-Recovered) model with constant birth and death rate μ. In this case, $w(p) = 1 - \frac{1}{R_0(1-p)}$ where R_0 is the* reproduction ratio *of the disease in question. For a detailed description of this model and how to derive its infection probability function, see 5.7. For this model, the disease will be eradicated if the vaccination level is at or above the critical vaccination threshold: $p_{crit} = 1 - 1/R_0$. In this example, the optimal vaccination coverage will be $p_{opt} = p_{crit}$, as the condition in* (5.18) *is satisfied for $w(p) = 1 - \frac{1}{R_0(1-p)}$, as long as $r < 1$, which is true by assumption.*

However, if we assume that individuals are allowed to make their own vaccination decisions, disease eradication will not be possible, and often the optimal vaccination coverage is not acheived. The privately optimal strategy p^* is always less than the

critical vaccination threshold, as shown in Figure 5.1. Even in the case where the socially optimal vaccination rate is less than the critical threshold, the privately optimal strategy is still less than the social optimum. Formally,

Theorem 5.2. *The private optimum $p^* \leq p_{opt}$ in the vaccination game with nonconforming peer effects.*

Proof. Differentiating the social welfare function when $p < p_{crit}$, we have

$$\frac{\partial W(p)}{\partial p} = [-d_v - \theta m + d_i w(p)] + (1-p)\left[-d_i \frac{\partial w(p)}{\partial p}\right] \tag{5.19}$$

$$= \frac{\partial E[P,p]}{\partial P} + \underbrace{(1-p)\left[-d_i \frac{\partial w(p)}{\partial p}\right]}_{>0 \text{ always, since } \frac{\partial w(p)}{\partial p} < 0} \tag{5.20}$$

The first term captures the private benefit from increasing vaccination and the second term captures the societal benefit which arises as increasing vaccination reduces the probability of infection for the entire population. At the private optimum $p = p^*$, the social welfare will be increasing with p, since $\frac{\partial E[P,p]}{\partial P} = 0$ for $p = p^*$. Further, for $p < p^*$, the social welfare will also be increasing with p, as

$$-d_v - \theta m + d_i w(p - \epsilon) > -d_v - \theta m + d_i w(p^*) = 0 \tag{5.21}$$

where the inequality comes from the fact that $w(p)$ is decreasing in p. So, the social welfare function is increasing in p for all $p \leq p^*$, and as a result, since $p_{opt} = \operatorname{argmax} W(p)$ and using the analysis above, we have

$$p^* \leq p_{opt} \leq p_{crit} \tag{5.22}$$

□

Exactly how much lower the social welfare is when individuals act selfishly from the optimal point depends on several factors. The social welfare at the socially optimal point, dividing by the constant d_i to obtain an expression in terms of the relative

cost, is

$$\frac{W(p_{opt})}{d_i} = \frac{1}{d_i}(p_{opt}[H + \theta(C - m) - d_v] + (1 - p_{opt})[H + \theta C - d_i w(p_{opt})]) \quad (5.23)$$

$$= \frac{H + \theta C}{d_i} - w(p_{opt}) + p_{opt}[-r + w(p_{opt})]. \quad (5.24)$$

The social welfare at the private optimum, again dividing by d_i, is

$$\frac{W(p^*)}{d_i} = \frac{1}{d_i}(p^*[H + \theta(C - m) - d_v] + (1 - p^*)[H + \theta C - d_i w(p^*]) \quad (5.25)$$

$$= \frac{H + \theta C}{d_i} - w(p^*) + p^*[-r + w(p^*)] \quad (5.26)$$

$$= \frac{H + \theta C}{d_i} - w(p^*) \quad (5.27)$$

since $w(p^*) = r$. We can easily calculate the difference between the two:

$$\frac{W(p_{opt}) - W(p^*)}{d_i} = \frac{H + \theta C}{d_i} - w(p_{opt}) + p_{opt}[-r + w(p_{opt})] - \frac{H + \theta C}{d_i} + w(p^*) \quad (5.28)$$

$$= (1 - p_{opt})(r - w(p_{opt})) \quad (5.29)$$

again using $w(p^*) = r$. The above equations show that as the cost of the vaccine (m and d_v) increases and as the cost of infection (d_i) decreases, this gap in welfare will increase; fewer people will voluntarily choose to vaccinate and the social welfare will decrease. We can lower bound the difference, relating it to the social welfare at the point where the disease is eradicated. This lower bound is less meaningful if the optimum vaccination rate is exactly the critical threshold.

5.2.4 Effect of government subsidies

If the government offers subsides of the monetary cost of the vaccine, individuals' expected payoff for vaccinating becomes a function of the subsidy:

$$E_{vac}(s) = H + \theta(C - m(1 - s)) - d_v \quad (5.30)$$

where s represents the percentage of the marginal production cost of the vaccine that the government is subsidizing. The private optimum, as a function of the subsidy,[1] becomes

$$p^*(s) = w^{-1}\left(\frac{\theta m(1-s)+d_v}{d_i}\right). \tag{5.31}$$

Note that this function is strictly decreasing in its argument, since the original probability of infection function $w(p)$ is also strictly decreasing. In general, the effectiveness of the subsidy is inversely related to the morbidity cost of the disease, d_i. That is, vaccine subsidies are less effective for more deadly diseases. However, the effectiveness of the subsidy is directly related to the morbidity (and monetary) cost of the vaccine, d_v — the vaccine subsides are more effective for more dangerous vaccines. Looking at (5.31) more closely, we see that it is an increasing function of s and d_i, but decreasing in m and d_v. Intuitively, as the government subsidy increases and lowers the monetary cost of the vaccine (or as the danger of infection increases), more people will be inclined to buy the vaccine. Similarly, as the cost and risk of the vaccine increases, less people will be inclined to vaccinate.

Continuing with our running example, we examine the private optimum as a function of the subsidy for a specific infection probability function $w(p) = 1 - \frac{1}{R_0(1-p)}$. In this case, the private optimum becomes

$$p^*(s) = 1 - \frac{1}{R_0\left(1-\frac{\theta m(1-s)+d_v}{d_i}\right)} \tag{5.32}$$

and the derivative with respect to s is

$$\frac{\partial p^*(s)}{\partial s} = \frac{\theta m}{d_i R_0\left(1-\frac{\theta m(1-s)+d_v}{d_i}\right)^2}. \tag{5.33}$$

Inspecting the above equation, we can see that the effectiveness of the subsidy will be *higher* for a higher cost and higher risk (larger m and d_v) vaccine, whereas for a more dangerous disease (larger d_i) the subsidy will not be as effective.

[1]Recall that the private optimum when subsidies are not present is $p^* = w^{-1}\left(\frac{\theta m+d_v}{d_i}\right)$.

Let $x(s) = \frac{\theta m(1-s)+d_v}{d_i}$ to simplify notation. If the goal is to eradicate the disease, then we need $x(s) = 0$ so that $p^*(s) = p_{crit}$. The subsidy that achieves disease eradication even when individuals behave selfishly is

$$s_{opt} = 1 + \frac{d_v}{\theta m} \tag{5.34}$$

obtained by setting $x(s) = 0$. Note that the optimal subsidy here is greater than one — the subsidy must compensate individuals for more than just the monetary cost of the vaccine in order to eradicate the disease. If we impose the constraint that $0 \leq s \leq 1$, the optimal subsidy will be exactly $s_{opt} = 1$.

The social welfare function, as a function of the subsidy, is

$$W(p^*(s)) = p^*(s)[H + \theta(C - m) - d_v] + (1 - p^*(s))[H + \theta C - d_i w(p^*(s))] \tag{5.35}$$

When $s = s_{opt}$, this simplifies to

$$W(p^*(s_{opt})) = p_{crit}[H + \theta(C - m) - d_v] + (1 - p_{crit})[H + \theta C] \tag{5.36}$$

$$= H + \theta(C - p_{crit}m) - p_{crit}d_v. \tag{5.37}$$

In contrast, if we look at the social welfare function when there is no subsidy and individuals behave selfishly, we have

$$W(p^*) = p^*[H + \theta(C - m) - d_v] + (1 - p^*)[H + \theta C - d_i w(p^*)] \tag{5.38}$$

$$= H + \theta(C - m) - d_v \tag{5.39}$$

which is always less than the social welfare at the optimum. Further, it is easy to show that $W(p^*(s)) > W(p^*)$ for any $s > 0$.

5.3 Standard economic model with conforming and nonconforming peer effects

In this section we add conforming peer effects to the standard model in Section 5.2, demonstrating the interaction between the desire to behave rationally and the desire to conform to what others are doing. We follow the same format as in the previous section, first describing the payoffs and equilibria of the model and then discussing the differences between the individually optimal strategies and the socially optimal vaccination coverage, as well as the effect of government subsidies in this new, more realistic model of human decisions.

5.3.1 Payoffs

We begin by defining payoff functions for following each strategy: vaccinating and not vaccinating. We use a linear combination of the payoff functions from Section 5.2 and new payoff functions capturing the reward one gets by conforming:

$$E_{vac}(p) = \gamma' f(p) + H - d_v + \theta(C - m) \tag{5.40}$$

$$E_{nv}(p) = \gamma' g(p) + H - d_i w(p) + \theta C \tag{5.41}$$

where $\gamma' \in (0, \infty]$ measures the strength of the desire to conform, $f(p)$ is a strictly increasing function representing the desire to conform to the vaccinating strategy, and $g(p)$ is a strictly decreasing function representing the desire to conform to the nonvaccinating strategy. Note that this general formulation can capture bias; for example, a given population might put more weight on conforming to the nonvaccinating, rather than vaccinating, strategy. All other variables are the same as defined in Section 5.2.

We can also describe a simpler game with symmetric linear payoff functions for

conformity, as follows. Let $f(p) = p$ and $g(p) = 1 - p$, so that

$$E_{vac}(p) = \gamma' p + H - d_v + \theta(C - m) \tag{5.42}$$

$$E_{nv}(p) = \gamma'(1 - p) + H - d_i w(p) + \theta C \tag{5.43}$$

The expected payoff for playing a mixed strategy P (vaccinating with probability P) when the vaccination coverage level is p is

$$\hat{E}[P, p] = P[\gamma' f(p) + H + \theta(C - m) - d_v] + (1 - P)[\gamma' g(p) + H + \theta C - d_i w(p)] \tag{5.44}$$

$$= H + \theta C - P[\theta m + d_v - \gamma' f(p)] - (1 - P)[d_i w(p) - \gamma' g(p)] \tag{5.45}$$

Again dividing through by d_i and using the relative cost of the vaccine, we can express the expected payoff as

$$E[P, p] = \frac{\hat{E}[P, p]}{d_i} = \frac{H + \theta C}{d_i} - P[r - \gamma f(p)] - (1 - P)[w(p) - \gamma g(p)] \tag{5.46}$$

where $\gamma = \frac{\gamma'}{d_i}$ is just a scaled constant measuring the strength of the desire to conform. Note that we retain the assumption that $0 \leq r \leq 1$. For convenience, let $h(p) = g(p) - f(p)$, a useful strictly decreasing summary function. We assume

$$h(0) = \alpha \tag{5.47}$$

$$h(1) = -\beta. \tag{5.48}$$

For reference, we also define the *pure conformity game*, where payoffs are only a function of the desire to conform to others, and there are no nonconforming peer effects.

$$E_{vac}(p) = \gamma' f(p) \tag{5.49}$$

$$E_{nv}(p) = \gamma' g(p) \tag{5.50}$$

The pure conformity game has two pure strict NE (and ESS's): $P = 0$ and $P = 1$, which can easily be shown to always exist. It further has a weak NE at $P = p^*$ where p^* is the solution to $0 = \gamma' h(p^*)$, but this equilibria is not an ESS. If we use the symmetric linear conformity payoff functions as described in (5.42) and (5.43), we have

$$E_{vac}(p) = \gamma' p \tag{5.51}$$

$$E_{nv}(p) = \gamma'(1 - p) \tag{5.52}$$

This simple pure conformity game will always have two pure strict NE (and ESS's): $P = 0$ and $P = 1$. It also has a weak NE at $P = p^* = 1/2$, where p^* is the solution to $0 = h(p^*) = \gamma'(1-2p^*)$, but this equilibria will not be an ESS. To illustrate this result, imagine the conformity game with exactly half of the population vaccinating. As soon as the fraction vaccinating slightly increases (or decreases), the majority strategy is no longer 50—50, and the population will converge to the strict NE $P = 1$, always vaccinating (or $P = 0$, never vaccinating).

5.3.2 Equilibria

Just as described in Section 5.2.2, individuals here will seek to maximize their expected payoff given the current vaccination coverage p. However, when the game also includes conforming peer effects, individual strategies become more complicated, reflecting the tension between the desire to conform and to free-ride on others' decisions to vaccinate. In this section, we show that the vaccination game with both conforming and nonconforming peer effects can have multiple stable equilibria whose existence and stability depend on the disease and cost parameters of the model, in contrast to the vaccination game with only nonconforming peer effects, which only has one stable equilibrium.

Lemma 5.3. *The pure nonvaccinating strategy $P = 0$ is a strict Nash Equilibrium and Evolutionarily Stable Strategy of the vaccination game with conforming and non-*

conforming peer effects if $r > w(0) - \gamma\alpha$.

Proof. Using Definition 7 from 5.5, the pure strategy $P = 0$ (never vaccinating) is a strict Nash Equilibrium (and thus an evolutionarily stable strategy) if $E(P, P) - E(Q, P) > 0$. Calculating this, we have

$$E(P, P) - E(Q, P) = (P - Q)(E_v(P) - E_{nv}(P)) \tag{5.53}$$

$$= -Q(E_v(0) - E_{nv}(0)) \tag{5.54}$$

$$= -Q(-\theta m - d_v + d_i w(0) - \gamma'\alpha) \tag{5.55}$$

Thus, $E(P, P) > E(Q, P)$ and $P = 0$ is a strict NE and ESS if

$$-\theta m - d_v + d_i w(0) - \gamma'\alpha < 0, \tag{5.56}$$

or equivalently, if $r > w(0) - \gamma\alpha$. □

The above lemma states that if the vaccine is sufficiently costly or has large side effects relative to the mortality costs of infection, never vaccinating will be a stable equilibrium strategy. Alternatively, if the disease is sufficiently not infectious, that is, $w(0)$ is small, then never vaccinating will be a stable equilibrium strategy. Note that as $\gamma \to 0$ and the desire to conform goes away, this approaches the condition for never vaccinating when only nonconforming peer effects are present. However, when $\gamma \to \infty$, and the conforming strategy dominates, never vaccinating will always be a stable equilibrium strategy, as in the pure conformity game.

Lemma 5.4. *The pure vaccinating strategy* $P = 1$ *is a strict Nash Equilibrium and Evolutionarily Stable Strategy of the vaccination game with conforming and nonconforming peer effects if* $r < \gamma\beta$.

Proof. Using Definition 7 from 5.5, the pure strategy $P = 1$ (always vaccinating) is a strict Nash Equilibrium (and thus an evolutionarily stable strategy) if $E(P, P) -$

$E(Q,P) > 0$. Calculating this, we have

$$E(P,P) - E(Q,P) = (P-Q)(E_v(P) - E_{nv}(P)) \tag{5.57}$$
$$= (1-Q)(E_v(1) - E_{nv}(1)) \tag{5.58}$$
$$= (1-Q)(-\theta m - d_v + \gamma'\beta) \tag{5.59}$$

since $w(1) = 0$. Thus, $E(P,P) > E(Q,P)$ and $P = 1$ is a strict NE and ESS if

$$-\theta m - d_v + \gamma'\beta > 0, \tag{5.60}$$

or equivalently, if $r < \gamma\beta$. □

The above lemma states that if the vaccine is sufficiently safe, always vaccinating will be a stable equilibrium strategy. Note that as $\gamma \to 0$ and the desire to conform goes away, always vaccinating will *never* be a stable equilibrium, as is the case for the vaccination game with only nonconforming peer effects. However, when $\gamma \to \infty$, and the conforming strategy dominates, always vaccinating becomes a stable equilibrium strategy, as in the pure conformity game.

Lemma 5.5. *The mixed strategy p^* satisfying $E_v(p^*) = E_{nv}(p^*)$ is a weak Nash Equilibrium and Evolutionarily Stable Strategy for the vaccination game with conforming and nonconforming peer effects if*

$$\frac{\partial w(p)}{\partial p} < \gamma \frac{\partial h(p)}{\partial p} \tag{5.61}$$

Proof. Consider a population following the mixed equilibrium strategy p^*, (vaccinating with probability p^*) where p^* is the solution to the equation

$$E_v(p^*) = E_{nv}(p^*) \tag{5.62}$$

This strategy is clearly a weak Nash Equilibrium, since

$$E(p^*, p^*) - E(Q, p^*) = (p^* - Q)(E_v(p^*) - E_{nv}(p^*)) = 0. \tag{5.63}$$

Using Definition 9 from 5.5, p^* will be an evolutionarily stable strategy if

$$E(p^*, Q) > E(Q, Q) \iff (p^* - Q)(E_v(Q) - E_{nv}(Q)) > 0. \tag{5.64}$$

This definition states that vaccinating with probability p^* is preferable to some other level Q, given that the current vaccination coverage is Q — the equilibrium strategy p^* will be able to successfully "invade" a population with coverage Q. It turns out that p^* will be an ESS if $E_v(p) - E_{nv}(p)$ is strictly decreasing in the vaccination coverage p. To see this, consider first the case where $Q > p^*$, where the current vaccination coverage is greater than the equilibrium p^*. If $E_v(p) - E_{nv}(p)$ is strictly decreasing in the vaccination coverage p, then

$$E_v(Q) - E_{nv}(Q) < E_v(p^*) - E_{nv}(p^*) = 0 \tag{5.65}$$

and so we have $(p^* - Q)(E_v(Q) - E_{nv}(Q)) > 0$, and individuals vaccinating with probability p^* will obtain a higher expected payoff than the rest of the population when the coverage level Q is greater than p^*.

Now consider the case where $Q < p^*$, where the current vaccination coverage is less than the equilibrium p^*. Again, if $E_v(p) - E_{nv}(p)$ is strictly decreasing in the vaccination coverage p, then

$$E_v(Q) - E_{nv}(Q) > E_v(p^*) - E_{nv}(p^*) = 0 \tag{5.66}$$

and so we have $(p^* - Q)(E_v(Q) - E_{nv}(Q)) > 0$, and individuals vaccinating with probability p^* will obtain a higher expected payoff than the rest of the population.

Thus, individuals vaccinating with probability p^* solving $E_v(p^*) = E_{nv}(p^*)$ will have higher expected payoffs than the rest of the population when the vaccination

coverage is at any level Q; i.e., p^* is not only a weak Nash Equilibrium, it is also an evolutionarily stable strategy if $E_v(p) - E_{nv}(p)$ is strictly decreasing in the vaccination coverage p. This condition is equivalent to

$$\begin{aligned}
&\frac{\partial}{\partial p}[E_v(p) - E_{nv}(p)] < 0 \\
&\iff \frac{\partial}{\partial p}[\gamma' f(p) + H - d_v + \theta(C - m) - \gamma' g(p) - H + d_i w(p) - \theta C] < 0 \\
&\iff \gamma' \frac{\partial f(p)}{\partial p} - \gamma' \frac{\partial g(p)}{\partial p} + d_i \frac{\partial w(p)}{\partial p} < 0 \\
&\iff \frac{\partial w(p)}{\partial p} < \gamma \frac{\partial h(p)}{\partial p}. \qquad (5.67)
\end{aligned}$$

For reference, we refer to (5.67) as the "mixed strategy ESS condition". □

We can explain the "mixed strategy ESS condition" above intuitively. Both the LHS and RHS of equation (5.67) are less than zero. The LHS shows how the probability of infection falls with an increase in vaccination coverage. The higher the absolute value of this gradient the greater the incentive to free-ride on others. The RHS shows how the payoff for conforming to the nonvaccinating strategy relative to the vaccination strategy changes with an increase in vaccination coverage. The higher the absolute value of this gradient the greater the desire to conform to the majority vaccination strategy. If the desire to conform is relatively high then it will overpower the desire to free-ride resulting in a corner solution with everyone following the same strategy, either 100% or 0% vaccinating. The equation shows that a mixed strategy ESS is only possible as long as the desire to conform does not completely offset the desire to free-ride.

Note that the vaccination game with conforming and nonconforming peer effects may have more than one weak Nash Equilibrium, in contrast to the game in Section 5.2.2, if (5.62) has more than one solution. However, in order for a given weak Nash Equilibrium to also be stable, the mixed strategy ESS condition in (5.67) must be satisfied at that point. Thus, depending on the disease and cost parameters of the model, the game here can have more than one stable equilibrium.

To illustrate the main results, we give here a specific example of a vaccination game with conforming and nonconforming peer effects. Assume symmetric linear conformity payoff functions:

$$f(p) = p \tag{5.68}$$

$$g(p) = (1 - p). \tag{5.69}$$

For these conformity functions, we have $h(0) = 1$ and $h(1) = -1$. The payoff functions become

$$E_{vac}(p) = \gamma' p + H - d_v + \theta(C - m) \tag{5.70}$$

$$E_{nv}(p) = \gamma'(1 - p) + H - d_i w(p) + \theta C \tag{5.71}$$

and the expected payoff is

$$\begin{aligned} \hat{E}[P, p] &= P[\gamma' p + H + \theta(C - m) - d_v] \\ &\quad + (1 - P)[\gamma'(1 - p) + H + \theta C - d_i w(p)] \qquad (5.72) \\ &= H + \theta C - P[\theta m + d_v - \gamma' p] - (1 - P)[d_i w(p) - \gamma'(1 - p)] \qquad (5.73) \end{aligned}$$

In terms of the relative cost, the expected payoff becomes

$$E[P, p] = \frac{\hat{E}[P, p]}{d_i} = \frac{H + \theta C}{d_i} - P[r - \gamma p] - (1 - P)[w(p) - \gamma(1 - p)] \tag{5.74}$$

For this example, let $w(p)$ be the SIR probability of infection: $w(p) = 1 - \frac{1}{R_0(1-p)}$, as described in 5.7. The parameter R_0 is the basic reproduction ratio of the disease and will vary for different diseases. Using the equilibrium strategy analysis from earlier, never vaccinating ($P = 0$) will be a pure strict NE (and an ESS) when $r > 1 - 1/R_0 - \gamma$; i.e., when the vaccine is sufficiently risky. Similarly, always vaccinating ($P = 1$) will be a pure strict NE (and an ESS) when $r < \gamma$; i.e., when the vaccine is sufficiently safe. Note that by making the desire to conform sufficiently

strong (increasing γ), we can achieve the same result. All solutions[2] to the equation

$$E_{vac}(p^*) = E_{nv}(p^*) \tag{5.75}$$

will be weak Nash Equilibria for this example. For $p < p_{crit}$ this becomes

$$\begin{aligned}\gamma' p^* + H - d_v + \theta(C - m) &= \gamma'(1 - p^*) + H - d_i \left[1 - \frac{1}{R_0(1 - p^*)}\right] + \theta C \\ -r &= \gamma(1 - 2p^*) - \left(1 - \frac{1}{R_0(1 - p^*)}\right).\end{aligned} \tag{5.76}$$

However, only one solution of (5.75) will satisfy the mixed strategy ESS condition in (5.67). This solution is given by

$$q^* = \frac{\sqrt{R_0}(3\gamma + r - 1) + \sqrt{R_0(\gamma - r + 1)^2 - 8\gamma}}{4\sqrt{R_0}\gamma}. \tag{5.77}$$

This solution will exist when

$$0 \leq \gamma \leq \frac{r}{1 - \frac{2}{R_0}} \tag{5.78}$$

or, in terms of r, when

$$\gamma\left(1 - \frac{2}{R_0}\right) \leq r \leq 1 + \gamma - 2\sqrt{2}\sqrt{\frac{\gamma}{R_0}}. \tag{5.79}$$

Note that as q^* is the solution to the quadratic equation, it will by necessity always be less than p_{crit}. We plot all of the evolutionarily stable strategies for this example as a function of γ in Figure 5.2, with $R_0 = 5$ and $r = 0.5$. The solid black horizontal line shows the vaccination coverage needed to eradicate the disease. Examining the

[2]There are three solutions to the equation in (5.75), two to the quadratic equation (5.76) and one to the linear equation which occurs when $p \geq p_{crit}$ and $w(p) = 0$. They are given by

$$\begin{aligned}q_{1,2} &= \frac{\sqrt{R_0}(3\gamma + r - 1) \pm \sqrt{R_0(\gamma - r + 1)^2 - 8\gamma}}{4\sqrt{R_0}\gamma} \\ l &= \frac{\gamma + r}{2\gamma}\end{aligned}$$

Using the mixed ESS condition in (5.67) we see that the linear solution l will never be an ESS, and when the quadratic solutions exist, only q_1 will be an ESS.

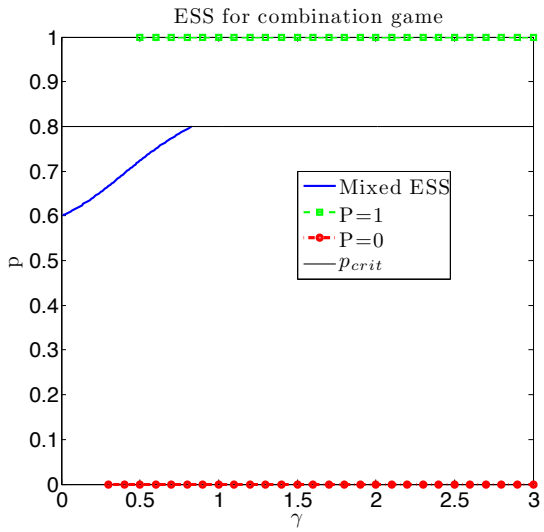

Figure 5.2: ESS as a function of γ

figure, we see that for $\gamma = 0$, the private optimum is lower than the social optimum. As we introduce conforming peer effects and γ increases, the private optimum mixed strategy approaches the social optimum. However, increasing the strength of conforming peer effects also leads to the emergence of pure strategies with either no vaccination coverage ($P = 0$) or full vaccination coverage ($P = 1$) as evolutionary stable equilibria. This means that as conformity begins to dominate we could end up in a situation where we eradicate the disease but incur excess social costs due to over-vaccination or a situation where no one vaccinates and we incur mortality and morbidity costs of high disease prevalence.

In Figure 5.3 we plot *all* Nash equilibria, both strict and weak. We note that the weak NE in this example will not be ESS's, but that they serve an important role in determining which ESS the system converges to. For example, imagine a case with $\gamma = 0.5$ and the current vaccination coverage at 5%, below the weak NE. In this case, the system will converge to the pure nonvaccinator equilibrium, $P = 0$. However, if instead the current vaccination coverage is 40%, above the weak NE, the system will converge to mixed ESS, at approximately 70% coverage. Similar examples can be proposed for convergence to the pure vaccinator equilibrium at $P = 1$. We examine this effect in more detail in Section 5.3.4 in the context of government subsidies.

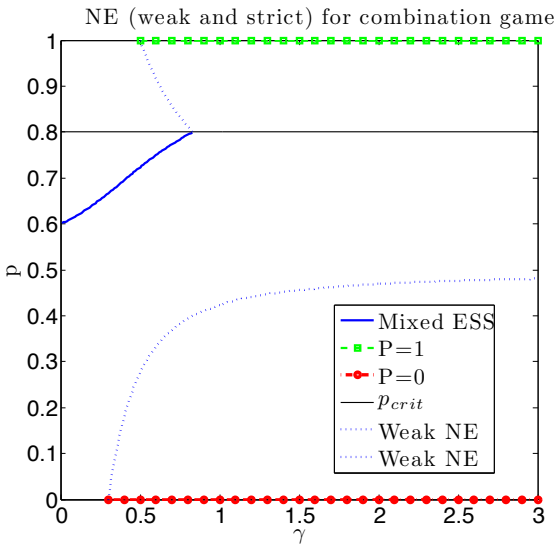

Figure 5.3: All NE as a function of γ

In summary, the game with only nonconforming peer effects, as described in Section 5.2, has only one unique evolutionarily stable strategy, either a mixed strategy below the social optimum, or the pure strategy with no vaccination coverage. In contrast, the game with both nonconforming and conforming peer effects has a much richer set of equilibria, admitting up to 3 evolutionarily stable strategies including a mixed strategy equilibrium and two pure strategy equilibria with either full or no vaccination coverage. The likelihood of observing pure strategy equilibria with full vaccination coverage increases with the strength of conforming peer effects and decreases with the relative cost of the vaccine. Similarly, the likelihood of observing pure strategy equilibria with no vaccination coverage increases with the strength of conforming peer effects and increases with the relative cost of the vaccine.

5.3.3 Social welfare and individually optimal strategies

For the game with both conforming and nonconforming peer effects, we consider the *same* social welfare as in Section 5.2, ignoring the additional utility given by the conformity functions. In other words, we assume that the value derived by individuals in conforming to a particular strategy does not have any social value. In theory, it is unclear whether the social value of utility derived from conforming is zero. We make

this assumption as most policymakers or public health officials in charge of vaccination policy will likely discount the pure utility from conforming in making policy decisions. They are likely to only consider the public health impact and monetary costs of alternate policy options. As a result, we have the same social optimum as before, $p_{opt} = p_{crit}$, if the condition in (5.18) is met; otherwise $p_{opt} \leq p_{crit}$. For our running example with $w(p) = 1 - \frac{1}{R_0(1-p)}$, we have $p_{opt} = p_{crit}$, as discussed in Remark 2 earlier.

In contrast to the model in Section 5.2, we note that when conforming peer effects are present in the standard economic model, the private vaccination level can be higher or lower than the social optimum. If the entire payoff function depends on conformity, there will only be two stable equilibria: one at everyone vaccinating and one at nobody vaccinating, while the social optimum remains constant at $p_{opt} = 1 - \frac{1}{R_0}$. When there is also a desire to behave "rationally," the regions where these pure strategy equilibria exist shrink, and a mixed strategy equilibria appears. This mixed stable strategy will always be less than the socially optimal level, as discussed in the derivation of the ESS's in the previous section, i.e., $q^* < p_{opt}$.

Define $p_{conform}$ as the weak NE (not ESS) of the pure conformity game, and $p_{non-conform}$ as the weak NE (ESS) of the vaccination game with nonconforming peer effects from Section 5.2.2. Also define $p_{combo} = q^*$ as the weak NE (ESS) of the vaccination game with both conforming and nonconforming peer effects from the previous section.

In terms of pure strategies, we have that if $p_{conform}$ decreases, we have a smaller α and a larger β, or *more pressure to vaccinate*. In this case, the range for which we have a pure (strict and ESS) NE at $P = 1$ will grow, while the range for which the pure strategy $P = 0$ is a strict NE (and ESS) shrinks. If we increase $p_{conform}$, however, increasing α and decreasing β, we will have *more pressure to not vaccinate*. In this case, the range for which we have a pure (strict and ESS) NE at $P = 1$ will shrink, while the range for which the pure strategy $P = 0$ is a strict NE (and ESS) grows.

In the case of mixed strategies, the advantage of having conformity will depend

on the relative values of $p_{non-conform}$ and $p_{conform}$. We state the formal conditions for conformity to provide an advantage in the theorem below.

Theorem 5.6. *The Evolutionarily Stable Strategy (if it exists) of the vaccination game with both conforming and nonconforming peer effects will be higher than that of the game with only nonconforming peer effects if and only if the mixed strict Nash Equilibrium of the vaccination game with nonconforming peer effects is higher than the mixed weak Nash Equilibrium of the pure conformity game, i.e.,*

$$p_{non-conform} > p_{conform} \iff p_{combo} > p_{non-conform}.$$

Proof. For simplicity, let $p_{non-conform} = p_{nc}$ and $p_{conform} = p_c$.

$$p_{nc} > p_c \tag{5.80}$$

$$\iff \gamma' h(p_{nc}) < \gamma' h(p_c) \tag{5.81}$$

$$\iff \gamma' h(p_{nc}) < 0 \tag{5.82}$$

$$\iff \gamma' h(p_{nc}) - [d_i w(p_{nc}) - \theta m - d_v] < [\gamma' h(p_{combo}) - d_i w(p_{combo}) + \theta m + d_v] \tag{5.83}$$

$$\iff \gamma h(p_{nc}) - w(p_{nc}) + r < \gamma h(p_{combo}) - w(p_{combo}) + r \tag{5.84}$$

$$\iff p_{nc} < p_{combo} \tag{5.85}$$

Line (5.81) come from the fact that $h(p)$ is decreasing in p; line (5.82) since $h(p_c) = 0$; and lines (5.83) and (5.84) use the equilibrium solutions of the vaccination games. The last line follows from the fact that, when p_{combo} exists, $\gamma h(p) - w(p)$ increases with p, according to mixed strategy ESS condition. □

We can see that under certain conditions, the private optimum achieved in the game with both conforming and nonconforming peer effects will be higher than that of the game with only nonconforming peer effects; i.e., under certain conditions, conformity "helps", bringing the private optimum closer to the socially optimal level. We illustrate this effect with our running example in Figure 5.4, plotting the ESS's as

a function of r, for various γ and R_0. The solid horizontal black line plots the coverage required for disease eradication ($p_{opt} = 1 - \frac{1}{R_0}$), while the black curved dashed line represents the mixed equilibrium strategy for the game with only nonconforming peer effects (Section 5.2).

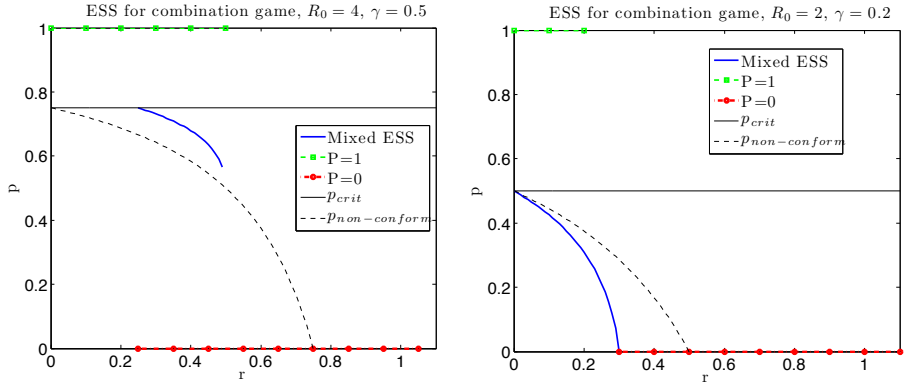

(a) $p_{combo} > p_{non-conform}$ (b) $p_{combo} < p_{non-conform}$

Figure 5.4: ESS as a function of r

As r increases, either through an increase of its monetary cost or risk of serious side effects, the privately optimal strategy will drop below the socially optimal level. Depending on the disease and cost parameters, the mixed strategy may be higher or lower than in the game with only nonconforming peer effects — we see both cases illustrated in Figures 5.4a and 5.4b.

Comparing the mixed strategy ESS with the socially optimal strategy, we see that $p_{combo} \leq p_{opt}$. Exactly how far the individually optimal mixed strategy is from the social optimum can be easily calculated, as follows. The welfare at the private optimum, using the social welfare expression from (5.13) is

$$\frac{W(p_{combo})}{d_i} = \frac{p_{combo}}{d_i}\left[H + \theta(C-m) - d_v\right] + \frac{(1-p_{combo})}{d_i}\left[H + \theta C - d_i w(p_{combo})\right] \tag{5.86}$$

$$= \frac{H+\theta C}{d_i} - w(p_{combo}) + p_{combo}(-r + w(p_{combo})) \tag{5.87}$$

$$= \frac{H+\theta C}{d_i} - r - (1-p_{combo})\gamma h(p_{combo}) \tag{5.88}$$

where we have taken advantage of the fact that $w(p_{combo}) = \gamma h(p_{combo}) + r$. Using this we have the difference between the social welfare at the optimum (using (5.24)) and private ESS as

$$\begin{aligned}\frac{W(p_{opt}) - W(p_{combo})}{d_i} &= \frac{H + \theta C}{d_i} - w(p_{opt}) + p_{opt}[-r + w(p_{opt})] \\ &\quad - \frac{H + \theta C}{d_i} + r + (1 - p_{combo})\gamma h(p_{combo}) \qquad (5.89) \\ &= (1 - p_{opt})(r - w(p_{opt})) + (1 - p_{combo})\gamma h(p_{combo}). \qquad (5.90)\end{aligned}$$

In our running example, $p_{opt} = p_{crit}$, so the difference becomes

$$\frac{W(p_{opt}) - W(p_{combo})}{d_i} = (1 - p_{opt})r + (1 - p_{combo})\gamma h(p_{combo}). \qquad (5.91)$$

Note that if $h(p_{combo}) > 0$, this implies that the difference between the social optimum and the private optimum will be less than in the game with only nonconforming peer effects and that $p_{combo} > p_{nc}$. In our specific example with linear symmetric conformity, this holds if $p_{combo} > 1/2$.

We note also that the major difference between this game and that with only nonconforming peer effects is the existence of the pure 100% vaccinator stable strategy. Lemma 5.4 states the formal conditions for this pure strategy to be stable. In this case, the classic "free-rider effect" does not hold, and the private optimum is in fact higher than the social optimum.

5.3.4 Effect of government subsidies

As before, if the government offers subsidies of the monetary cost of the vaccine, individuals' expected payoff for vaccinating becomes a function of the subsidy. However, in contrast to the earlier section, with conforming peer effects present, it will also be a function of the current coverage:

$$E_{vac}(p, s) = H + \theta(C - m(1 - s)) - d_v + \gamma' f(p) \qquad (5.92)$$

where s represents the percentage of the marginal production cost of the vaccine that the government is subsidizing. Unlike the game with only nonconforming peer effects, there is no simple way to write the private optimum as a function of the subsidy, so we instead focus on general effects and the optimal subsidy in the presence of conforming peer effects.

In general, when the monetary cost of the vaccine is lowered, the vaccination coverage will increase, as can be seen by decreasing r and looking at the mixed ESS in Figure 5.4. When only nonconforming peer effects are present, this produces a counter effect — as the vaccination coverage goes up, individuals' incentive to vaccinate goes down, as their probability of getting infected decreases with the coverage. So, the advantage gained by lowering the monetary cost of the vaccine is mitigated by the nonconforming peer effects, and subsides are less effective. However, when conforming peer effects are present, there is a third effect that can play a role — the individual desire to vaccinate less as more people vaccinate is balanced by the desire to conform, resulting in more effective subsidies than when only nonconforming peer effects are present.

To illustrate these concepts more concretely, we return to our running example, where $f(p) = p$, $g(p) = 1 - p$, and $w(p) = 1 - \frac{1}{R_0(1-p)}$. In this case, the optimal coverage is p_{crit}, and in order to achieve this level of vaccination, we solve for the optimal subsidy. It is easily verified (setting $E_{vac}(p_{crit}, s_{opt}) = E_{nv}(p_{crit})$ and solving for s_{opt}) that

$$s_{opt} = 1 + \frac{d_v - \gamma'\left(1 - \frac{2}{R_0}\right)}{\theta m}. \tag{5.93}$$

Comparing this optimal subsidy to that in Section 5.2.4, we see that if $R_0 > 2$

$$s_{opt}^{combo} < s_{opt}^{nc} \tag{5.94}$$

always — we require less subsidy to achieve the same level of vaccination coverage. Examining the optimal subsidy further, we look at when conformity "helps" and when it can "hurt." In the original game, the optimal subsidy was greater than one

— individuals needed to be paid extra, not just have the cost subsidized, in order to eradicate the disease. When conforming peer effects are present, it is possible to avoid this problem. To see this, look at the case where $s_{opt} \leq 1$. Rearranging and solving for γ', we see that this is equivalent to

$$\gamma \geq \frac{d_v}{d_i \left(1 - \frac{2}{R_0}\right)} \tag{5.95}$$

In other words, if the conformity effect is strong enough, individuals do not need to be paid extra to achieve the social optimum. However, if the conformity effect is too strong, we might need to impose a "tax" to bring the coverage level down to the social optimum. Recall that in this combination game, a pure NE and ESS exists at $P = 1$; if the conformity is strong enough and a subsidy is used, it is possible that individuals would choose to always vaccinate. This would certainly lead to disease eradication, but the extra cost incurred would not make this a socially optimal strategy. Formally, $s_{opt} \leq 0$ if

$$\gamma \geq \frac{r}{1 - \frac{2}{R_0}}. \tag{5.96}$$

In other words, the optimal subsidy will be negative (a tax) if the conforming peer effects are too strong.

Figure 5.5 plots all Nash equilibrium (weak and strict) of the vaccination game with conforming and nonconforming peer effects as a function of r. Using this figure, we can again see the importance of the starting point and the weak NE, as discussed at the end of Section 5.3.2 in the context of γ. Here, we can see that the subsidy will also play a role. For example, assume that a new vaccine is being introduced, and so the starting point is at 0% coverage and suppose $r = 0.5$. In order to bump up the coverage to the social optimum, we need to reduce r to approximately $r_1 = 0.3$. However, if we use too large a subsidy and decrease r to $r_2 = 0.2$, the only equilibrium will be at 100% coverage, incurring too much extra cost. The weak NE come into play if the starting point is somewhere between 0–100%, as discussed before. With conforming peer effects, we gain in that the required subsidy to achieve

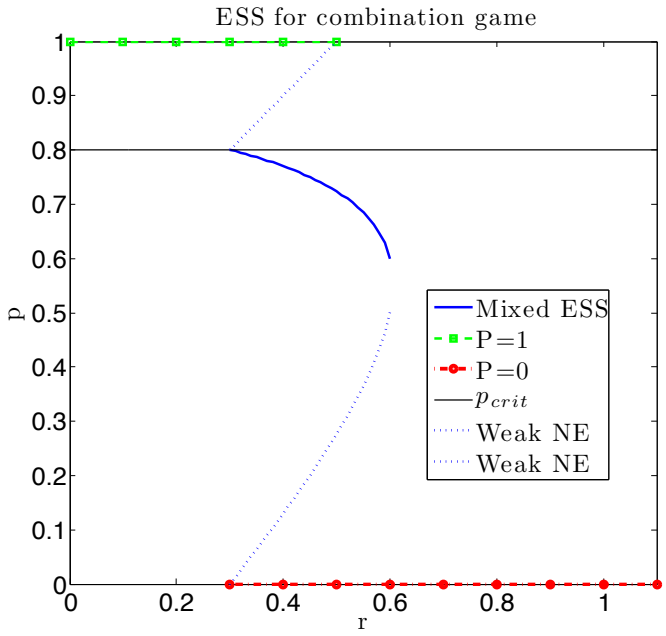

Figure 5.5: All NE as a function of r

the social optimum is less, but there is now the possibility to over-subsidize, leading to over-vaccination. Knowing the current vaccination level and the value placed on conforming are both key to determining the appropriate subsidy.

5.4 Conclusions

In this chapter we contrasted the positive and normative implications of two alternate models of vaccination decisions. In the first or traditional model, rational agents desire to free-ride on the vaccination decisions of others. In the second model, agents have an additional desire to conform to the vaccination decisions of their peers. We demonstrated that adding conforming peer effects to the traditional model of vaccination decisions can have important implications for understanding vaccination decisions and designing public health policy.

Adding conforming peer effects overturns several important results from traditional vaccination models. In most traditional models, privately optimal vaccination rates are always below the socially optimal vaccination rate. These models also produce a unique evolutionarily stable equilibrium. In contrast, in the model with con-

forming peer effects, privately optimal vaccination rates can be above or below the social optimum. In fact, the model produces several evolutionarily stable equilibria including no vaccination coverage, full vaccination coverage and a mixed strategy equilibrium. Since this model produces several equilibria vaccination rates, the final state not only depends on the vaccine and disease parameters but also on the initial conditions. This means that the effect of changes in the cost of vaccines or new side effect information might depend on the vaccination rate under the initial equilibrium.

Traditional models also imply that vaccine subsidies are always optimal as private vaccination rates are always below the social optimum. Given the free-rider problem these models also imply that even when vaccines are free, coverage required to achieve disease eradication is impossible. In contrast, in the model with conforming peer effects, subsidies for vaccination are not always optimal as the privately optimal vaccination coverage might be above the social optimum. However, in certain cases, depending on the disease and vaccine parameters, even small subsidies can achieve disease eradication. In addition, the effects of subsidies can also depend on the initial conditions.

Overall, these results suggest that conforming peer effects can have important implications for designing effective public health policy and understanding the effectiveness of interventions for improving vaccination coverage. Yet we know little about the magnitude of conforming peer effects and the extent to which these peer effects might vary across diseases, geography, and age group. We also know little about what factors influence peer effects in vaccination decisions and whether we can design interventions to change their magnitude. These are all fruitful avenues for future research.

5.5 Appendix: Definitions

Within the vaccination game with nonconforming peer effects, we are interested in equilibrium strategies to determine the behavior of rational agents. We define a Nash Equilibrium and an Evolutionarily Stable Strategy (ESS) as given in [62].

Definition 7. *A strategy P is a Nash Equilibrium if for all strategies $Q \neq P$*

$$E(Q, P) \leq E(P, P). \tag{5.97}$$

Note that P is referred to a *strict NE* if the inequality is strict, or as a *weak NE* if the equality holds.

Definition 8. *Let $p_{tot} = \epsilon Q + (1 - \epsilon)P$ represent the total vaccination coverage when ϵ-fraction of the population deviates from strategy P to Q. A strategy P is an Evolutionarily Stable Strategy (ESS) if for all $Q \neq P$*

$$E(Q, p_{tot}) < E(P, p_{tot}) \tag{5.98}$$

holds for all $\epsilon > 0$ sufficiently small.

An alternate definition of an ESS is useful for proving when it exists:

Definition 9. *A strategy P is an ESS $\iff$ for all strategies $Q \neq P$*

$$\textit{(i) } E(P, P) > E(Q, P), \textit{ or} \tag{5.99}$$

$$\textit{(ii) } E(P, P) = E(Q, P) \textit{ and } E(P, Q) > E(Q, Q) \tag{5.100}$$

Note that the following relations hold for NE and ESS's:

$$\text{strict NE} \implies \text{ESS}$$

$$\text{ESS} \implies \text{NE}$$

5.6 Appendix: Proofs

In this section we present formal proofs not included in the main body of the chapter.

Proof. (Lemma 5.1) In the context of the vaccination game with only nonconforming peer effects, the Nash Equilibrium condition from Definition 7 can be rewritten as, for all $Q \neq P$,

$$E(P,P) - E(Q,P) \geq 0 \tag{5.101}$$

$$\iff P[E_{vac}] + (1-P)[E_{nv}(P)] - Q[E_{vac}] - (1-Q)[E_{nv}(P)] \geq 0 \tag{5.102}$$

$$\iff (P-Q)[E_{vac} - E_{nv}(P)] \geq 0 \tag{5.103}$$

$$\iff (P-Q)[-r + w(P)] \geq 0. \tag{5.104}$$

Consider a population following the mixed equilibrium strategy p^* satisfying $w(p^*) = r$. This strategy is clearly a weak NE, since (using the rewritten NE condition from 5.104)

$$E(p^*,p^*) - E(Q,p^*) = (p^* - Q)(-r + w(p^*)) = 0. \tag{5.105}$$

Using Definition 9, p^* will be an ESS if

$$E(p^*,Q) > E(Q,Q) \iff (p^* - Q)(-r + w(Q)) > 0. \tag{5.106}$$

Consider first the case where $Q > p^*$. In this case, we have $p^* - Q < 0$ and

$$-r + w(Q) < -r + w(p^*) = 0 \tag{5.107}$$

since by assumption the probability of getting infected $w(p)$ is a strictly decreasing function with vaccination coverage p (i.e., an individual's probability of getting infected goes down as more people choose to vaccinate). As a result, $(p^* - Q)(-r + w(Q)) > 0$.

Now consider the second case where $Q < p^*$. In this case, we have $p^* - Q > 0$ and

$$-r + w(Q) > -r + w(p^*) = 0 \tag{5.108}$$

again since the probability of getting infected $w(p)$ is a strictly decreasing function with vaccination coverage p. Note however that if $r > w(0)$, we have

$$-r + w(Q) < -w(0) + w(Q) < 0 \tag{5.109}$$

always. Thus, $(p^* - Q)(-r + w(Q)) > 0$ and the mixed equilibrium is an ESS only if $r < w(0)$, i.e., if the vaccine is sufficiently inexpensive and safe.[3] □

5.7 Appendix: The SIR model with constant population size and vaccination

Using the SIR model with constant population model (birth rate = death rate = μ) in [13], often used to model childhood diseases, we have,

$$\frac{dS}{dt} = \mu(1-p) - \beta SI - \mu S \tag{5.111}$$

$$\frac{dI}{dt} = \beta SI - \gamma I - \mu I \tag{5.112}$$

$$\frac{dR}{dt} = \mu p + \gamma I - \mu R \tag{5.113}$$

[3] In the case where $r > w(0)$ (when the relative cost of vaccination to being infected is smaller than the probability of being infected with zero coverage), there exists a pure strict NE and ESS at $P = 0$, nobody vaccinating. In this case,

$$E(P,P) - E(Q,P) = (P-Q)(E_v(P) - E_{nv}(P)) = -Q(E_v(0) - E_{nv}(0)) = -Q(-r + w(0)) \tag{5.110}$$

Thus, $E(Q,P) < E(P,P)$ if $w(0) < r$. If $r = 0$ (there is no cost or risk associated with the vaccine), any strategy $P \geq p_{crit}$ will be a weak NE, including the pure strategy $P = 1$, everyone vaccinating. However, none of these weak NE will be evolutionarily stable, since they are not resistant to a decrease in vaccination coverage. As a result, everyone will converge to the mixed strategy $p^* = p_{crit}$.

where p is vaccination uptake, β is the mean transmission rate, $1/\gamma$ is the mean infectious period, and μ is the mean birth and death rate. We can reduce these equations to the following dimensionless form:

$$\frac{dS}{d\tau} = f(1-p) - R_0(1+f)SI - fS \tag{5.114}$$

$$\frac{dI}{d\tau} = R_0(1+f)SI - (1+f)I \tag{5.115}$$

where $\tau = t\gamma$ is time measured in units of the mean infectious period, $f = \mu/\gamma$ is the infectious period as a fraction of mean lifetime, and $R_0 = \beta/(\gamma+\mu)$ is the basic reproductive ratio (the average number of secondary cases produced by a typical primary case in a fully susceptible population). (From [4], we have for childhood diseases, $f < .001$ and $R_0 \sim 5 - 20$.)

The predictions of the SIR model depend on the critical coverage level that eliminates the disease from the population, p_{crit}:

$$p_{crit} = \begin{cases} 0 & R_0 \leq 1 \\ 1 - \frac{1}{R_0} & R_0 > 1 \end{cases} \tag{5.116}$$

If $p \geq p_{crit}$, then the system converges to the disease-free state $(\hat{S}, \hat{I}) = (1-p, 0)$, whereas if $p < p_{crit}$, it converges to a stable endemic state given by

$$\hat{S} = 1 - p_{crit} \tag{5.117}$$

$$\hat{I} = \frac{f}{1+f}(p_{crit} - p) \tag{5.118}$$

Because S and I are constant in this situation, the probability that an unvaccinated individual eventually becomes infected can be expressed, using the above equations, as the proportion of susceptible individuals becoming infected versus dying in any unit time,

$$w(p) = \frac{R_0(1+f)\hat{S}\hat{I}}{R_0(1+f)\hat{S}\hat{I} + f\hat{S}} = 1 - \frac{1}{R_0(1-p)}. \tag{5.119}$$

Thus, we have our infection probability:

$$w(p) = \begin{cases} 1 - \frac{1}{R_0(1-p)} & 0 \leq p \leq p_{crit} \\ 0 & p_{crit} < p \leq 1 \end{cases} \tag{5.120}$$

Note that $w(p)$ is a decreasing function of p, as shown in Figure 5.6.

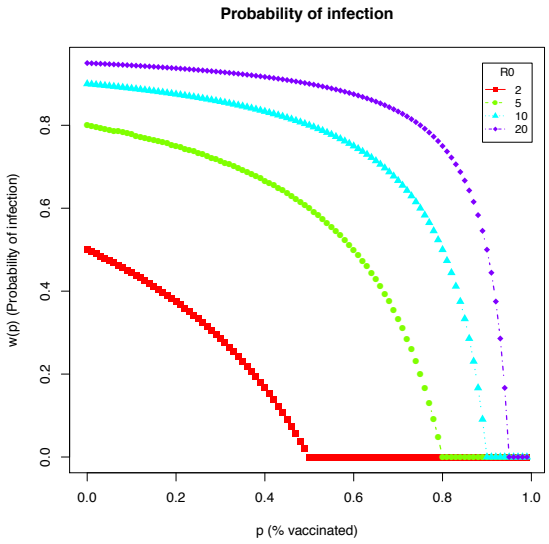

Figure 5.6: Probability of infection

Chapter 6

Conclusion

6.1 Summary of contributions

In this thesis, we have focused on the role of peer effects in social networks, examining their impact on distributed search, matching markets, epidemic spread, and human behavior. The goal in each chapter was to leverage these peer effects to reach a deeper understanding of the problem at hand. For example, in the case of distributed search, we explored how a distance-dependent probability of connection between peers is required for a social network to be searchable and developed a novel random network model: distance-dependent Kronecker graphs. Investigating two very different problems, matching markets and vaccination decisions, we examined the impact of peer effects on individual agents' preferences and decisions. In the context of matching markets, our focus on peer effects in social networks allowed us to achieve positive results where most earlier work has only negative results. In our work on epidemics, we used random social network models to calculate the expected cost of an epidemic when infection in transmitted between peers (contact-based infection). The common thread connecting these rather different problems is that each has an underlying social network; in each case, we asked the question: *How might we exploit our knowledge of peer effects in social networks to use this underlying social network to our advantage?* For the remainder of this chapter, we summarize our answer to this question, restating our major results and describing possible future directions. We conclude with some general thoughts on the nature of social network research and why it is

such an interesting and promising area of investigation.

Distributed Search. In order to determine what makes a social network searchable by a distributed algorithm using only local information, we used Kleinberg's idea of distance-dependent connection probability [75] to generalize a promising random graph model, Kronecker graphs [81]. Specifically, we developed a mathematically tractable random network model (distance-dependent Kronecker graphs) incorporating searchability, where individuals use their local and long-distance connections to their peers to optimally route a message through the network. This model generalizes Kronecker graphs, using a family of "distance"-dependent matrices and a new Kronecker-like operation, as opposed to the static generator matrix used in the original Kronecker graph model. As a result, our network model defines both local regular structures and global distance-dependent connections. While this model is more complicated than the original model, it is more general, as it can generate existing social network models, and more importantly, networks that are searchable. These properties emerge naturally from the definition of the embedding of the nodes and the probability of connection within the family of generator matrices. More generally, any lattice-based network model with distance-dependent connection probabilities can be analyzed using the framework described in Chapter 2 for exploring degree distribution, diameter, and searchability. In particular, our searchability analysis shows how to make any network model searchable by defining the appropriate probability of connection. Using this analysis, we are able to show a particularly nice aspect of our model; i.e., it is rather robust to changes in the long-distance connection probability, as opposed to earlier models.

Matching Markets with Externalities. Looking at matching markets, we used a social network to capture the impact of peer effects on individual preferences, proving that even in the presence of these types of externalities, stable matchings exist and are achievable by a distributed matching mechanism. Typically, results on this topic tend to be negative, either proving that stable matchings may not exist, or that stable matchings are computationally difficult to find. Our goal has been to provide positive results. To this end, we focused on the case when peer effects are the result

of an underlying social network, using utility functions to capture preferences and examining a new notion of stability, namely, two-sided exchange stability. With this framework, we proved that a two-sided exchange-stable matching always exists and that under certain conditions, socially optimal matchings are always stable. Further, we proved that the impact of the social network structure on the price of anarchy in such markets happens only through the clustering of the network, which is well understood for social networks. Interestingly, in our context the price of anarchy has a dual interpretation as characterizing the degree of inefficiency caused by peer effects. Our algorithms and efficiency bounds provide a promising approach for designing optimal matching mechanisms, for the specific housing market considered in Chapter 3 as well as any general market where peer effects change the space of stable matchings.

Epidemic Spread on Complex Networks. Turning to epidemic spread, we examined the social cost of an epidemic when a disease is spread by social contact, using tools from random matrix theory to obtain simple solutions highlighting the importance of the structure of the underlying social network in the final cost of an epidemic. Using a linearized dynamical system based on the popular SIS model and a random graph as the underlying network, we calculated the cost of the disease in the large graph limit and derived bounds for the disease cost for a given graph. This cost depends on the entire transient behavior of the system and hence this analysis differs from previous work that usually focuses on the steady-state equilibrium. Our calculation shows that the disease cost depends on the entire eigen-distribution of the system matrix, whereas the upper bound depends only on the largest eigenvalue. Despite its simpler form, the upper bound appears to be tight for some random graphs, as shown by our simulations. Applying these results to the social cost of an epidemic (accounting for both the disease cost and the mechanism used to control the disease), we briefly analyzed the cost of some simple immunization strategies: random and degree-based one-shot vaccination. We also carefully analyzed the assumptions made in our linear model and showed graph regimes where our assumptions are valid. To the best of our knowledge, our approach in Chapter 4 using random matrices is novel to the study of epidemic processes.

Human Behavior in Vaccination Decisions. Motivated by our work in disease cost, we moved to studying the role of peer effects in vaccination decisions, in order to explore the impact of (selfish) human behavior in vaccination health policy. We proposed a game-theoretical model to capture both conforming and nonconforming peer effects and used this model to determine optimal public health policies regarding vaccination subsidies. In traditional vaccination decision models with only nonconforming peer effects, rational agents desire to free-ride on the vaccination decision of others. In our model, agents have an additional desire to conform to the vaccination decisions of their peers. Adding conforming peer effects overturns several important results from the traditional model. In particular, when only nonconforming peer effects are present, the privately optimal vaccination rate is a unique evolutionarily stable strategy and is always below the social optimum. In contrast, when conforming peer effects are added to the model, privately optimal vaccination rates can be above or below the social optimum. In fact, the model produces several evolutionary stable equilibria including no vaccination coverage, full vaccination coverage and a mixed strategy equilibrium. Since this model produces several equilibria vaccination rates, the final state not only depends on the vaccine and disease parameters but also on the initial conditions. In a practical sense this means that the effects of changes in vaccine cost, or new information on side effects, might depend on the vaccination rate under the initial equilibrium. The traditional model also implies that vaccine subsidies are always optimal, since private vaccination rates are always below the social optimum. Given the free-rider problem, this model also implies that even when vaccines are free, coverage required to achieve disease eradication is impossible. In contrast, in our model with nonconforming peer effects, subsidies for vaccination are not always optimal, since privately optimal vaccination coverage might be above the social optimum. However, in certain cases, depending on disease and vaccine parameters, even small subsidies can achieve disease eradication. Overall, our results in Chapter 5 suggest that conforming peer effects can have important implications for designing effective public health policy and understanding the effectiveness of interventions for improving vaccination coverage.

6.2 Future work and applications

The research presented here lays the foundation for further investigation of peer effects in social networks. Each of the specific topics explored, search, matching markets, and epidemics, can be extended both theoretically and practically, as described below. More generally, however, our approach of using network structure and peer effects to explore problems in diverse areas, from economics to engineering to computer science, is a promising direction for future social network research. In any problem where there is an underlying network or process operating on a network, understanding the structure of that network will be key, and our research provides a useful approach for tackling these sorts of problems.

Search. While our work in Chapter 2 gives a near complete description of the characteristics of "distance"-dependent Kronecker graphs, there are many interesting questions that remain. These include how to parameterize the model from real-world data sets, and how to incorporate network dynamics. Ideally, given any data set, i.e., any collection of related real-world social networks, we would like to be able to find an appropriate family of distance-dependent matrices to match any desired characteristic of the data set. First, we will need to determine the appropriate embedding of the network (yielding the first few generator matrices and the "distance" measure) and then the long-distance probability of connection (giving the rule for the rest of the generator matrices). Possible approaches include exploring current methods for embedding networks in Euclidean and hyperbolic spaces, but much work still remains to determine how exactly to separate out and learn the embedding and the long-distance probability of connection from a real-world social network. Additionally, while the current model incorporates some measure of growth, growing from a small initiator matrix to a final $n \times n$ adjacency matrix, we would like to better incorporate mobility into the model so that it is not just a static description of the network at one point in time. Ideally, our model of growth should mimic the way real social networks grow and evolve with time, something the current distance-dependent Kronecker graph model does not capture.

Matching Markets. Our current results in Chapter 3 represent only a starting point for research into the interaction of social networks and many-to-one matchings. There are a number of simplifying assumptions in this work which would be interesting to relax. For example, the efficiency bounds we have proven consider only a one-sided market, where houses do not have preferences over students, students rate houses similarly, and quotas are exactly met. These assumptions are key to providing simpler bounds, and they certainly are valid in some matching markets; however relaxing these assumptions would broaden the applicability of the work greatly.

There are numerous examples of many-to-one matching markets where our results can provide insight; one of particular interest to us is the matching of incoming undergraduates to residential houses which happens yearly at Caltech and other universities. Currently incoming students only report a preference order for houses, and so are incentivized to collude with friends and not reveal their true preferences. For such settings, our results highlight the importance of having students report not only their preference order on houses, but also a list of friends with whom they would like to be matched. In particular, our simulations clearly show an improvement in social welfare by considering the social network in the matching mechanism, even with the very simple mechanisms we examine. Extending this work, we would like to explore more sophisticated matching mechanisms, perhaps determining the impact of peer effects on mechanism design (i.e., incentive compatibility and complexity).

Other markets where our approach could prove beneficial include team formation problems, resource allocation, and on-line ad auctions. When forming teams, whether in industry or academia, it is important to consider the makeup of the team (diverse skills and backgrounds) as well as the ability of team members to work together. Our model can easily be extended to this scenario, using a weighted social network to capture team members' affinity for each other and our utility functions to capture complementarities. In terms of on-line ad auctions, we would like to use our model to explore the impact of ad placement on effectiveness — examining the impact of neighboring competing or complementary ads on click-through rate. If neighboring ads do have a positive and/or negative impact, we could use our model to design ad

auctions that take this effect into account. In general, we should be able to extend our results to any sort of market where peer effects change the space of stable matchings.

Epidemics. To extend the work on epidemics on complex networks, we would like to investigate both theoretical and practical refinements of our model. We can consider more sophisticated epidemic models (SIR, etc.) as well as immunization based on the strategic behavior of agents. Moreover, a case study with real data from communicable diseases like influenza or herpes would provide more insight into the accuracy and predictive power of these models in real-world scenarios, as well as help refine the per node cost of disease which we have assumed is a single parameter. In general, our random network approach is a promising direction to tackle the problem of epidemic spread on network — our simulations show that at least under certain infection and graph parameters, our results are fairly accurate, giving us hope to quantify the cost of an epidemic on real-world networks. The approach and the random matrix tools we use are fairly general; we hope to extend the tools, techniques and ideas in our results to further study complex processes on complex networks.

For example, we can combine our work on epidemics and vaccination decisions to investigate dynamic vaccination games on networks, where individuals make vaccination decisions at each point in time, based on their local information about the current epidemic state and perhaps influenced by their peers to make particular choices. This is a very interesting and challenging theoretical problem to pursue, but unfortunately, we know little about real-world peer effects. Practically, we know little about the magnitude of conforming peer effects and the extent to which these peer effects might vary across diseases, geography, and age group, what factors influence peer effects in vaccination decisions and whether we can design interventions to change their magnitude. Quantifying real-world peer effects is a fruitful avenue for future research, perhaps requiring some sort of real-world data gathering and study. On the theoretical side, this general approach can also be applied to other problems such as technology adoption, dynamic patching of viruses on computer networks, and others — any problem where individual agents make decisions based on information available through their peers and perhaps can be influenced by conforming peer effects.

6.3 Concluding thoughts

Social network research requires translation between the fields of engineering, computer science, economics, public policy and sociology. Often, the challenge can be simply to find a common language; a thorough literature search on a given topic may require multiple searches across disciplines using different keywords. As with all interdisciplinary research, in order to not reinvent the wheel, one must be careful to examine the research in each area to determine where novel contribution can be made. Despite the challenges, the potential benefit of such research is huge. Leveraging knowledge from one area not only allows us to reach deeper insights about problems in a different one, but also can influence the questions we ask and the research problems we decide to study. For example, existing research in sociology on real-world data sets may point to an underlying phenomenon. This knowledge provides the motivation for computer scientists and statistical physicists to propose and study various random network models explaining the origin of said phenomenon. Closing the loop, real-world studies can then be used to validate these random network models, determining which model is most appropriate for studying a particular topic. Economists can then apply such models to studying economic interactions in networked markets, while engineers can use the same models to design protocols and algorithms to facilitate such markets. This is just one rather general example where this type of interdisciplinary research provides a large reward — many more specific examples exist, including the work presented here.

In many cases, the results in one area lead to questions in another. For example, in our attempt to define a mathematically tractable searchable network model, we discovered a tension between searchability and a heavy-tailed degree distribution. Our results state that at least in the case of lattice-based network models, the two characteristics are incompatible. Yet, both have been observed in social networks. This apparent contradiction points to the need for more careful investigation using real-world and on-line data sets, determining the exact circumstances under which both characteristics exist, and hopefully determining an improvement to the model

to make it more realistic. In another example, we found that while our matching mechanisms incorporating social network knowledge yield a better match than the existing one for the Caltech housing market, the improvement is not drastic. The existing match of students to houses already does a pretty good job of matching friends together. At first glance, this is a negative result, but upon further investigation, it is pointing to a deeper issue: causation and network formation. The current data set we use includes all undergraduate students, freshman through senior. Seniors have been living in their respective houses for four years and likely have formed many friendships within their houses. Thus, the network is already rather well clustered into the various houses, and while our matching mechanisms do provide some improvement, this increase in social welfare is not as much as would be expected compared to starting at a purely random match. This rather simple observation leads to more questions involving network formation, and further avenues of investigation. Perhaps we can use our data set, differentiating between each class of students, to determine the effect of housing assignment on the social network and vice versa.

In conclusion, using the interdisciplinary knowledge required for social network research can help us understand our role in an increasingly (social-)networked world, as well as design better solutions to the problems our networked world poses.

Bibliography

[1] R. Albert and A. Barabási. Statistical mechanics of complex networks. *Reviews of Modern Physics*, 74, 2002.

[2] J. Alcalde. Exchange-proofness or divorce-proofness? Stability in one-sided matching markets. *Review of Economic Design*, 1:275–287, 1994.

[3] G.W. Anderson, A. Guionnet, and O. Zeitouni. *An Introduction to Random Matrices*, volume 118 of *Cambridge Studies in Advanced Mathematics*. Cambridge University Press, 2010.

[4] R.M. Anderson and R.M. May. *Infectious Diseases of Humans*. Oxford University Press, 1991.

[5] M. Ángeles Serrano, D. Krioukov, and M. Boguñá. Self-similarity of complex networks and hidden metric spaces. *Physics Review Letters*, 100, 2008.

[6] E. Anshelevich, S. Das, and Y. Naamad. Anarchy, stability, and utopia: Creating better matchings. In *SAGT '09*, pages 159–170, 2009.

[7] H. Aziz, F. Brandt, and H.G. Seedig. Stable partitions in additively separable hedonic games. *Computing Research Repository*, 2010.

[8] M. Baccara, A. Imrohoroglu, A. Wilson, and L. Yariv. A field study on matching with network externalities. *The American Economic Review*, 102, 2012.

[9] P. Bajari and J. Fox. Measuring the efficiency of an FCC spectrum auction. Working Paper 11671, National Bureau of Economic Research, 2009.

[10] P. Bak, K. Chen, and C. Tang. A forest-fire model and some thoughts on turbulence. *Phys. Lett. A*, 147:297300, 1990.

[11] A. Barabási and R. Albert. Emergence of scaling in random networks. *Science*, 286:509–512, 1999.

[12] M. Barthelemy, A. Barrat, R. Pastor-Satorras, and A. Vespignani. Velocity and Hierarchical Spread of Epidemic Outbreaks in Scale-Free Networks. *Phys. Rev. Lett.*, 92(17), 2004.

[13] C.T. Bauch. Vaccination and the theory of games. *Proceedings of The National Academy of Sciences*, 101:13391–13394, 2004.

[14] C.T. Bauch. Imitation dynamics predict vaccinating behavior. *Proceedings of the Royal Society B: Biological Sciences*, 272(1573):1669–1675, 2005.

[15] C.T. Bauch, A.P. Galvani, and D.J. Earn. Group interest versus self-interest in smallpox vaccination policy. *Proceedings of the National Academy of Sciences*, 100(18):10564–10567, 2003.

[16] E. Bodine, B. Hassibi, and A. Weirman. Generalizing Kronecker graphs in order to model searchable networks. In *Proc. Forty-Seventh Annual Allerton Conference*, 2009.

[17] E. Bodine-Baron, S. Bose, B. Hassibi, and A. Wierman. Minimizing the social cost of an epidemic. *LNICST, Proc. GameNets 2011*, 2011.

[18] E. Bodine-Baron, B. Hassibi, and A. Wierman. Distance-dependent Kronecker graphs for modeling social networks. *IEEE Journal of Selected Topics in Signal Processing*, 4(4):718–731, Aug. 2010.

[19] E. Bodine-Baron, C. Lee, A. Chong, B. Hassibi, and A. Wierman. Peer effects and stability in matching markets. In Giuseppe Persiano, editor, *Algorithmic Game Theory*, volume 6982 of *Lecture Notes in Computer Science*, pages 117–129. Springer Berlin/Heidelberg, 2011.

[20] E. Bodine-Baron, S. Nowak, N. Sood, and R. Vardavas. Conforming and non-conforming peer effects in vaccination decisions. Working paper, 2012.

[21] A. Bogomolnaia and M. Jackson. The stability of hedonic coalition structures. *Games and Economic Behavior*, 38(2):201–230, 2002.

[22] M. Boguñá and D. Krioukov. Navigating ultrasmall worlds in ultrashort time. *Physical Review Letters*, 102:058701, 2009.

[23] M. Boguñá, D. Krioukov, and kc claffy. Navigability of complex networks. *Nature Physics*, 5:74–80, 2009.

[24] M. Boguna, R. Pastor-Satorras, and A. Vespignani. Absence of Epidemic Threshold in Scale-Free Networks with Degree Correlations. *Phys. Rev. Lett.*, 90(2), 2003.

[25] B. Bollobás. *Random Graphs*. Academic Press, Inc., 1985.

[26] S. Bose, E. Bodine-Baron, B. Hassibi, and A. Wierman. Cost of epidemic spread on complex networks: A random matrix approach. Working paper, 2012.

[27] L. Bownds, R. Lindekugel, and P. Stepak. Economic impact of a Hepatitis A epidemic in a mid-sized urban community: The case of Spokane, Washington. *Journal of Community Health*, 38(4), 2003.

[28] S. Brânzei and K. Larson. Coalitional affinity games and the stability gap. In *Proc. 21st Intl. Joint Conf. on Artificial Intelligence (IJCAI)*, pages 1319–1320, 2009.

[29] N. Burani and W.S. Zwicker. Coalition formation games with separable preferences. *Mathematical Social Sciences*, 45:27–52, 2003.

[30] K. Cechlarova and D. Manlove. On the complexity of exchange-stable roommates. *Discrete Applied Mathematics*, 116(3):279–287, 2002.

[31] K. Cechlarova and D. Manlove. The exchange-stable marriage problem. *Discrete Applied Mathematics*, 152(1–3):109–122, 2005.

[32] M. Cha, A. Mislove, and K.P. Gummadi. A measurement-driven analysis of information propagation in the flickr social network. *Proc. 18th WWW Conf.*, pages 721–730, 2009.

[33] D. Chakrabarti, Y. Wang, C. Wang, J. Leskovec, and C. Faloutsos. Epidemic thresholds in real networks. *ACM Trans. on Info. and System Security (TISSEC)*, 10(4), 2008.

[34] H. Chen, H. Jin, J. Sun, and Z. Han. Efficient immunization algorithm for peer-to-peer networks. *Lec. Notes in Comp. Sci.*, 3296:143–178, 2005.

[35] F. Chung and L. Lu. *Complex Graphs and Networks*. AMS, 2006.

[36] S. Clark, A. Cowan, and P. Wortley. Influenza vaccination attitudes and practices among US registered nurses. *American Journal of Infection Control*, 37(7):551–556, 2009.

[37] R. Cohen, S. Havlin, and D. ben Avraham. Efficient immunization strategies for computer networks and populations. *Phys. Rev. Lett.*, 91(24), 2003.

[38] A. Cvetkovski and M. Crovella. Hyperbolic embedding and routing for dynamic graphs. In *Proc. of Infocom*, 2009.

[39] D. Daley and J. Gani. *Epidemic Modeling: An Introduction*. Cambridge University Press, 2005.

[40] A. Datar, A. Mukherji, and N. Sood. Health infrastructure and immunization coverage in rural India. *Indian Journal of Medicine*, 125:31–42, January 2007.

[41] Wikipedia vote data set: Stanford large network dataset collection. `http://snap.stanford.edu/data/wiki-Vote.html`.

[42] J.H. Dreze and J. Greenberg. Hedonic coalitions: Optimality and stability. *Econometrica*, 48(4):987–1003, 1980.

[43] B. Dutta and J. Masso. Stability of matchings when individuals have preferences over colleagues. *Journal of Economic Theory*, 75(2):464–475, 1997.

[44] F. Echenique and M. Yenmez. A solution to matching with preferences over colleagues. *Games and Economic Behavior*, 59(1):46–71, 2007.

[45] A. Edelman and N.R. Rao. Random matrix theory. *Acta Numerica*, 14:233–297, 2005.

[46] E. Elkind and M. Wooldridge. Hedonic coalition nets. In *Proc. 8th Intl. Joint Conf. on Autonomous Agents and Multi-Agent Systems (AAMAS)*, pages 417–424, 2009.

[47] J. Ensminger. The Caltech Project, 2010. Unpublished dataset.

[48] W. Evans, W. Oates, and R. Schwab. Measuring peer group effects: A study of teenage behavior. *Journal of Political Economy*, 100(5):966–91, 1992.

[49] F. Fenner. *Smallpox and Its Eradication (History of International Public Health), No. 6*. Geneva: World Health Organization, 1988.

[50] J. Fox. Estimating matching games with transfers. Working Paper 14382, National Bureau of Economic Research, October 2008.

[51] L. Freeman. *The Development of Social Network Analysis*. Empirical Press, 2006.

[52] F. Fu, D. Rosenbloom, L. Wang, and M. Nowak. Imitation dynamics of vaccination behavior on social networks. *Proceedings of the Royal Society Biological Sciences*, 2010.

[53] M. Gairing and R. Savani. Computing stable outcomes in hedonic games. In *Proc. 3rd Intl. Sym. on Algorithmic Game Theory (SAGT)*, 2010.

[54] D. Gale and L.S. Shapley. College admissions and the stability of marriage. *The American Mathematical Monthly*, 69(1):9–15, January 1962.

[55] A. Gaviria and S. Raphael. School-based peer effects and juvenile behavior. *The Review of Economics and Statistics*, 83(2):257–268, 2001.

[56] M. S. Granovetter. The strength of weak ties. *The American Journal of Sociology*, 78(6):13601380, 1973.

[57] Q. Gu and N. Sood. Do people taking flu vaccines need them the most? *PLoS ONE*, 6(12), 12 2011.

[58] I.E. Hafalir. Stability of marriage with externalities. *International Journal of Game Theory*, 37:353–370, 2008.

[59] O. Häggström. *Finite Markov Chains and Algorithmic Applications*. Cambridge University Press, 2001.

[60] B. Hanratty, T. Holt, E. Duffell, W. Patterson, M. Ramsay, J.M. White, L. Jin, and P. Litton. UK measles outbreak in non-immune anthroposophic communities: the implications for the elimination of measles from Europe. *Epidemiology and Infection*, 125:377–383, 2000.

[61] L. Henderson, C. Millett, and N. Thorogood. Perceptions of childhood immunizations in a minority community: qualitative study. *Journal of the Royal Society of Medicine*, 101(5):244–251, 2008.

[62] J. Hofbauer and K. Sigmund. *Evolutionary Games and Population Dynamics*. Cambridge University Press, 1998.

[63] P. W. Holland and S. Leinhardt. Transitivity in structural models of small groups. *Comparative Group Studies*, 2:107–124, 1971.

[64] R.A. Horn and C.R. Johnson. *Matrix Analysis*. Cambridge University Press, 2005.

[65] L. Huang, K. Park, and Y. C. Lai. Information propagation on modular networks. *Phys. Rev. E*, 73(3), Mar 2006.

[66] R. Irving. Stable matching problems with exchange restrictions. *Journal of Combinatorial Optimization*, 16:344–360, 2008.

[67] M. Jackson. *Social and Economic Networks*. Princeton University Press, 2008.

[68] P. Jacquet, B. Mans, and G. Rodolakis. Information propagation speed in mobile and delay tolerant networks. *IEEE Trans. on Info. Theory*, 56(10):5001 –5015, 2010.

[69] D. Johnson, K. Nichol, and K. Lipczynski. Barriers to adult immunization. *The American Journal of Medicine*, 121(7, Supplement 2):S28–S35, 2008.

[70] R. Kannan, S. Vempala, and A. Vetta. On clusterings: Good, bad and spectral. *Journal of the ACM*, 51(3):497–515, 2004.

[71] E. Kenah and James M. Robins. Second look at the spread of epidemics on networks. *Physical Review E (Statistical, Nonlinear, and Soft Matter Physics)*, 76:036113, 2007.

[72] W.O. Kermack and A.G. McKendrick. A contribution to the mathematical theory of epidemics. *Proc. Roy. Soc. Lond. A*, 115:700–721, 1927.

[73] B. Klaus and F. Klijn. Stable matchings and preferences of couples. *Journal of Economic Theory*, 121:75–106, 2005.

[74] B. Klaus and F. Klijn. Paths to stability for matching markets with couples. *Games and Economic Behavior*, 58:154–171, 2007.

[75] J. Kleinberg. The small-world phenomenon: An algorithmic perspective. In *Proc. of the 32nd ACM Symposium on Theory of Computing*, pages 163–170, 2000.

[76] J. Kleinberg. Complex networks and decentralized search algorithms. In *Proc. of International Conference of Mathematicians*, 2006.

[77] F. Kojima and P. Pathak. Incentives and stability in large two-sided matching markets. *American Economic Review*, 99(3):608–627, 2009.

[78] D. Krioukov, F. Papadopoulos, M. Boguñá, and A. Vahdat. Greedy forwarding in scale-free networks embedded in hyperbolic metric spaces. In *Proc. of MAMA Workshop at Sigmetrics*, 2009.

[79] D. Krioukov, F. Papadopoulos, A. Vahdat, and M. Boguñá. Curvature and temperature of complex networks. *Physical Review E*, 80:635101, 2009.

[80] J. Leskovec. *Dynamics of Large Networks.* PhD thesis in Computer Science, Carnegie Mellon University, 2008.

[81] J. Leskovec, D. Chakrabarti, J. Kleinberg, and C. Faloutsos. Realistic, mathematically tractable graph generation and evolution, using Kronecker multiplication. In *Conf. on Principles and Practice of Knowledge Discovery in Databases*, 2005.

[82] J. Leskovec, J. Kleinberg, and C. Faloutsos. Graphs over time: densification laws, shrinking diameters and possible explanations. In *Proc. of ACM SIGKDD Conf. on Knowledge Discovery in Data Mining*, pages 177–187, 2005.

[83] J. Logan. Disparities in influenza immunization among US adults. *Journal of the National Medical Association*, 101(2):161–166, 2009.

[84] P. Lundborg. Having the wrong friends? Peer effects in adolescent substance use. *Journal of Health Economics*, 25, 2006.

[85] M. Mahdian and Y. Xu. Stochastic Kronecker graphs. In *In WAW07: Proc. of Workshop On Algorithms And Models For The Web-Graph*, pages 179–186, 2007.

[86] C. Martel and V. Nguyen. Analyzing Kleinberg's and other small-world models. In *In PODC '04: Proc. of ACM Symposium on Principles of Distributed Computing*, pages 179–188, 2004.

[87] T. May and R. Silverman. Clustering of exemptions as a collective action threat to herd immunity. *Vaccine*, 21(11–12):1048–1051, 2003.

[88] M. McPherson, L. Smith-Lovin, and J. Cook. Birds of a feather: Homophily in social networks. *Annual Review of Sociology*, 27:414–444, 2001.

[89] S. Milgram. The small-world problem. *Psychology Today*, 2:60, 1967.

[90] J. Miller and J. Hyman. Effective vaccination strategies for realistic social networks. *Physica A: Statistical Mechanics and its Applications*, 386(2):780–785, 2007.

[91] C. Moore and M.E.J. Newman. Epidemics and percolation in small-world networks. *Physical Review E*, 61(5):5678, 2000.

[92] M.E.J. Newman. Spread of epidemic disease on networks. *Physical Review E*, 66(1):016128, 2002.

[93] M.E.J. Newman. The structure and function of complex networks. *SIAM Review*, 2003.

[94] M.E.J. Newman. Random graphs as models of networks. In *Handbook of Graphs and Networks*, pages 35–68. Wiley-VCH, 2005.

[95] M. Olsen. Nash stability in additively separable hedonic games and community structures. *Theory Comput Sys.*, 45:917–925, 2009.

[96] F.W. O'Reilly, G.W. Cran, and A.B. Stevens. Factors affecting influenza vaccine uptake among health care workers. *Occupational Medicine*, 55(6):474–479, 2005.

[97] P. Erdős and A. Rényi. On random graphs. *Publicationes Mathematicae 6*, page 290297, 1959.

[98] M. Ostrovsky. Stability in supply chain networks. *The American Economic Review*, 98(3):897–923, 2008.

[99] A. Parker, W. Staggs, G. Dayan, I. Ortega-Sánchez, P. Rota, L. Lowe, P. Boardman, R. Teclaw, C. Graves, and C. LeBaron. Implications of a 2005 measles outbreak in Indiana for sustained elimination of measles in the United States. *New England Journal of Medicine*, 355(5):447–455, 2006.

[100] R. Pastor-Satorras and A. Vespignani. Epidemic Spreading in Scale-Free Networks. *Phys. Rev. Lett.*, 86:3200–3203, 2001.

[101] R. Pastor-Satorras and A. Vespignani. Epidemic dynamics in finite size scale-free networks. *Phys. Rev. E*, 65, 2002.

[102] R. Pastor-Satorras and A. Vespignani. Immunization of complex networks. *Phys. Rev. E*, 65, 2002.

[103] C. Peng, X. Jin, and M. Shi. Epidemic threshold and immunization on generalized networks. *Physica A: Statistical Mechanics and its Applications*, 389(3):549–560, 2010.

[104] J. Phelps, R. Lewis, L. Mobilio, D. Perry, and N. Raman. Viral marketing or electronic word-of-mouth advertising: Examining consumer responses and motivations to pass along email. *Journal of Advertising Research*, 44, 2004.

[105] T. Philipson. Economic epidemiology and infectious diseases. In A. J. Culyer and J. P. Newhouse, editors, *Handbook of Health Economics*, volume 1 of *Handbook of Health Economics*, chapter 33, pages 1761–1799. Elsevier, 2000.

[106] M. Pycia. Stability and preference alignment in matching and coalition formation. *Econometrica*, 80(1):323–362, 2012.

[107] F. Radicchi, C. Castellano, F. Cecconi, V. Loreto, and D. Parisi. Defining and identifying communities in networks. *Proc. National Academy of Sciences USA*, 101(9):2658–2663, 2004.

[108] V. Ramasubramanian and D. Malkhi. On the treeness of internet latency and bandwidth. In *Proc. of ACM Sigmetrics*, pages 61–72, 2009.

[109] N. Rao, M. Mobius, and T. Rosenblat. Social networks and vaccination decisions. *Federal Reserve Bank of Boston Working Papers*, 2007.

[110] P. Revilla. Many-to-one matching when colleagues matter. Working paper 146, Fondazione Eni Enrico Mattei Working Papers, 2007.

[111] M. Richardson and P. Domingos. Mining knowledge-sharing sites for viral marketing. *Proc. 8th ACM SIGKDD*, pages 61–70, 2002.

[112] E. Ronn. NP-complete stable matching problems. *Journal of Algorithms*, 11:285–304, 1990.

[113] A.E. Roth. The evolution of the labor market for medical interns and residents: A case study in game theory. *Journal of Political Economics*, 92:991–1016, 1984.

[114] A.E. Roth, U.G. Rothblum, and J.H. Vande Vate. Stable matchings, optimal assignments and linear programming. *Mathematics of Operations Research*, 18(4):803–828, 1993.

[115] A.E. Roth and M. Sotomayor. *Two-sided matching: A study in game-theoretic modeling and analysis*. Cambridge University Press, 1990.

[116] A.E. Roth and J.H. Vande Vate. Random paths to stability in two-sided matching. *Econometrica*, 58:1475–1480, 1990.

[117] R. Rubin, C. Harrington, A. Poon, K. Dietrich, J. Greene, and A. Moiduddin. The Economic Impact of Staphylococcus aureus Infection in New York City Hospitals. *Emerging Infectious Diseases*, 5(1), 1999.

[118] B. Sacerdote. Peer effects with random assignment: Results for Dartmouth roommates. *Quarterly Journal of Economics*, 116:681–704, 2001.

[119] T. Santibanez, M. Nowalk, R. Zimmerman, I. Jewell, I. Bardella, S. Wilson, and M. Terry. Knowledge and beliefs about influenza, pneumococcal disease, and immunizations among older people. *Journal of the American Geriatrics Society*, 50(10):1711–1716, 2002.

[120] H. Sasaki and M. Toda. Two-sided matching problems with externalities. *Journal of Economic Theory*, 70(1):93–108, 1996.

[121] D. Schmid, H. Holzmann, S. Abele, S. Kasper, S. König, S. Meusburger, H. Hrabcik, A. Luckner-Hornischer, E. Bechter, A. DeMartin, J. Stirling, A. Heißenhuber, A. Siedler, H. Bernard, G. Pfaff, D. Schorr, M.S. Ludwig, H.P. Zimmerman, Ø. Løvoll, P. Aavitsland, and F. Allerberger. An ongoing multi-state outbreak of measles linked to non-immune anthoposophic communities in Austria, Germany, and Norway. *Eurosurveillance*, 13(16):18838, 2008.

[122] J. Scott. *Social Network Analysis: A Handbook*. Sage, 2nd edition, 2000.

[123] J. Shi and J. Malik. Normalized cuts and image segmentation. *IEEE Trans. of Pattern Analysis and Machine Intelligence*, 22(8):888–905, 2000.

[124] B. Stewart-Freedman and N. Kovalsky. An ongoing outbreak of measles linked to the UK in an ultra-orthodox Jewish community in Israel. *Eurosurveillance*, 12(38):3270, 2007.

[125] T. Tao. *Topics in random matrix theory*, volume 132 of *Graduate Studies in Mathematics*. American Mathematical Society, 2012.

[126] A.M. Tulino and S. Verdú. *Random matrix theory and wireless communications*, volume 1. Now Publishers, Inc., 2004.

[127] G. Van Essen, M. Kuyvenhoven, and R. De Melker. Why do healthy elderly people fail to comply with influenza vaccination? *Age and Ageing*, 26(4):275–279, 1997.

[128] P. Van Mieghem. *Graph spectra for complex networks*. Cambridge University Press, 2011.

[129] C. Wang, J.C. Knight, and M.C. Elder. On computer viral infection and the effect of immunization. *Proc. ACSAC '00*, pages 246–256, 2000.

[130] Y. Wang, D. Chakrabarti, C. Wang, and C. Faloutsos. Epidemic spreading in real networks: An eigenvalue viewpoint. *Proc. Symp. Reliable Dist. Systems*, 2003.

[131] S. Wasserman and K. Faust. *Social Network Analysis: Methods and Applications*. Cambridge University Press, 1994.

[132] D. Watts. *Six Degrees: The Science of a Connected Age*. W. W. Norton and Company, 2003.

[133] D.J. Watts and S.H. Strogatz. Collective dynamics of small-world networks. *Nature*, 393:440, 1998.

[134] C. Winston, P. Wortley, and K. Lees. Factors associated with vaccination of medicare beneficiaries in five u.s. communities: Results from the racial and ethnic adult disparities in immunization initiative survey, 2003. *Journal of the American Geriatrics Society*, 54(2):303–310, 2006.